



Original document stored on the publication server of the University of Basel
edoc.unibas.ch



This work is licensed under the agreement "Attribution Non-Commercial No Derivatives – 2.5 Switzerland". The complete text may be viewed here:
creativecommons.org/licenses/by-nc-nd/2.5/ch/deed.en

INSTRUMENTATION OF TABLETING MACHINES: HIGH SPEED COMPACTION INVESTIGATION THROUGH SIMULATION AND RADIAL DIE-WALL PRESSURE MONITORING

**INAUGURALDISSERTATION
ZUR
ERLANGUNG DER WÜRDE EINES DOKTORS DER PHILOSOPHIE
VORGELEGT DER
PHILOSOPHISCH-NATURWISSENSCHAFTLICHEN FAKULTÄT
DER UNIVERSITÄT BASEL**

**VON
SAMEH MOHAMED ABDEL-HAMID ABD-RABO
AUS KAIRO (ÄGYPTEN)**

BASEL, 2011



Attribution-Noncommercial-No Derivative Works 2.5 Switzerland

You are free:



to Share — to copy, distribute and transmit the work

Under the following conditions:



Attribution. You must attribute the work in the manner specified by the author or licensor (but not in any way that suggests that they endorse you or your use of the work).



Noncommercial. You may not use this work for commercial purposes.



No Derivative Works. You may not alter, transform, or build upon this work.

- For any reuse or distribution, you must make clear to others the license terms of this work. The best way to do this is with a link to this web page.
- Any of the above conditions can be waived if you get permission from the copyright holder.
- Nothing in this license impairs or restricts the author's moral rights.

Your fair dealing and other rights are in no way affected by the above.

This is a human-readable summary of the Legal Code (the full license) available in German:
<http://creativecommons.org/licenses/by-nc-nd/2.5/ch/legalcode.de>

Disclaimer:

The Commons Deed is not a license. It is simply a handy reference for understanding the Legal Code (the full license) — it is a human-readable expression of some of its key terms. Think of it as the user-friendly interface to the Legal Code beneath. This Deed itself has no legal value, and its contents do not appear in the actual license. Creative Commons is not a law firm and does not provide legal services. Distributing of, displaying of, or linking to this Commons Deed does not create an attorney-client relationship.

Genehmigt von der Philosophisch-Naturwissenschaftlichen Fakultät

auf Antrag von

Prof. Dr. Matthias Hamburger

und

PD Dr. Gabriele Betz

und

Prof. Dr. Adel Sakr

Basel, den 26. April, 2011

Prof. Dr. Martin Spiess
Dekan

To my Dad who waited for this moment but could not live it

الى ابي الذي طالما انتظر هذه اللحظة لكنه لم يستطع ان يعيشها

To all those who sacrificed themselves for the Egyptian Revolution on 25 January

الى كل هؤلاء الذين ضحوا بانفسهم من اجل الثورة المصرية يوم 25 يناير

“ الحرية ، والمعرفة ، والإيمان هي الأسس لتحقيق التقدم والنهضة ”

أحمد زويل (1946-)

الحائز على جائزة نوبل في الكيمياء لعام 1999

“Freedom, knowledge, faith are the basics for progress and Renaissance

Ahmed Zewail (1946-)

Nobel Prize winner for chemistry in 1999

Acknowledgements

This work was carried out at the Industrial Pharmacy Lab, Department of Pharmaceutical Sciences; University of Basel during the years 2007-2011.

I would like to express my sincere gratefulness and appreciation to:

PD Dr. Gabriele Betz, my Thesis Advisor, for her wonderful supervision, continuous support, trust and encouragement.

Prof. Dr. Matthias Hamburger, for accepting to be my Faculty Responsible.

Prof. Dr. Adel Sakr, for accepting to assume the co-refereeing of this work.

Egyptian Ministry for Higher Education and Research for the financial support of my PhD.

Metropolitan Computation Corporation (NJ, US) and ***AICOS*** (Basel, Switzerland) for the support for Presster[®] and STAVEX[®], respectively.

Former and Present Industrial Pharmacy Research Group colleagues:

Dr. Imjak Jeon, Dr. Elaine Darronqui (dear cute mates in liquid sterile dosage forms practical), Dr. Muhanned Saeed (continuous IT support), Dr. Murad Rumman (great support on my arrival to Switzerland), Dr. Krisanin Chansanroj (scientific help), Mr. Mirko Koziolk (co-author in Publication 2), Mr. Shady Mansour (helping in Publication 1), Mr. Firas Alshihabi (Fluidized bed granulation), Miss Neha Ladha (Roll compaction), Mrs. Felicia Flicker, Mrs. Lizbeth Martinez, Mr. Branko Vranic, Mr. Nicolaos Gentis, Mr. Yuya Yonezawa, Mr. Miki Yamashita, Mr. Hiroshi Yamaguchi for making IPL warm, cozy, with funny and unforgettable memories.

My precious friend in Basel, Frau Regina Winter for invaluable friendship and support.

Finally, I do not find enough words to thank my mom and dad for unlimited support and love, my dear sisters Eman and Nesma, and my beloved nephew Ahmed.

Sameh Abdel-Hamid

Basel, 2011

Table of Contents

List of Figures	15
List of Tables.....	18
List of Original Publications	20
List of Abbreviations	21
Summary.....	23
Theoretical Background.....	27
Tablet Press Instrumentation.....	29
Calibration.....	34
Shunt calibration.....	34
Dynamic LVDT calibration (correction of deformation)	34
Die-wall Instrumentation	35
Compaction simulators	36
Compaction scaling-up.....	45
References	48
Aims of the Thesis	59
Chapter I: Study of radial die-wall pressure changes during pharmaceutical powder compaction.....	60
Abstract	60
Introduction	62
Materials and Methods	65
Materials.....	65
Methods	65
Powder Characterization.....	65
True density.....	65
Particle-size distribution	66

Powder compaction.....	66
Compact characterization.....	68
Radial tensile strength (RTS).....	68
Elastic recovery (% ER ₀).....	68
Change in void fraction (VC).....	68
Data interpretation.....	69
Results and Discussion.....	71
Effect of compression pressure on radial die wall parameters.....	71
Effect of precompression pressure on radial die wall parameters.....	76
Effect of compaction speed on radial die wall parameters.....	77
Effect of radial die wall pressure changes on compacts' physical properties.....	78
Conclusion.....	82
References.....	83
Chapter 2: Study of radial die-wall pressure during high speed tableting: effect of formulation variables.....	90
Abstract.....	90
Introduction.....	92
Materials and Methods.....	94
Materials.....	94
Methods.....	95
Powder Characterization.....	95
True density.....	95
Particle-size distribution.....	95
Morphological studies.....	95
Preparation of mixtures.....	96
Powder compaction.....	96
Radial tensile strength (RTS).....	98
Data interpretation.....	99
Results and Discussion.....	101

True density and particle size distribution	101
Effect of lubricant on radial die-wall pressure and friction	103
Mg stearate.....	103
Polyethylene glycol PEG 6000	106
External lubrication	107
Effect of binder on radial die wall pressure and friction.....	109
Copovidone.....	109
Hydroxypropyl cellulose HPC	110
Effect of Drug loading on radial die wall pressure and compressibility	114
References.....	120
 Chapter 3: Investigating the effect of particle size and shape on high speed tableting through radial die-wall pressure monitoring	 130
Abstract	130
Introduction	132
Materials and Methods	134
Materials.....	134
Methods	134
Granulation	134
Granulation in fluidized bed granulator	134
Granulation in roller compactor	135
Powder/Granules Characterization	135
True density.....	135
Particle-size distribution	135
Morphological studies.....	136
Powder/ Granules compaction.....	136
Compact characterization.....	137
Radial tensile strength (RTS).....	137
Porosity	138
Elastic recovery (% ER ₀)	138

Data interpretation.....	139
Results and Discussion	141
True density and particle size distribution.....	141
Particle shape.....	142
Effect of particle size and shape on radial die-wall pressure.....	144
Effect of size and shape on RDP and EF.....	147
Effect of size and shape on MDP and SR.....	149
Effect of particle size and shape on ER_0 , WC, RTS, and Porosity.....	151
Conclusion	153
References	154
Chapter 4: Radial die-wall pressure as a reliable tool for studying the effect of powder water activity on high speed tableting	161
Abstract	161
Introduction	163
Materials and Methods	165
Materials.....	165
Methods.....	165
Powder storage.....	165
Powder Characterization.....	166
Water activity (A_w).....	166
True density.....	167
Differential scanning calorimetry (DSC).....	167
Powder compaction.....	167
Compact characterization.....	169
Radial tensile strength (RTS).....	169
Porosity.....	169
Elastic recovery (% ER_0).....	170
Differential scanning calorimetry (DSC).....	170

Data interpretation.....	170
Results and Discussion	173
True density and Differential Scanning Calorimetry (DSC).....	173
Effect of A_w on Residual Die-wall Pressure (RDP)	174
Effect of A_w on Maximum Die-wall Pressure (MDP)	175
Effect of A_w on Stress Ratio (SR).....	177
Effect of A_w on Ejection Force (EF)	178
Effect of A_w on Friction Coefficient during Compaction (FCC) and Friction Coefficient during Ejection (FCE).....	178
Effect of A_w on Take-off force (TD) and Effective Fall Time (EFT) (sticking prediction tools)	180
Effect of A_w on Elastic Recovery (ER_0) and Radial Tensile Strength (RTS).....	182
Effect of A_w on Work of Compaction (WC)	184
Effect of A_w on Porosity.....	185
Effect of A_w on Ejection Angle (EA)	185
Conclusion.....	187
References.....	188
Chapter 5: Investigating the effect of punch geometry on high speed tableting through radial die-wall pressure monitoring	197
Abstract	197
Introduction	199
Materials and Methods	201
Materials.....	201
Methods	201
Powder Characterization.....	201
True density.....	201
Particle-size distribution	202
Powder compaction.....	202
Compact characterization.....	203
Radial tensile strength (RTS).....	203

Porosity	204
Elastic recovery (% ER_0)	205
Data interpretation.....	205
Results and Discussion	207
True density and particle size distribution	207
Effect of punch geometry on Residual Die-wall Pressure (RDP), Maximum Die-wall Pressure (MDP), and Stress Ratio (SR)	208
Effect of punch geometry on Friction Coefficient during Ejection (FCE)	211
Effect of punch geometry on Elastic Recovery (ER_0) and Radial Tensile Strength (RTS)	212
Effect of punch geometry on Work of Compaction (WC) and porosity	214
Conclusion	217
References.....	218
Chapter 6: A novel tool for the prediction of tablet sticking during high speed compaction.....	222
Abstract	222
Introduction	224
Materials and Methods	227
Materials.....	227
Methods	227
Preparation of powder mixtures	227
True density.....	228
Particle-size distribution	228
Morphological studies.....	228
Powder compaction.....	229
Compact characterization.....	230
Radial tensile strength (RTS).....	230
Porosity	230
Elastic recovery (% ER_0)	231
Data interpretation.....	231

Results and Discussion	233
Effect of particle size and surface, and MA loading on sticking	233
Effect of compression pressure and speed on sticking	236
Radial die-wall pressure for sticking prediction	236
Take-off force for sticking prediction	239
Effect of MA loading on Radial Tensile Strength (RTS), Elastic Recovery (ER_0), Work of Compaction (WC), and Porosity	240
Conclusion	243
References	244
Discussion and Outlook	251
Curriculum Vitae	252

List of Figures

Figure 1 Stages of powder compaction	28
Figure 2 Foil strain gauge with six terminal contacts.....	32
Figure 3 LVDT for punch displacement measurement	33
Figure 4 Presster™ die-wall instrumentation	36
Figure 5 Presster™ linear compaction replicator	39
Figure 6 The Presster™ main screen, stepper motor adjustment, dwell time calculator, and tooling selection	40
Figure 7 Schematic diagram of the Presster™ (Model 104)	41
Figure 8 Compression waveform of the Presster™ showing 1.Upper and 2.Lower compression (UC/LC), 3.Upper and 4.Lower punch displacement (UPD/LPD), and 5.Radial die-wall pressure (RDWP) curves	43
Figure 9 Plots of the Presster™ software showing 1.Ejection force, 2.Take-off force, and 3. Lower punch displacement.....	43
Figure 10 Summary results spreadsheet of the Presster™ software.....	44
Figure 11 Effect of compaction pressure on RDP at compaction speed 0.5 m/s	74
Figure 12 Effect of compaction pressure on MDP at compaction speed 0.5 m/s.....	75
Figure 13 Effect of compaction pressure on RDP/MDP ratio at compaction speed 0.5 m/s.....	75
Figure 14 Effect of compaction pressure on axial to radial stresses ratio SR at compaction speed 0.5 m/s	76
Figure 15 Change of RDP with ER_0 at compaction speed 0.5 m/s	80
Figure 16 Change of RDP with void volume change at compaction speed 0.5 m/s	80
Figure 17 Change of RDP with RTS at compaction speed 0.5 m/s.....	81
Figure 18 Schematic diagram for MDP and RDP [F_c - Compaction Force, F_e - Ejection Force]	98
Figure 19 Contour plots showing the effect of the lubricant Mg stearate on RDP (values in black on the right) for (a) Pregelatinized starch, (b) Mannitol at compaction speed 2 m/s	103
Figure 20 Contour plots showing the effect of the lubricant PEG 6000 on RDP (values in black on the right) for (a) MCC, (b) Mannitol at compaction speed 2 m/s	107
Figure 21 Plots for different runs comparing the effect on RDP of no lubrication (on the left) versus external lubrication with the lubricant PEG 6000 for (a) MCC, (b) Pregelatinized starch.....	108

Figure 22 Contour plots showing the effect of the binder copovidone on RDP (values in black on the right) for (a) Mannitol, (b) MCC at compaction speed 2 m/s.....	110
Figure 23 Contour plots showing the effect of the binder HPC on (a) F_e , (b) RTS, (values in black on the right) for lactose at compaction speed 2 m/s.....	111
Figure 24 SEM pictures showing the particles for (a) HPC and (b) Copovidone.....	113
Figure 25 Contour plots showing the effect of drug loading on RDP (values in black on the right) for (a) MCC, (b) Lactose at compaction speed 2 m/s.....	115
Figure 26 SEM pictures of the particles of (a) MCC PH101, (b) Parateck M200, and (c) Emcompress.....	142
Figure 27 SEM pictures of the granules of (a) MCC PH101/Paracetamol, (b) Parateck M200, and (c) Sorbolac 400.....	143
Figure 28 Effect of powders with different mean particle size on RDP	145
Figure 29 Effect of powders with different mean particle size on MDP	145
Figure 30 ER_0 of MCC PH102 and Parateck M200	146
Figure 31 Effect of particle size of Parateck M200 granules on RDP at high compression pressure (300MPa) and speed (2 m/s) ($RSE= 0.4$)	147
Figure 32 Effect of particle size of Sorbolac 400 granules on EF at high compression pressure (300MPa) and speed (2 m/s) ($RSE= 3.06$).....	149
Figure 33 Effect of particle size of MCC PH101/ Paracetamol granules on MDP at high compression pressure (300MPa) and speed (2 m/s) ($RSE= 1.13$).....	150
Figure 34 Effect of A_w on RDP for MCC.....	174
Figure 35 Effect of A_w on MDP for MCC	175
Figure 36 Effect of A_w on SR for pregelatinized starch.....	177
Figure 37 Effect of A_w on FCC for MCC	179
Figure 38 Effect of A_w on FCE for mannitol	180
Figure 39 Effect of A_w on TO for pregelatinized starch.....	180
Figure 40 Effect of A_w on EFT for pregelatinized starch.....	182
Figure 41 Effect of A_w on ER_0 for pregelatinized starch.....	183
Figure 42 Effect of A_w on RTS for lactose.....	183
Figure 43 Effect of ejection angle change on FCE for MCC at high speed and A_w (LCP= Low compression pressure; HCP= High compression pressure) ($RSE=0.01$)	186
Figure 44 Contour plots showing the effect of flat (F) and concave (C) punch shapes on RDP for MCC.....	208

Figure 45 Contour plots showing the effect of flat (F) and concave (C) punch shapes on RDP for lactose	209
Figure 46 Contour plots showing the effect of flat (F) and concave (C) punch shapes on MDP for CHPD	209
Figure 47 Contour plots showing the effect of flat (F) and concave (C) punch shapes on SR for pregelatinized starch	210
Figure 48 Contour plots showing the effect of flat (F) and concave (C) punch shapes on FCE for MCC	212
Figure 49 Contour plots showing the effect of flat (F) and concave (C) punch shapes on ER_0 for CHPD	213
Figure 50 Contour plots showing the effect of flat (F) and concave (C) punch shapes on RTS for mannitol	214
Figure 51 Contour plots showing the effect of flat (F) and concave (C) punch shapes on WC for CHPD	215
Figure 52 Contour plots showing the effect of flat (F) and concave (C) punch shapes on porosity for mannitol	216
Figure 53 Sticking and capping of different MA formulations	235
Figure 54 SEM picture for MA particles	235
Figure 55 Contour plots of MDP for (a) Lactose (b) CHPD	238
Figure 56 Contour plots of SR for (a) Lactose (b) CHPD	238
Figure 57 Linear plots for MCC showing (a) RDP (b) EF	239
Figure 58 Linear plots of RTS for (a) MCC (b) Lactose	241
Figure 59 Contour plot of ER_0 for lactose	242
Figure 60 Contour plot of WC for lactose	242

List of Tables

Table 1 Comparison of the equipment used for tableting studies	29
Table 2 Advantages and Disadvantages of strain gauges and piezoelectric transducers.....	32
Table 3 Presster™ standard specifications.....	42
Table 4 True density and mean particle size of the powders.....	66
Table 5 Pentagon factorial design for compaction variables	70
Table 6 Models suggested for different materials showing the compaction variables, compression (C), precompression (P) and compaction speed (S) and their interactions.....	72
Table 7 Classification of the materials regarding their deformation behavior upon compaction.....	73
Table 8 Different levels for compaction parameters in relation to materials' deformation behavior	81
Table 9 Different experimental designs generated by STAVEX® 5.0 to study the impact of lubricant, binder, and drug loading on RDWP	100
Table 10 Median, and mean diameters, span, specific surface area, and true density of the investigated powders.....	102
Table 11 Compressibility slopes of different fillers at different paracetamol loadings (20, 50, 80 % w/w) at low and high compaction speeds (0.5, 2 m/s)	117
Table 12 Pearson correlation between compact volume and MDP.....	118
Table 13 Effect of formulation variables on RDWP and other compaction parameters	118
Table 14 Experimental design generated by STAVEX® 5.0 to study the impact of particle size on radial die-wall pressure and friction tendency	140
Table 15 Median, and mean diameters, span, specific surface area, and true density of the investigated powders.....	141
Table 16 Average water activity (Aw) values of powders before, during, and after compaction.....	166
Table 17 Experimental design generated by STAVEX® 5.0 to study the effect of powder water activity (Aw) and machine's ejection cam angle (EA) on radial die-wall pressure at high/low compression pressures and speeds.....	172
Table 18 True density and DSC parameters of the investigated powders	173
Table 19 Experimental design generated by STAVEX® 5.0 to study the effect of tooling shape on radial die-wall pressure ...	206
Table 20 Median, and mean diameters, span, and true density of the investigated powders	207
Table 21 Comparison between the effect of flat-faced and standard concave punches on compaction parameters	216

Table 22 Experimental design generated by STAVEX [®] 5.0 to study the effect of mefenamic acid (MA) loading on radial die-wall pressure	232
Table 23 Median, and mean diameters, span, and true density of the investigated powders	234

List of Original Publications

This thesis is based on the following publications:

1. **Sameh Abdel-Hamid**, G.Betz. Study of radial die-wall pressure changes during pharmaceutical powder compaction. *Drug Dev Ind Pharm* 2011, 37(4): 387–395.
2. **Sameh Abdel-Hamid**, M. Koziolk, G.Betz. Study of radial die-wall pressure during high speed tableting: effect of formulation variables. *Drug Dev Ind Pharm*. Article in press
3. **Sameh Abdel-Hamid**, F. Alshihabi, G.Betz. Investigating the effect of particle size and shape on high speed tableting through radial die-wall pressure monitoring. *Int J Pharm* 2011, 413: 29-35.
4. **Sameh Abdel-Hamid**, G.Betz. Radial die-wall pressure as a reliable tool for studying the effect of powder water activity on high speed tableting. *Int J Pharm* 2011, 411: 152-161.
5. **Sameh Abdel-Hamid**, G.Betz. Investigating the effect of punch geometry on high speed tableting through radial die-wall pressure monitoring. *Pharm Dev Technol*. Article in press
6. **Sameh Abdel-Hamid**, G.Betz. A novel tool for the prediction of tablet sticking during high speed compaction. *Pharm Dev Technol*. Article in press

Reprints were made with permission from the journals' Publishers.

List of Abbreviations

CHPD	Calcium hydrogen phosphate dihydrate
CF	Calibration factor
DCL	Direct compressible lactose
EF	Ejection force
EFT	Effective fall time
ER ₀	Elastic recovery within the die at zero pressure
F _e	Ejection force
HPC	Hydroxypropylcellulose
LC	Lower compression
LPD	Lower punch displacement
LVDTs	Linear Variable Differential Transformers
MCC	Microcrystalline cellulose
MDP	Maximum die wall pressure
PEG	Polyethylene glycol
RDP	Residual die wall pressure
RDW	Radial die wall
RDWP	Radial die wall pressure
RTS	Radial tensile strength
SDL	Spray dried lactose
SEM	Scanning electron microscopy
SR	Axial to radial stress transmission ratio
TO	Take-off Force

UC	Upper compression
UPD	Upper punch displacement
VC	Change in void fraction
WC	Work of Compaction
μ_c (FCC)	Friction coefficient during compaction
μ_e (FCE)	Friction coefficient during ejection

Summary

Background: The complexity of the compaction process specially with using high-speed tablet presses necessitates the use of robust monitoring tools during the process. The use of an instrumented compaction simulator in the early stage of development has a significant benefit for product development and scaling-up. Up to now, in tableting research rare attention has been paid to the measurement of die-wall pressure. Die-wall instrumentation would be essential to understand the deformation of particles under axial pressure during the compaction cycle. It would be also of great help to investigate particle–die-wall shear stresses or friction, which is the cause of many tableting problems such as capping, lamination, and sticking.

Purpose: To investigate the effect of compaction process variables ((pre) compression pressure, speed, ejection angle, tooling shape), formulation variables (filler, lubricant, binder, drug loading), powder physico-chemical properties (particle size and shape, water activity) on the compaction process through radial die-wall monitoring. Common tableting problems such as capping, lamination, and sticking were also investigated.

Materials and Methods: Using a fully instrumented compaction simulator, the Presster™ guided by mathematical modeling and experimental design. Materials with different compaction behaviors: viscoelastic, plastic, brittle, plastic/brittle.

Results and Discussion: Regarding tablet press parameters, by increasing compaction pressure radial die-wall pressure was increased for all materials (RDP and MDP), while with increasing pre-compaction residual die-wall pressure (RDP) was decreased for plastic materials, whereas by increasing speed maximum die-wall pressure (MDP) was decreased for all materials. Plastic and brittle materials showed increased tendencies for friction because of high radial relaxation. An increasing RDP value during compaction would indicate higher tendency for friction, whereas a high constant value of MDP would provide an evidence for plastic behavior. High compaction force combined with high speed should be avoided to prevent capping. Increasing ejection angle increased friction tendencies and ejection force for powders. Effective Fall Time (EFT) derived from decompression time was a reliable tool for sticking prediction. Moreover, radial die-wall monitoring was a more sensitive tool to detect sticking in comparison to take-off force. Flat shape tooling increased radial die-wall pressure while it was reduced by concave tooling due to more homogeneity in density distribution as well as greater area of contact. However, concave tooling showed higher friction and capping in comparison to flat tooling

due to more radial movement for the powder, which resulted in higher densification at the edges in comparison to flat tooling.

Concerning formulation variables, additives enhancing the elasticity or weakening the bonds such as lubricants or increasing drug loading promoted the occurrence of capping, while additives improving the mechanical strength such as binders reduced capping. The RDP/MDP ratio was not suitable as a sensitive parameter for the evaluation of lubricants, since it was only changed for plastic and/or brittle materials. Also, MDP was a good predictor for axial pressure transmission to the die-wall. External lubrication reduced the die-wall-compact friction without affecting the deformation behavior of the formulation. High RDP values were not always responsible for capping, because MCC exhibited low RDP values and still showed capping, therefore, other parameters such ER_0 and tensile strength should also be considered.

Regarding physico-chemical properties of powders, small / irregular particles acted more plastically at high compression, showed better axial pressure transmission, more porous and stronger compacts, and had higher tendency for friction and sticking than bigger particles. On the other hand, high water activity resulted in a low RDP and friction for all materials, and a high MDP for plastic materials. This was due to the lubricating and plasticizing effects of water, respectively.

Conclusion: Radial die-wall pressure monitoring is recommended as a valuable tool to assess the deformation behavior of materials and detect friction and adhesion at early stages of development and during production as well, which would be of great help to predict common scaling-up tableting problems such as capping, lamination, and sticking.

Theoretical Background

Tablets represent the most popular dosage form in the pharmaceutical market. It is very important to select the most suitable excipient and manufacturing process to develop a formulation. Moreover, understanding of the physicochemical and mechanical properties of pharmaceutical powders and granules is required to compact them successfully to tablets with the desired quality and transferring this technology from an art to a science. There is a continuous need to constrain variability and find new tools to develop traditional manufacturing procedures.

Powder Compaction

Compression is reduction of powder volume while compaction (solid consolidation) is an increase in the mechanical strength [1-3]. Compaction steps [4-6] include: particle rearrangement, fragmentation, and deformation which may be elastic, plastic, brittle, viscoelastic, or plastic/brittle, and finally fusion, **Figure 1**. Elastic is reversible, and plastic, viscoelastic, plastic/brittle are time dependent [7, 8].

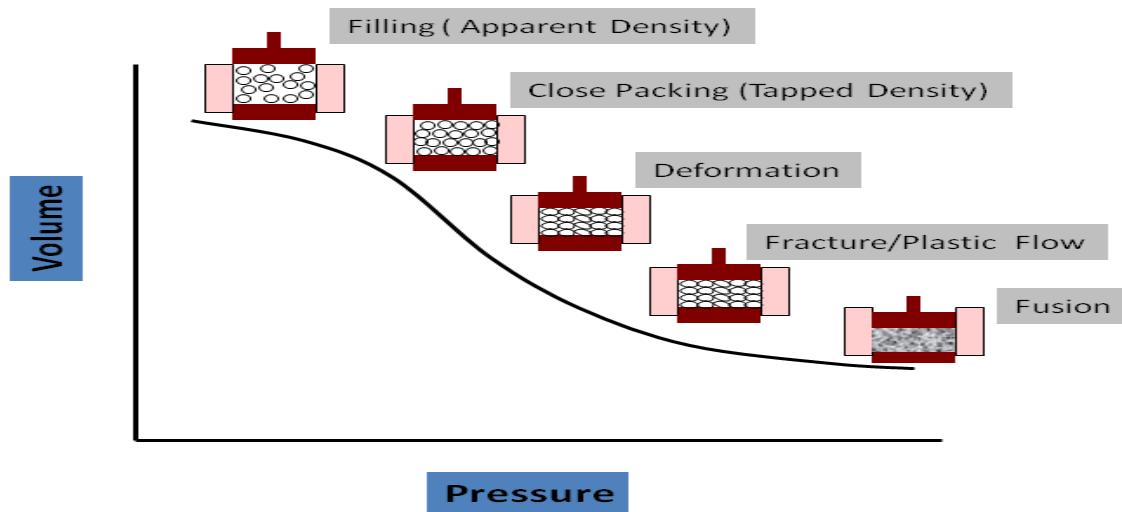


Figure 1 Stages of powder compaction

Assessment of powder compaction behavior includes many parameters: Heckel equation [9, 10], strain rate sensitivity [11], Hiestand tableting indices [12-14], force displacement curves [15, 16], and friction [17]. However, the USP (1999) recommended three factors for presenting the compactability test [18] which are:

- (1) Consolidation factor: area under the breaking force – log applied pressure plot.
- (2) Compressibility factor: area under the average porosity – log applied pressure plot.

- (3) Compaction Rate Sensitivity factor: area between the breaking force – log applied pressure plots for two compaction rates, where the rates differ by a factor of 10.

Types of tablet presses used for tableting studies are either single-station (eccentric), multi-station (rotary), or simulator [19], **Table 1**.

Table 1 Comparison of the equipment used for tableting studies

Feature	Eccentric Press	Rotary Press	Simulator
Mimic production conditions	no	yes	yes
Mimic cycles of many presses	no	no	yes
Require small amount of material	yes	no	yes
Easy to instrument	yes	no	yes
Price	low	high	high
Ease to Set up	yes	no	yes
Used for strain/stress studies	no	no	yes

Tablet Press Instrumentation

Using of instrumented tableting machines in early stages of development is no more an accessory. To have good manufacture productivity for tableting, a thorough scientific understanding of the process could only be done by

instrumentation. Instrumentation turns tablet press into an analytical tool beside its normal function in production [20, 21]. Tablet press instrumentation helps greatly in a quick scaling up from the R&D to production stage which saves a lot of time and money. Instrumentation could be applied to eccentric [22], and rotary presses [23], as well as compaction simulators. Components of an instrumentation or data acquisition system for a tablet press include [24]:

(1) Sensors

(a) Piezoelectric

(b) Strain gauge

(i) Wheatstone Bridge

(ii) Temperature compensation

(iii) Bridge balance

(c) Displacement (LVDTs)

(2) Signal conditioning

(a) Power supply

(b) Differential amplifier

(3) Analog to digital conversion

(a) Resolution

(b) Aliasing filters

(4) Representative tablet press sensors for (pre) compression, ejection and take-off

(5) Calibration (precision, accuracy, and repeatability)

(6) Analysis software

Tablet press sensors typically measure applied force, compaction speed or punch displacement [25]. The sensors used are mainly strain gauges and piezoelectric transducers. They are fitted to the tablet press for force measurement like (pre)compression, ejection, and take-off forces. A strain gauge is a network of wires, through which an electric current is passed, **Figure 2**. Under stress, the wires of the strain gauge deform and hence, its electrical resistance changes. The size of the signal is proportional to the deformation, which in turn is a function of the applied force. Wheatstone bridge is a special arrangement of strain gauges which is composed of two pairs of resistors in a circle to ensure signal balancing. This technique is used to increase the sensitivity of the sensors and to erase the impact of temperature on the signal.

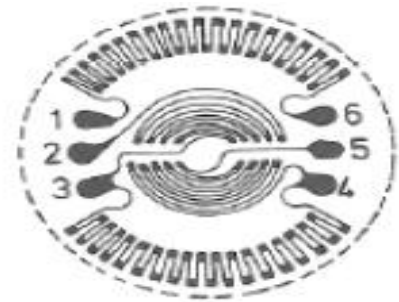


Figure 2 Foil strain gauge with six terminal contacts [26]

Piezoelectric force transducers generally consist of quartz crystals, which accumulate electrical charge when subjected to stress. This charge is proportional to the applied force, but signal drifting occurs due to charge leakage. The most precise results can be obtained if the measurement is done as close as possible to the tip of the punch. Further, calibration affects the results [27]. Comparison between strain gauges and piezoelectric transducers are shown in **Table 2** [7, 24-28].

Table 2 Advantages and Disadvantages of strain gauges and piezoelectric transducers

Strain Gauges	Piezoelectric Transducers
<ul style="list-style-type: none"> - Easy to mount - Narrow measurement range - Space-saving - Static and dynamic measurements possible - Great influence of mounting position - Temperature sensitivity - Hysteresis 	<ul style="list-style-type: none"> - High frequency response - Broad measurement range - High required space - Use limited to dynamic events - Great influence of mounting position - Longer calibration interval - Certain biasing voltage necessary

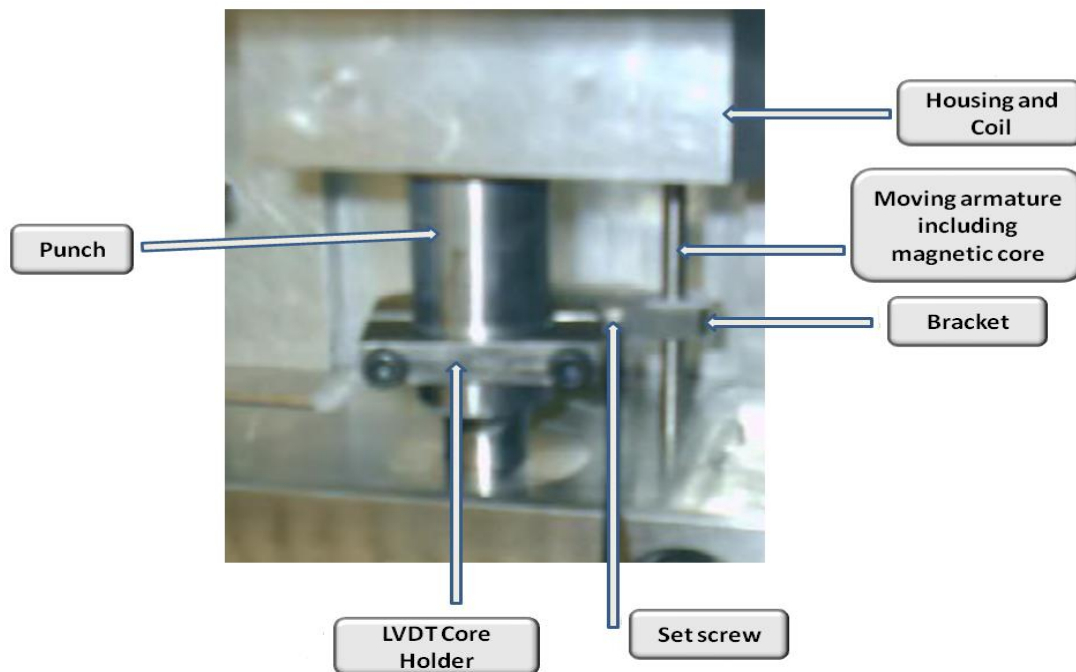


Figure 3 LVDT for punch displacement measurement

For the measurement of punch displacement, linear variable differential transformers (LVDTs) are used, **Figure 3**. The position of a core rod inside a cylinder is measured relative to a predefined zero position. The resulting voltage is proportional to the displacement of the object. LVDTs are also used for in-die thickness measurements. Another type of sensors is the proximity switches which are non-contact electromagnetic pick-up devices that are often used for speed measurements. These sensors are able to sense the presence of nearby objects or metal, because they emit electromagnetic fields and register occurring changes in these fields [25].

Calibration

“Calibration of sensors is performed for comparing transducer outputs at standard test loads to output of a known standard at the same load levels. A calibration graph representing the best fitting line for data is plotted and a calibration factor which is the load value in engineering units that a transducer indicates for each volt of output, after amplifier gain and balance is calculated” [25].

Shunt calibration

“Shunt calibration of a strain gauge based transducer is a procedure for verifying its condition. It is a procedure of transducer testing when a resistor with a known value is connected to one leg of the bridge. The output should correspond to the voltage specified in the calibration certificate. If it does not, something is wrong and the transducer needs to be inspected for possible damage or recalibrated” [29].

Dynamic LVDT calibration (correction of deformation)

“A set of runs can be performed on the simulator using metal tablets of various thicknesses, at different forces and speeds. The resulting gap (punch separation) measurements are then compared with the actual tablet thickness and a correction is calculated following a multivariable regression procedure. If enabled, such correction can drastically reduce the gap measurement error under dynamic

conditions, usually, well below $\pm 30 \mu\text{m}$, to improve Heckel analysis, estimates of elastic recovery, work of compaction, etc.” [29].

Die-wall Instrumentation

Rare attention is paid to die-wall instrumentation because of difficulty in installation and calibration due to non-homogenous pressure distribution relative to tablet position within the die and its thickness [30-32]. To overcome this problem, accurate calibration and complex mathematical corrections were carried out [33-35]. Moreover, many designs like a three layered die and a die with piston inserted through the wall were proposed [36-38]. This variability in the die-wall design and mathematical models used for calibration caused many conflicts in the data reported in literature. Radial die-wall measurement helps in the understanding of the material compaction behavior under pressure and indicates adhesion and friction which are related to common tableting problems such as capping and sticking [39-45]. In-die temperature can be monitored for heat-sensitive materials such as ibuprofen [46, 47]. The Presster™ radial die- wall (RDW) transducer used in this study is a solid die with a cut-out that creates two sensing elements of a uniform section area on the opposite sides of the die opening along its entire height, **Figure 4.** Two pairs of tension-compression strain gauges are positioned in such a way that the tablet compaction on Presster™ always takes place between them. The

upper pair covers the area of upper punch penetration (4 mm from the die's top), the second pair is placed 6 mm lower. The recommended maximum tablet thickness for RDWP measurements is 4.5 mm. The voltage output of the transducer is proportional to the radial force transmitted to the die wall. During calibration, this force is calculated as a product of the applied axial pressure by the area of cylindrical portion of the tablet. Calibration factor CF is calculated as RDW force per voltage output. During tablet compaction, the measured voltage output is multiplied by CF and the product RDW force value is referred to the area of cylindrical portion of the tablet to obtain the RDWP value. The transducer is calibrated with a polyurethane 4.5 mm height insert and B-type 10 mm round flat face punch.

Figure 4 Presster™ die-wall instrumentation



Compaction simulators

All compaction simulators have the same main three units; a load frame, a hydraulic unit, and a data acquisition system [48]. Usually simulators accept F-tooling but nowadays standard European and IPT B- and D- tooling are also possible. Small amounts of

material are required and similar dwell times of rotary presses are attainable.

Compaction simulators are ideally suited for raw material evaluation to:

- (1) Study the basic compaction mechanisms.
- (2) Evaluate and optimize excipients such as lubricants and binders with respect to the desired tablet properties such as disintegration and dissolution.
- (3) Study process and scale up variables like (pre) compression pressure and speed.
- (4) Compare production presses with respect to ability to handle different compounds.
- (5) Study physicochemical properties effect such as particle size, moisture content on formulations with respect to the desired tablet properties.
- (6) Practically eliminate or minimize the need for scale-up in the formulation development process and predicting common tableting problems such as capping, lamination, and sticking.

Factors that could be simulated to be the same like production presses are: tooling, upper and lower (pre) compression rolls, applied force, punch velocity and speed, consolidation, dwell, relaxation, and contact times. Factors that are hard to be

simulated until now include: feeding process, turret movement, and building up of turret temperature due to long term running at high speed.

In this study the PressterTM developed by Metropolitan Computing Corporation Inc., NJ, US, **Figures 5-7** was used. It is a mechanical compaction replicator where it combines the attributes of a high-speed single-station press and a compaction simulator which allows mimicking production presses without any application of hydraulic control and hence, works under conditions close to production [49, 50]. Standard specifications of the PressterTM are shown in **Table 3**. Raw data could be displayed in a graphical representation after specifying batch and tablet numbers, **Figure 8** and **9**. Summary results could be also displayed in spreadsheets, **Figure 10**. Resolution for force and displacement measurements on Presster are interpreted as the accuracy of signal voltage measurements (in Volts) multiplied by respective calibration factors of the transducers (in kN/V or mm/V). Absolute Accuracy of the data acquisition board installed on the Presster is +/- 0.0015% of Full Scale value which is +/-10 V. Calibration factors were 5.81 kN/V for upper compression; 5.61 kN/V for lower compression; 1.38 mm/V for upper punch displacement; -1.35 mm/V for lower punch displacement. The sampling rate was 1 kHz.

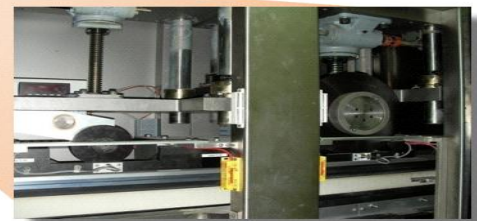
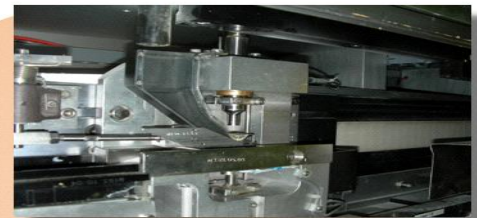
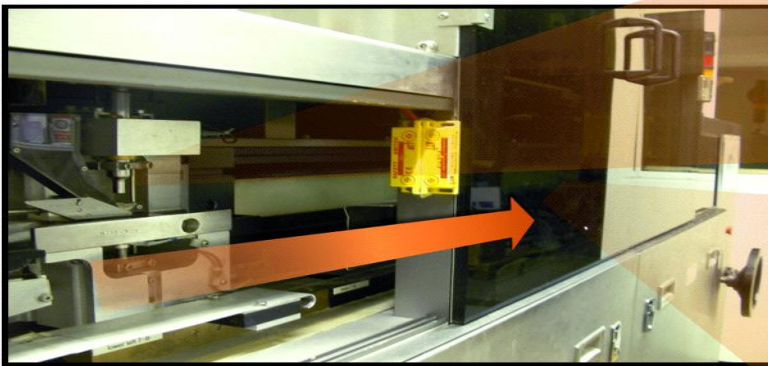


Figure 5 PressterTM linear compaction replicator

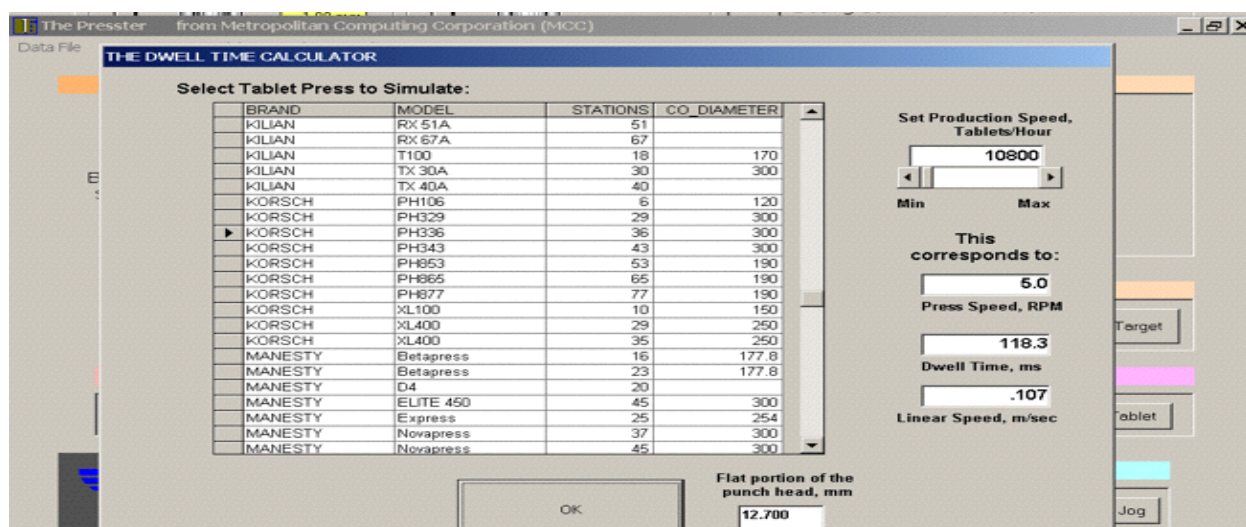
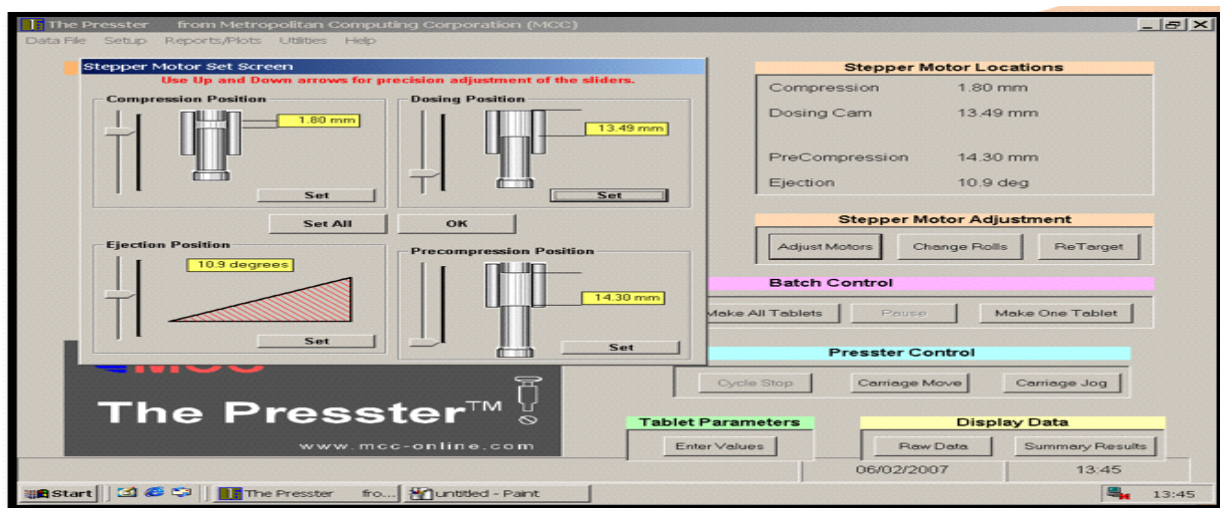
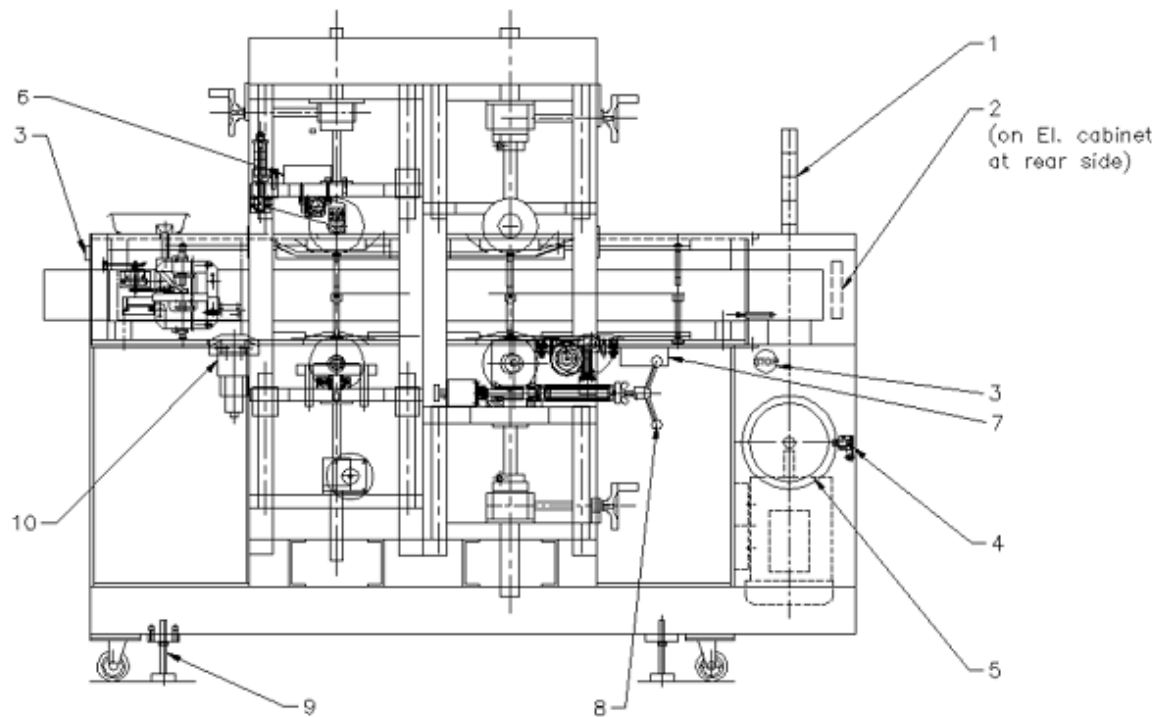


Figure 6 The Presster™ main screen, stepper motor adjustment, dwell time calculator, and tooling selection



1. Signal lamp Indicator
2. Main Power Switch
3. Emergency Stop Buttons
4. Hand Wheel Restraint
5. Main Hand Wheel
6. Precompression Overload Meter
7. Compression Overload Meter
8. Overload Protection Lever
9. Leveling Pads
10. Dosing Mechanism

Figure 7 Schematic diagram of the Presster™ (Model 104) [29]

Table 3 Presster™ standard specifications

Maximum compression force	50 kN
Maximum precompression force	10 kN
Maximum depth of fill	17.4 mm
Maximum tablet thickness	8 mm
Number of stations	1 station
Minimum punch velocity (in horizontal plane)	0.055 m/s
Maximum punch velocity (in horizontal plane)	2.2 m/s
Minimum dwell time	4.4 ms
Maximum dwell time	230 ms
Die feeding	Manual or force feed shoe
Maximum output	4 tablets/min
Motor specifications	1800 rpm 7.5 HP

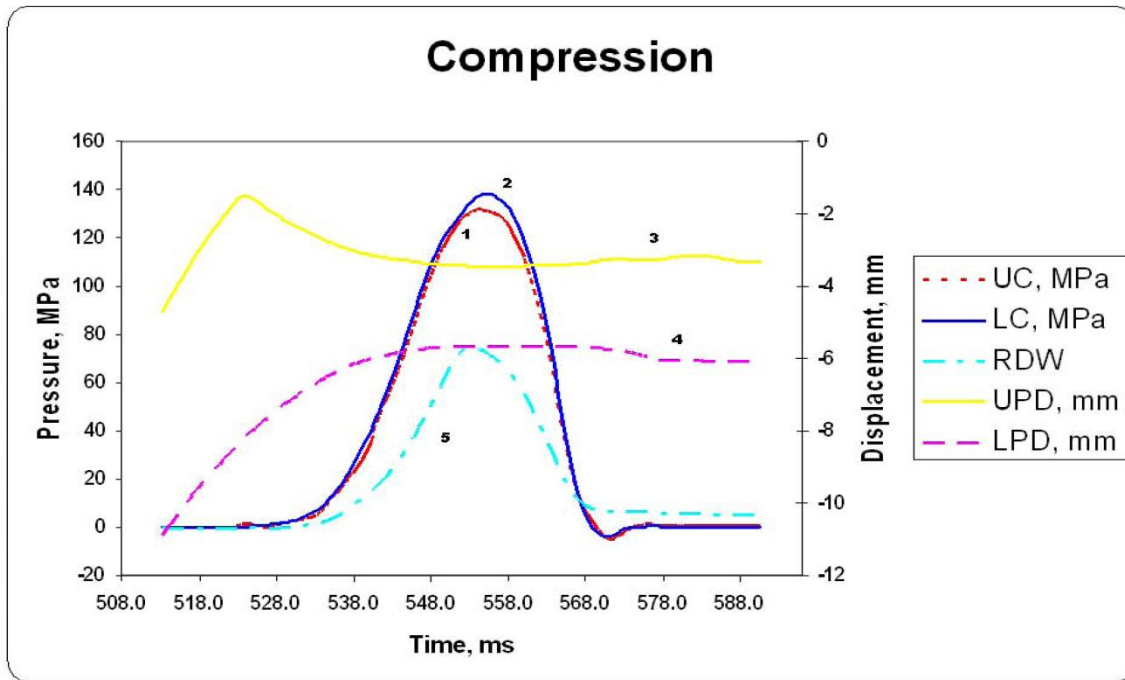


Figure 8 Compression waveform of the Presster™ showing 1.Upper and 2.Lower compression (UC/LC), 3.Upper and 4.Lower punch displacement (UPD/LPD), and 5.Radial die-wall pressure (RDWP) curves

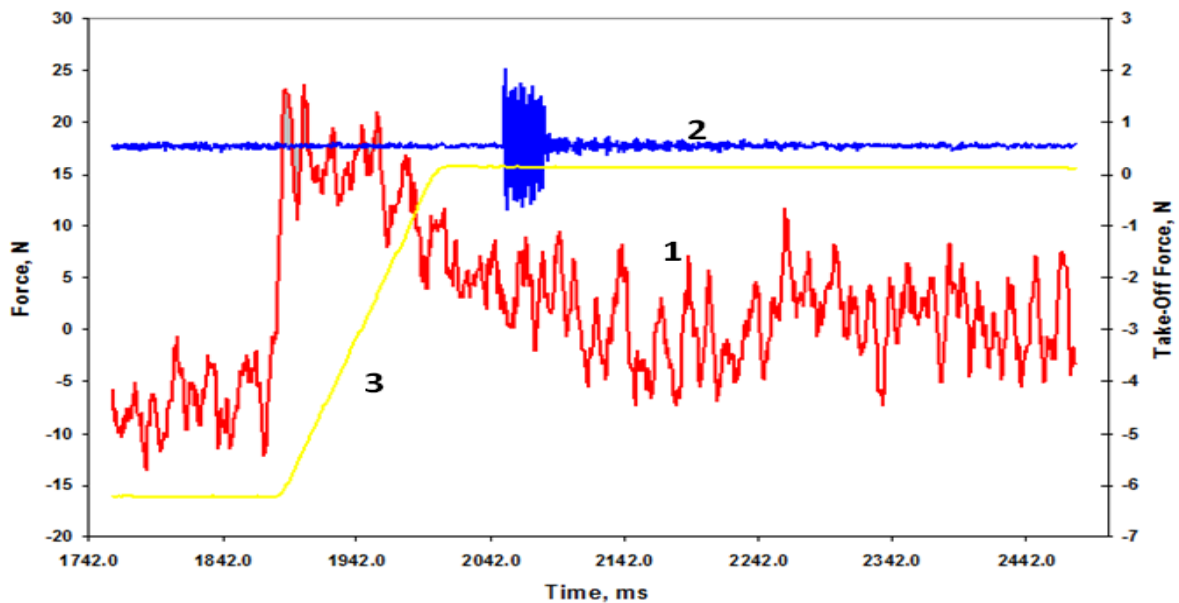


Figure 9 Plots of the Presster™ software showing 1.Ejection force, 2.Take-off force, and 3.Lower punch displacement

Batch No.	Tablet No.	Press Brand	Press Model	Desired Press Speed (TPH)	Desired Dwell Time (ms)	Achieved Dwell Time (ms)	Effective Dwell Time (ms)	Upper Pre-compression Peak (kN)	Lower Pre-compression Peak (kN)	Upper Compression Peak (kN)	Lower Compression Peak (kN)	Maximum Upper Punch Displacement (mm)	Maximum Lower Punch Displacement (mm)	Peak Ejection (N)	Peak Take-Off (N)	Peak Radial Die Wall Pressure (MPa)	Tablet Weight (mg)	Tablet Thickness (mm)
Batch Name: trial	1	KORSCH	PH336	50,300	19.1	18.8	17.1	0.0	0.0	4.1	4.6	3.490	6.220	218.9	1.0100	23.9800		
Batch Name: 1	1	KORSCH	PH336	50,300	19.1	18.8	17.9	0.0	0.0	4.2	4.7	3.490	6.220	223.5	1.2500	25.2000		
	2	KORSCH	PH336	50,300	19.1	18.8	17.9	0.0	0.0	4.0	4.5	3.490	6.230	215.6	1.0100	24.0500		
	3	KORSCH	PH336	50,300	19.1	18.8	17.1	0.0	0.0	4.1	4.7	3.500	6.230	217.8	1.5400	24.8300		
	4	KORSCH	PH336	50,300	19.1	18.8	17.9	0.0	0.0	4.0	4.4	3.490	6.230	212.3	1.5300	24.4800		
	5	KORSCH	PH336	50,300	19.1	18.8	17.9	0.0	0.0	4.3	4.9	3.490	6.230	224.4	2.5300	26.2200		
	6	KORSCH	PH336	50,300	19.1	18.9	17.9	0.0	0.0	4.1	4.7	3.500	6.240	213.8	1.5600	25.3700		
Batch Name: 2	1	KORSCH	PH336	201,200	4.8	4.8	4.1	0.0	0.0	4.1	4.5	3.500	6.230	391.0	1.2100	17.4700		
	2	KORSCH	PH336	201,200	4.8	4.8	4.1	0.0	0.0	4.3	4.9	3.510	6.240	383.1	1.3500	17.7900		
	3	KORSCH	PH336	201,200	4.8	4.8	4.3	0.0	0.0	4.1	4.6	3.510	6.240	310.9	1.2000	16.0500		
	4	KORSCH	PH336	201,200	4.8	4.8	4.3	0.0	0.0	3.9	4.3	3.510	6.240	376.1	1.2500	15.1800		
	5	KORSCH	PH336	201,200	4.8	4.8	4.3	0.0	0.0	4.2	4.8	3.520	6.240	394.7	1.6800	16.7900		
	6	KORSCH	PH336	201,200	4.8	4.8	4.1	0.0	0.0	4.2	4.8	3.510	6.240	428.9	1.1900	17.6900		
Batch Name: 3	1	KORSCH	PH336	100,600	9.5	9.6	8.5	0.0	0.0	4.5	4.9	3.520	6.120	293.0	0.8100	23.3900		
	2	KORSCH	PH336	100,600	9.5	9.6	8.5	0.0	0.0	4.0	4.4	3.530	6.150	259.7	0.7400	18.0700		
	3	KORSCH	PH336	100,600	9.5	9.6	8.5	0.0	0.0	4.0	4.5	3.510	6.140	255.7	0.7700	17.2000		
	4	KORSCH	PH336	100,600	9.5	9.6	8.1	0.0	0.0	3.8	4.1	3.510	6.140	236.8	0.6300	17.2800		
	5	KORSCH	PH336	100,600	9.5	9.6	8.5	0.0	0.0	3.9	4.2	3.510	6.140	235.7	0.6300	15.1300		
	6	KORSCH	PH336	100,600	9.5	9.6	8.1	0.0	0.0	4.0	4.2	3.530	6.140	236.5	0.5900	17.5000		
	7	KORSCH	PH336	100,600	9.5	9.6	9.0	0.0	0.0	4.1	4.5	3.510	6.130	243.1	0.5700	17.6900		
Batch Name: 4	1	KORSCH	PH336	100,600	9.5	9.6	9.0	0.0	0.0	4.2	4.7	3.510	6.320	247.4	0.8400	22.2800		
	2	KORSCH	PH336	100,600	9.5	9.6	8.1	0.0	0.0	4.0	4.4	3.520	6.320	231.6	0.6700	20.9600		
	3	KORSCH	PH336	100,600	9.5	9.7	9.4	0.0	0.0	4.0	4.4	3.510	6.310	246.3	0.8200	19.5000		

Figure 10 Summary results spreadsheet of the Presster™ software

For the users of hydraulic simulators, the need for precise separate measurements of upper and lower punch displacement is absolutely vital because of the feedback to the hydraulic actuators under the position control operation. Unlike Presster™, a hydraulic simulator requires the correction for machine deformation in order to operate [51]. In Presster™, both LVDTs are installed into the same carrier as the die. As the carrier does not support the compression force, the distances among each LVDT and die do not change with the force. The LVDT cores are fastened to the punches in close proximity to the punch tips thus minimizing the influence of the applied force on the measurements. Only punch tips deformation might be taken in

consideration. The calculated combined elasticity of 10 mm round punch tips used with the instrumented die is 0.003 mm/kN (0.002 for the lower punch and 0.001 for the upper one). In many cases, the involved error can be considered negligible. However, the PressterTM has some limitations [52, 53] which are powder loss after filling due to high speed, the lack of simulation for the feeding process, the lack of simulation for the heat effect on tablets due to long term running at high speed, and machine vibrations. Moreover, the distance between pre and compression rolls is not adjustable. However, during this work new cams were installed to close the die by the upper punch before starting of the compaction cycle to avoid the loss of powder at high speeds. Secondly, a Butterworth filter was added to the machine to eliminate noise from machine vibrations.

Compaction scaling-up

Scaling-up of compression causes many tableting problems due to increased speed.

These problems include:

1. Capping and Lamination: tendency for capping and lamination is usually increasing with tableting speed, (pre) compression force, punch penetration depth, and tablet thickness [54-62].

2. Picking and Sticking: formulation factors, process and tooling dependent [63-67].
3. Chipping: formulation dependent, take-off misalignment, and low moisture content [68, 69].

“Unlike other unit operations in solid dosage development and production, scale-up of compression on a tablet press takes place in the same volume (die) using the same process geometry (tooling) and dynamic factors (compression force). The only practical differences between development and production presses are the compression speed and die table” [70].

During scale-up or transferring powders from one tablet press to another different press, tablets may change with respect to weight, hardness, friability, disintegration, dissolution, and other properties. This is due to change in porosity attributes, such as pore size and surface area that are dependent on compression force and speed.

“Contact time refers to the time when both punches are moving having their tips in contact with the material that is being compacted, and their heads are in contact with the pressure rolls. It is divided to three phases: consolidation, dwell, and decompression times [71]. Consolidation or solidification time is the time when punches are changing their vertical position in reference to the rolls decreasing the

distance between their tips. Dwell time is the time when the punches are not changing their vertical position in reference to the rolls. Decompression time is the time when the punches are changing their vertical position in reference to the rolls, increasing the distance between their tips before losing a contact with the rolls. Another term is the compression time which is the consolidation and dwell times". For scaling up a new formulation, it is necessary to evaluate the minimum consolidation time (maximum compaction speed) at which tablets of a reasonable quality can be produced. In comparison to contact time, dwell time depends on punch geometry rather than roll diameter. So in order to scale up properly, matching compression force and tooling is not enough but you have to match contact, consolidation, and dwell times.

References

- [1] Yang L, Venkatesh G, Fassihi R. Characterization of compressibility and compactability of poly (ethylene oxide) polymers for modified release application by compaction simulator. *J Pharm Sci* 1996; 85:1085-1090.
- [2] Hardy IJ, Cook WG, Melia CD. Compression and compaction properties of plasticized high molecular weight hydroxypropylmethylcellulose (HPMC) as a hydrophilic matrix carrier. *Int J Pharm* 2006; 311: 26-32.
- [3] Leuenberger H. The compressibility and compactibility of powder systems. *Int J Pharm* 1982; 12: 41-55.
- [4] Rowe RC, Roberts RJ. The mechanical properties of powders. *Adv Pharm Sci*; Academic Press, 1995.
- [5] Bogda MJ. Tablet Compression: Machine Theory, Design and Process Troubleshooting. In: *Encyclopedia of Pharmaceutical Technology*, Swarbrick J.,ed., Informa Healthcare, New York; 2007: 3612-3630.
- [6] Armstrong NA. Time-dependent factors involved in powder compression and tablet manufacture. *Int J Pharm* 1989; 49: 1-13.

- [7] Ritschel WA, Bauer-Brandl A. Die Tablette : Handbuch der Entwicklung, Herstellung und Qualitätssicherung. 2. ed., vollständig überarbeitete und erw. Aufl. ed. Pharmazeutische Betrieb Bd. 7, Aulendorf: ECV - Editio Cantor Verlag. Xvi; 2002: 647.
- [8] Jain S. Mechanical properties of powders for compaction and tableting: an overview. Pharm Sci Technol Today 1999; 2: 20-31.
- [9] Heckel RW. Density-pressure relationships in powder compaction. Trans Metall Soc AIME, 1961; 221: 671-675.
- [10] Heckel RW. An analysis of powder compaction phenomena. Trans Metall Soc AIME 1961; 221: 1001-1008.
- [11] Roberts RJ, Rowe RC. The effect of punch velocity on the compaction of a variety of materials. J Pharm Pharmacol 1985; 37: 377-384.
- [12] Hiestand EN, Smith DP. Indices of tableting performance. Powder Technol 1984; 38: 145-149.
- [13] Hiestand EN. Rationale for and the measurement of tableting indices, In: Pharmaceutical powder compaction technology, Alderborn G, Nyström C, Marcel Dekker: New York, 1996; 219-244.
- [14] Davar N, Shah R. A critical comparison of Hiestand's tableting indices and traditional measures of compactibility to predict tableting behavior. Pharm Res 1995; 12:168.

- [15] De Blaey CJ, Polderman J. Compression of pharmaceuticals. I. The quantitative interpretation of force-displacement curves. *Pharm Weekbl* 1970; 105: 241-250.
- [16] Ragnarsson G, Sjogren J. Force-displacement measurements in tableting. *J Pharm Pharmacol* 1985; 37: 145-150.
- [17] Holzer AW, Sjogren J. Friction coefficients of tablet masses. *Int J Pharm* 1981; 7: 269-277.
- [18] Marshall K. Report and Recommendation of the USP Advisory Panel on Physical Test Methods: Compactability Test. *Pharm Forum*, May-June: 1999; 8293-8297.
- [19] Çelik M, Marshall K. Use of compaction simulator system in tableting research I. Introduction to and initial experiments with the system. *Drug Dev Ind Pharm* 1989; 15: 759-800.
- [20] Belda PM, Mielck JB. The tableting machine as an analytical instrument: qualification of the measurement devices for punch forces and validation of the calibration procedures. *Eur J Pharm Biopharm* 1998; 46: 381-395.
- [21] Belda PM, Mielck JB. The tableting machine as an analytical instrument: consequences of uncertainties in punch force and punch separation data on some parameters describing the course of the tableting process. *Eur J Pharm Biopharm* 1999; 48: 157-170.

- [22] Barra J, Doelker E. Instrumentation of an eccentric tablet press. In: Data acquisition and measurement techniques, Muñoz-Ruiz A, Vromans H., eds., Interpharm press Inc. US; 1998: 189- 238.
- [23] Ilkka J. Instrumentation of rotary tablet machines by a portable measuring system. In: Data acquisition and measurement techniques, Muñoz-Ruiz A, Vromans H., eds., Interpharm press Inc. US; 1998: 239-258.
- [24] Bubb GE. Tablet press instrumentation in the research and development environment. In: Pharmaceutical dosage forms: Tablets, vol. 3: Manufacture and process control, 3rd ed. , Augsburger LL, Hoag SW, eds. , Informa Healthcare, New York ; 2008: 49-83.
- [25] Levin M. Tablet Press Instrumentation. In: Encyclopedia of Pharmaceutical Technology, Swarbrick J, Informa Healthcare: New York; 2007: 3684-3706.
- [26] Bauer KH, Frömmering KH, Führer C, Egermann H, Graf H, Leuenberger H. Lehrbuch der Pharmazeutischen Technologie, 6 ed. Auflage Stuttgart: Wissenschaftliche Verlagsgesellschaft, 1999, 329.
- [27] Leitritz M, Krumme M, Schmidt PC. Effects of applied load and particle size on the plastoelasticity and tablet strength of some directly compressible powders. Pharm Ind 1995; 57: 1033-1038.

- [28] Schlack H. Kompressibilität und Kompaktibilität von Hilfsstoffen bei der Tablettierung, PhD Thesis, Fakultät für Chemie und Pharmazie, Albert-Ludwigs Universität Freiburg, Freiburg, Germany, 2001.
- [29] PressterTM user manual 3.6.4. Metropolitan Computing Corporation, East Hanover NJ, US, 2009.
- [30] Ridgway K. The use of photoelastic techniques in the measurement of die-wall stress in tableting. *J Pharm Pharmacol* 1966; 18:176S-181S.
- [31] Hoag S, Renuka N, Muller F. Force –Transducer-Design optimization for the measurement of die-wall stress in a compaction simulator. *Pharm Pharmacol Commun* 2000; 6: 293-298.
- [32] Doelker E, Massuelle D. Benefits of die-wall instrumentation for research and development in tableting. *Eur J Pharm Biopharm* 2004; 58: 427-444.
- [33] Cocolas HG, Lordi NG. Axial to radial pressure transmission of tablet excipients using a novel instrumented die. *Drug Dev Ind Pharm* 1993; 19: 2473-2497.
- [34] Hölzer AW, Sjögren J. Instrumentation and calibration of a single punch press for measuring the radial force during tableting. *Int J Pharm* 1979; 3: 221-230.
- [35] Huckle PD, Summers MP. The use of strain gauges for radial stress measurement during tableting. *J Pharm Pharmacol* 1985; 37: 722-725.

- [36] Rippie EG, Danielson DW. Viscoelastic stress/strain behavior of pharmaceutical tablets: analysis during unloading and post-compression periods. *J Pharm Sci* 1981; 70: 476-482.
- [37] Yeh C, Altaf SA, Hoag SW. Theory of force transducer design optimization for die wall stress measurement during tablet compaction: optimization and validation of split-web die using finite element analysis. *Pharm Res* 1997; 14: 1161-1170.
- [38] Millet J, Paris J, Duchene D, Puisieux F. Etude de comprime's. XII. Mise au point d'un nouvel équipement pour la mesure des forces au niveau des différents organes d'une machine à comprimer alternative. *Pharm Acta Helv* 1975; 50: 109-115.
- [39] Walter JT, Augsburger LA. Computerized force-displacement instrumentation system for a rotary Press. *Pharm Tech* 1986; 9: 26-43.
- [40] Nelson E. The physics of tablet compression VIII: Some preliminary measurements of die wall pressure during tablet compression. *J Am Pharm Assoc* 1955; 44: 494-497.
- [41] Long WM. Radial pressures in powder compaction. *Powder Met* 1960; 6: 73-86.

- [42] Windheuser JJ, Misra J, Eriksen SP, Higuchi T. The physics of tablet compression XIII. Development of die wall pressure during compression of various materials. *J Pharm Sci* 1963; 52: 767-772.
- [43] Carless JE, Leigh S. Compression characteristics of powders: Radial die wall pressure transmission and density changes. *J Pharm Pharmacol* 1974; 26: 289-297.
- [44] Carstensen JT, Toure P. Correlation between hysteresis loop areas of lower punch and of die pressures versus upper punch pressures. *Drug Dev Ind Pharm* 1981; 7: 645-648.
- [45] Schrank-Junghani H, Bier HP, Sucker H. The Measurement of die wall forces to determine the minimum concentration of lubricant needed for tablet formulations. *Acta Pharm Technol* 1984; 30:224-234.
- [46] Nurnberg E, Hopp A. Temperature measurement during tableting. *Pharm Technol* 1981; 9: 81-101.
- [47] Travers DN, Merriman MPH. Temperature changes occurring during the compression and the recompression of solids. *J Pharm Pharmacol* 1970; 22S: 11S-16S.
- [48] Bourland ME, Mullarney MP. Compaction Simulation, In: *Pharmaceutical dosage forms: Tablets Vol.1*, Augsburger LL, Hoag SW, eds., Informa Healthcare US: New York; 2008:519-554.

- [49] Levin M, Tsygan L, Dukler S. Tablet Press Apparatus, U.S. Patent, eds., Metropolitan Computing Corporation, East Hanover NJ, US, 2000.
- [50] Picker KM. The 3-D Model: Comparison of parameters obtained from and by simulating different tableting machines. AAPS PharmSciTech 2003; 4 (3): E35, 1-7.
- [51] Lloyd J, York P, Cook GD. Punch elasticity compensation in the calibration of displacement measurements on a compaction simulator. J Pharm Pharmacol 1991; 43:80.
- [52] Guntermann A. Untersuchung der Tablettiersimulation mit dem PressterTM in Abhängigkeit von der Formulierung, Chargengrösse und der Tablettenpresse, PhD Dissertation, Philosophisch-Naturwissenschaftliche Fakultät der Universität Basel, Basel, Switzerland, 2008.
- [53] Neuhaus T. Investigation and Optimisation of the Presster – A Linear Compaction Simulator for Rotary Tablet Presses, PhD Dissertation, Mathematisch-Naturwissenschaftliche Fakultät, University of Bonn, Bonn, Germany, 2007.
- [54] Van der voort maarschalk K, Zuurman K, Vromans H, Bolhuis GK, Lerk CF. Stress relaxation of compacts produced from viscoelastic materials. Int J Pharm 1997; 151: 27-34.

- [55] Bozic DZ, Dreu R, Vrecer F. Influence of dry granulation on compactability and capping tendency of macrolide antibiotic formulation. *Int J Pharm* 2008; 357:44-54.
- [56] Garr JSM, Rubinstein MH. An investigation into the capping of paracetamol at increasing speeds of compression. *Int J Pharm* 1991; 72: 117-122.
- [57] Ruegger CE, Çelik M. The effect of compression and decompression speed on the mechanical strength of compacts. *Pharm Dev Technol* 2000; 5: 485-494.
- [58] Mann C, Roberts RJ, Rowe RC, Hunter BM, Rees JE. The effect of high speed of compression at sub-atmospheric pressures on the capping tendency of pharmaceutical tablets. *J Pharm Pharmacol* 1983; 35: 44.
- [59] Hoblitzell JR, Rhodes CT. Determination of a relationship between force-displacement and force-time compression curves. *Drug Dev Ind Pharm* 1990; 16: 201-229.
- [60] Von Schmidt PC, Tenter U. Displacement measurements of rotary presses. *Pharm Ind* 1985; 47: 426-430.
- [61] Ritter A, Sucker HB. Studies of variables that affect tablet capping. *Pharm Technol* 1980; 4:56-65.

- [62] Parrot EL. Compression. In: Pharmaceutical Dosage Forms: Tablets, vol. 2, 2nd ed., Lieberman HA, Lachman L, Schwartz JB, eds., Marcel Dekker, New York; 1990: 201-243.
- [63] Mitrevej A, Augsburger LL. Adhesion of tablets in a rotary tablet press I. Instrumentation and preliminary study of variables affecting adhesion. *Drug Dev Ind Pharm* 1980; 6: 331-377.
- [64] Roberts M, Ford JL, MacLeod GS, Fell JT, Smith GW, Rowe PH, Dyas AM. Effect of lubricant type and concentration on the punch tip adherence of model ibuprofen formulations. *J Pharm Pharmacol* 2004; 56: 299-305.
- [65] Lam KK, Newton JM. Investigation of applied compression on the adhesion of powders to a substrate surface. *Powder Technol* 1991; 65:167-175.
- [66] Lam KK, Newton JM. Influence of particle size on the adhesion behavior of powders, after application of an initial press-on force. *Powder Technol* 1992; 73:117-125.
- [67] Lam KK, Newton JM. Effect of temperature on particle solid adhesion to a substrate surface. *Powder Technol* 1992; 73:267-274.
- [68] Zografi G, Kontny MJ. The interactions of water with cellulose and starch-derived pharmaceutical excipients. *Pharm Res* 1986; 3: 187-194.

- [69] Mitrevej KT, Augsburger LL. Adhesion of tablets in a rotary tablet press II. Effects of blending time, running time, and lubricant concentration. *Drug Dev Ind Pharm* 1982; 8: 237-282.
- [70] Muzzio FJ et al. A forward-looking approach to process scale-up for solid dose manufacturing. In: *Pharmaceutical dosage forms: Tablets*, vol.3: *Manufacture and process control*, 3rd ed. , Augsburger LL, Hoag SW, eds. , Informa Healthcare, New York ; 2008: 119-152.
- [71] Tsygan L, Murphy S, Levin M. New dimensionless performance factors of rotary tablet presses for scale-up of time-dependent formulations. Baltimore: Poster, AAPS General Meeting, 2004.

Aims of the Thesis

The overall aim of this thesis was to investigate pharmaceutical powder compaction at high speed using die-wall instrumentation to gain deep understanding of the process.

The specific aims of this thesis were to:

1. Study the effect of tablet press variables: (pre) compression pressures, speed, ejection angle, and tooling geometry on compaction.
2. Study the effect of common formulation variables: lubricant, binder, and drug loading on compaction.
3. Study the effect of some powder physico-chemical properties: particle size, shape, and water activity on compaction.
4. Investigate common tableting problems such as capping and sticking.

Chapter 1: Study of radial die-wall pressure changes during pharmaceutical powder compaction

Abstract

Context: In tablet manufacturing, less attention is paid to the measurement of die-wall pressure than to force-displacement diagrams. **Objective:** Therefore, the aim of this chapter was to investigate radial stress change during pharmaceutical compaction. **Materials and Methods:** The PressterTM, a tablet press replicator was used to characterize compaction behavior of microcrystalline cellulose MCC (viscoelastic), calcium hydrogen phosphate dihydrate CHPD (brittle), direct compressible mannitol (plastic), pregelatinized starch (plastic/elastic) and spray dried lactose (plastic/brittle) by measuring radial die-wall pressure; therefore powders were compacted at different (pre) compaction pressures as well as different speeds. Residual die-wall pressure (RDP) and maximum die-wall pressure (MDP) were measured. Various tablet physical properties were correlated to radial die wall pressure. **Results and Discussion:** With increasing compaction pressure RDP and MDP ($p < 0.0001$) increased for all materials, with increasing pre-compaction, RDP decreased for plastic materials ($p < 0.05$) while with increasing speed MDP decreased for all materials, ($p < 0.05$). During decompression, MCC

¹ "Reprinted from Drug Dev Ind Pharm, Vol.37 /No.4, S. Abdel-Hamid and G.Betz, Study of radial die-wall pressure changes during pharmaceutical powder compaction, Pages 387-395, Copyright (2011), with permission from Informa Healthcare"

and pregelatinized starch showed higher axial relaxation, whereas mannitol and lactose showed higher radial relaxation, CHPD showed high axial and radial relaxations. Plastic and brittle materials showed increased tendencies for friction due to high radial relaxation. **Conclusion:** Die-wall monitoring is suggested as a valuable tool for characterizing compaction behavior of materials and detecting friction phenomena in the early stage of development.

Keywords: capping, compaction simulation, die-wall instrumentation, friction, (pre) compaction pressure, radial die-wall pressure, speed

Introduction

Understanding the behavior of particles during each stage of powder compaction is very important. Parameters used to assess the compaction behavior of powders include Heckel analysis [1], stress relaxation [2], and elastic recovery [3]. Heckel equation [4, 5] has been the most frequently used method to characterize powder compaction behavior. However, this equation has some drawbacks like the curvature at low pressures due to particle rearrangement and the exponential curvature at high pressures due to elastic deformation as well as high error probability at relative density higher than 0.95 [6]. Powder behavior under very low compaction pressures was described by a modified Heckel equation [7], which investigates the conversion of particles into a solid compact. However, most of these approaches do not consider the radial stress transmission and powder-die wall friction where the latter is mainly responsible for density in-homogeneity within the compact [8-11]. This can lead to a non-uniform stress distribution which may result in problems like capping and lamination on decompression [12]. Radial versus axial pressure cycles introduced by Long, 1960 [13], can give an idea about the different deformation behaviors of materials such as Mohr body, brittle fracture, plastic deformation, and a perfect elastic body [14-17]. However, it is rare in reality to find such cycles typically as most powders are anisotropic and non homogeneous in density during compaction [18].

The complexity of compaction process specially with using high-speed tablet presses necessitates the use of robust monitoring tools during the process. The use of an instrumented compaction simulator in the early stage of development has a significant benefit for product development process.

The Presster™ is a linear mechanical replicator for rotary tablet machines designed by Metropolitan Computing Corporation to match compression force and dwell time as well as to mimic the punch displacement profile of any press. It is a high-speed, single-station, tablet press simulator with standard tooling (IPT B, D-type). It is also a powerhouse computer for compressibility profiles, Heckel and Picker plots, lubricant studies, and others. The Presster™ instrumentation includes Linear Variable Differential Transformers (LVDTs) for upper and lower punch displacement as well as strain gauges for (pre) compression, ejection, and take-off forces, and radial die-wall pressure. The Presster™ radial die-wall (RDW) transducer is a solid die with a cut-out that creates two sensing elements of a uniform section area on the opposite sides of the die opening along its entire height where the tablet compaction always takes place between them. The voltage output of the transducer is proportional to the radial force transmitted to the die wall.

The recent quality-by-design (Q-b-D) initiative by the Food and Drug Administration (FDA) stresses the need for development of process simulation

tools to identify optimal and efficient processes that can be easily scaled up. Up to now, in tablet production little attention has been paid to the measurement of die-wall pressure. Die-wall instrumentation [19-21] would be essential to understand the deformation of particles under axial pressure during the compaction cycle. It would be also of great help to investigate particle-die wall shear stresses or friction, which is the cause of many tableting problems such as capping, lamination, tooling wear, and sticking [17]. RDP was reported as one of the key factors for capping, like elastic recovery during decompression [22, 23].

The aim of this chapter was to use RDWP as a tool for characterizing the compaction behavior of pharmaceutical powders as well as to predict capping tendency during compaction. Further, to correlate various physical tablet properties such as tensile strength and elastic recovery to RDWP.

Materials and Methods

Materials

Microcrystalline cellulose MCC (Avicel[®] PH102, FMC Corporation, Delaware, US), directly compressible mannitol (Pardeck[®] M200, Merck KGaA, Darmstadt, Germany), calcium hydrogen phosphate dihydrate CHPD (Emcompress[®], JRS Pharma, Germany), pregelatinized starch (Sta-Rx[®] 1500, Colorcon, Germany), spray dried lactose monohydrate (Flowlac[®] 100, Meggle, Wasserburg, Germany), and magnesium stearate (N.F. Novartis, Switzerland) were used in the present chapter.

Methods

Powder Characterization

True density

True density of powders was measured by AccuPyc 1330 helium pycnometer (Micrometrics, Norcross, US). A known weight (2.5 g) of the samples was placed into the sample cell. Values were expressed as the mean of five parallel measurements, **Table 4**.

Particle-size distribution

The average particle size was determined by laser diffraction with a Malvern Mastersizer X (Malvern Instruments, Worcestershire, UK). The measurements were carried out three times for each sample. Obscuration value between 10 to 30% was got in all measurements. The function “polydisperse” was activated, **Table 4**.

Table 4 True density and mean particle size of the powders

Powder	True density [g/cm³] ± SD	Mean particle size [μm] ± SD
MCC	1.5589 ± 0.0009	127.6 ± 0.33
Mannitol	1.4902 ± 0.0005	146.3 ± 6.20
Lactose	1.5419 ± 0.0012	131.44 ± 1.005
Pregelatinized Starch	1.4790 ± 0.0018	93.74 ± 0.13
CHPD	2.4741 ± 0.0028	191.20 ± 7.07

Powder compaction

Powder compaction was carried out using a compaction replicator (Presster[™], Metropolitan Computing Corp., NJ, US) simulating the tablet press Korsch PH336 (36 stations). The compaction rolls used were 300 mm in diameter. Accordingly, a

flat-faced B-tooling with a diameter of 10 mm was used to make tablets of 250 mg in weight. Powder feed was manually done. Punches and dies were dusted with magnesium stearate powder before each compaction cycle for lubrication. The machine was set to perform compression pressures in the range of 50 to 300 MPa and precompression pressures in the range of 10 to 70 MPa at the compaction speeds of 0.5 and 2.147 m/s corresponding to the following dwell times (19 and 4.4 ms), respectively. Six tablets were compressed at the same experimental conditions and the mean of each parameter was calculated. During RDW sensor calibration, the radial force was calculated as a product of the applied axial pressure by the area of cylindrical portion of the tablet. Calibration factor CF was calculated as RDW force per voltage output (10.08 kN/volt). During tablet compaction, the measured voltage output was multiplied by CF and the product RDW force value was referred to the area of cylindrical portion of the tablet to obtain the RDWP value. RDP, MDP were measured and, RDP/MDP ratio was calculated. The die-wall pressure reaches a maximum value, MDP, just after the upper and lower punches show maximum compression values, and shows a constant residual value, RDP, after upper and lower punch forces become zero. Axial to radial stress ratio (SR) (the average of upper and lower compression pressures to MDP) was also calculated.

Compact characterization

Radial tensile strength (RTS)

Crushing strength of a compact was determined by pressing it diametrically [24] on a Pharmatron tablet tester (model 8D, Dr Schleuniger Pharmatron Inc., Solothurn, Switzerland). Radial tensile strength σ (MPa) was calculated according to:

$$\sigma = 2F/\pi dh \quad (1)$$

Where F is the force required to cause failure in tension (N), d is the compact diameter (mm), h is the compact thickness (mm), and π is a constant equals 3.1416. Compacts dimensions were measured using a micrometer with a precision of 0.01mm (Mitutoyo, Japan).

Elastic recovery (% ER_0)

The % ER_0 for a compact was calculated from “zero pressure thickness” that could be seen from the force vs. thickness plot, and “minimum punch gap” (thickness at maximum compression), features of Presster[®] software.

Change in void fraction (VC)

$$VC = \Delta\varepsilon/1 - \Delta\varepsilon \quad (2)$$

Where $\Delta\varepsilon$ is the change in porosity of the compact (difference between out and inside porosities).

Data interpretation

To study the effect of different compaction variables, runs were generated according to an experimental design using STAVEX[®] 5.0 (Aicos, Switzerland) applying Pentagon factorial design; optimization mode, see **Table 5**. Compression pressure (5 levels), precompression pressure (4 levels), and speed (2 levels) were the factors. RDP, MDP, RDP/MDP, SR, ER_0 , RTS, and VC were the responses. Least squares analysis was applied for the fitted model. The model was evaluated in terms of statistical significance using analysis of variance (ANOVA) at a level of significance ($p < 0.05$).

Table 5 Pentagon factorial design for compaction variables

Run	Compression Pressure C (MPa)	Precompression Pressure P (MPa)	Compaction Speed S (m/s)
1	50	50	0.5
2	50	50	2.0
3	80	10	0.5
4	80	10	2.0
5	120	30	0.5
6	120	30	2.0
7	120	70	0.5
8	120	70	2.0
9	170	10	0.5
10	170	10	2.0
11	200	50	0.5
12	200	50	2.0

Results and Discussion

Effect of compression pressure on radial die wall parameters

Table 6 shows the models suggested for different materials showing the compaction variables; compression, precompression pressures and compaction speed and their interactions. A qualitative classification for the materials under investigation regarding their deformation behavior [25-29] is given in **Table 7**. For all materials, increasing compression pressure significantly increased both RDP ($p < 0.0001$), and MDP ($p < 0.0001$), while decreased both RDP/MDP ratio ($p < 0.003$), and SR ($p < 0.0001$). **Figure 11** shows that the plastic material mannitol had the highest RDP followed by lactose (plastic/brittle), then CHPD (brittle), and finally MCC and pregelatinized starch (plastic/elastic). It is clear that plastic materials displayed the highest RDP while materials with an elastic component displayed the lowest RDP and materials with brittle character laid in between. Regarding MDP, see **Figure 12**, at higher pressures (200 MPa and above) materials with plastic/elastic behavior (MCC and pregelatinized starch) showed the highest MDP values followed by the plastic material mannitol, then the plastic/brittle lactose, and finally the brittle CHPD. MDP describes both elastic and plastic components, where it was clear in **Figure 12** that MDP could not clearly differentiate between materials at lower pressures, while RDP shows only permanent deformation after compaction [30].

Table 6 Models suggested for different materials showing the compaction variables, compression (C), precompression (P), and compaction speed (S) and their interactions

Material	Equation	Goodness of fit	
		R ²	R _c ²
CHPD	RDP = -1.757+0.09243 C +0.02666 P +0.08435 S +5.374E-0.0002014 P ² -0.0001033 CP -0.001225 CS - 0.001976 PS	0.9981	0.9931
	MDP = -8.585 +0.4103 C +0.1826 P -6.662 S +0.0009373 C ² -0.0007913 P ² -0.001214 CP +0.002614 CS - 0.02599 PS	0.9956	0.9838
MCC	RDP = 4.327+0.02462 C -0.05231 P -0.2226 S -7.245E-05 C ² +0.0002541 P ² +0.0001992 CP -0.001599 CS + 0.003609 PS	0.976	0.9122
	MDP = 0.6125 +0.5372 C -0.2768 P -1.357 S +0.0008899 C ² +0.003295 P ² -0.0003050 CP -0.02209 CS - 0.007288 PS	0.9996	0.9985
Mannitol	RDP = 2.145+ 0.08482 C - 0.05365 P + 0.1784 S + 0.0001936 C ² + 0.0004361 P ² + 6.694E-05 CP - 0.01017 CS + 0.001765 PS	0.9995	0.9982
	MDP = - 0.1144 + 0.4770 C - 0.09218 P - 0.9937 S + 0.0009111 C ² + 0.001167 P ² - 0.0002378 CP - 0.02897 CS - 0.02950 PS	0.9994	0.9978
Lactose	RDP = 1.956 + 0.08445 C - 0.04192 P - 1.010 S +2.443E-05 C ² + 0.0001850 P ² + 0.0001275 CP - 0.004313 CS + 0.01027 PS	0.9995	0.9983
	MDP =10.38 + 0.2405 C - 0.1535 P -3.895 S + 0.001192 C ² + 0.001094 P ² + 3.639E-05 CP - 0.03444 CS + 0.01328 PS	0.9990	0.9962
Pregelatinized starch	RDP = 8638+0.03348 C +0.001427 P -0.2748 S -8.650E-05 C ² -7.135E-05 P ² -1.389E05 CP -0.0008719 CS + 0.005358 PS	0.9799	0.9263
	MDP = -14.61+ 0.6541 C + 0.2226 P -3.103 S +0.001214 C ² -0.001357 P ² -0.001385 CP -0.05388 CS + 0.05732 PS	0.9999	0.9995

Table 7 Classification of the materials regarding their deformation behavior upon compaction

Material	Deformation behavior		
	Plastic	Elastic	Brittle
CHPD	-	-	+++
MCC	++	++	-
Mannitol	++	-	-
Lactose	+	-	+
Pregelatinized Starch	++	+++	-

+++ **High**; ++ = **medium**; + = **low**; - = **not present**

RDP was used as a guide to detect capping problem in some formulations [15, 31].

The relation between compression pressure and RDP/MDP ratio, **Figure 13**, followed the same sequence for different materials behavior with RDP but in a decreasing trend, where materials with plastic behavior (mannitol and lactose) showed the highest ratio values and materials with elastic component (MCC and pregelatinized starch) showed the least ratio values. Plastic behavior increases RDP while elastic behavior decreases RDP [32]. RDP/MDP ratio could be more useful

in describing the compaction behavior as it involves both die-wall related parameters, which provide a thorough profile regardless of the compaction pressure or speed. Generally, in tableting it would be desirable to have low RDP and high MDP values, hence low RDP/MDP values. This is in accordance with the results reported by Takeuchi et al [33]. On the other hand, compaction pressure showed no effect on SR for the brittle CHPD, but in case of materials with elastic component (MCC and pregelatinized starch), SR values were the lowest “i.e. low axial to radial stress transmission”, while materials with only plastic behavior such as mannitol and lactose showed the highest SR values “i.e. high axial to radial stress transmission”, which is a typical indicator for plasticity, **Figure 14**.

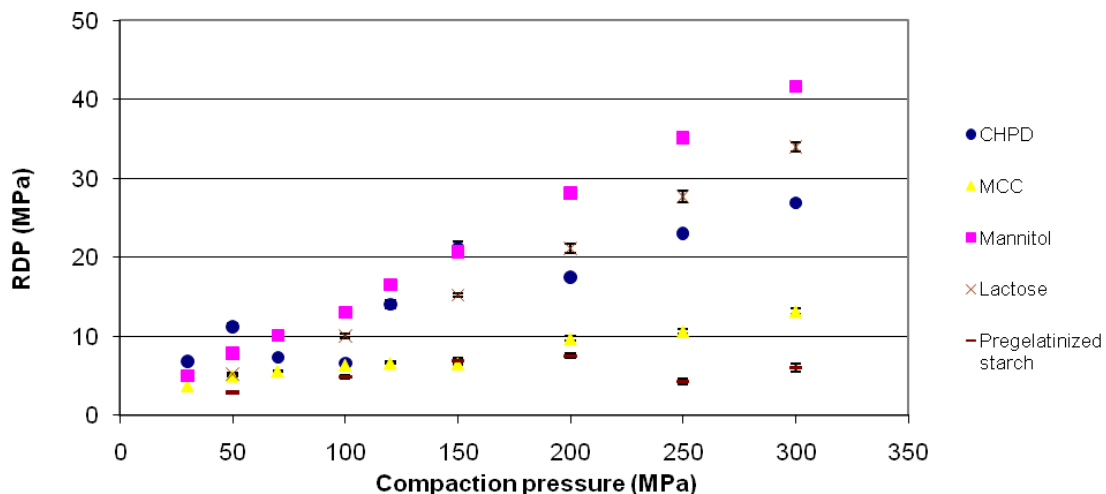


Figure 11 Effect of compaction pressure on RDP at compaction speed 0.5 m/s

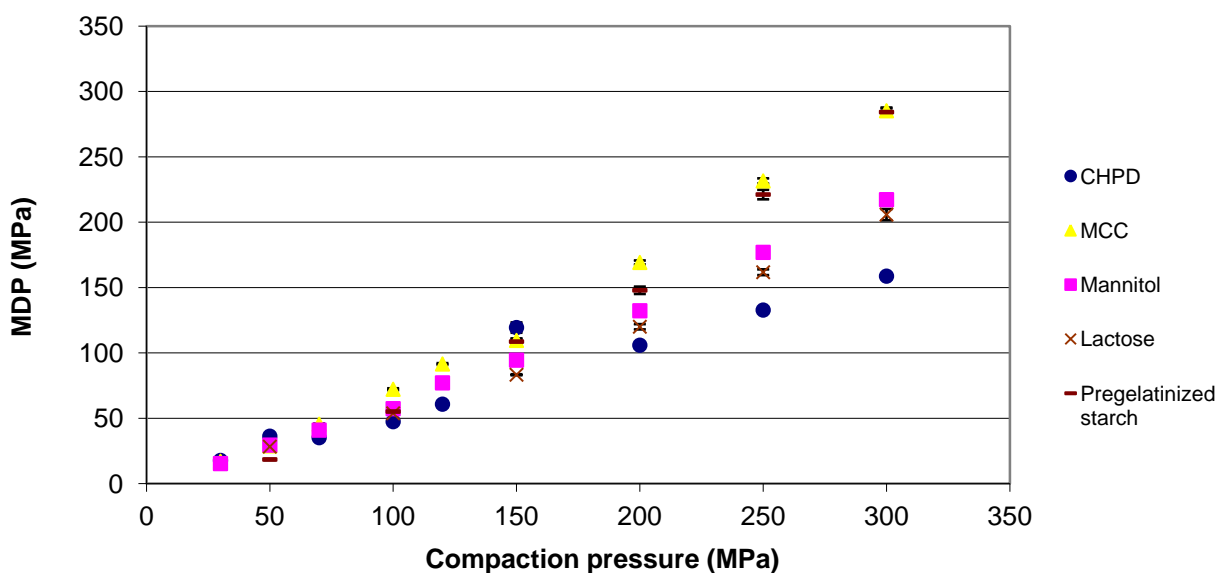


Figure 12 Effect of compaction pressure on MDP at compaction speed 0.5 m/s

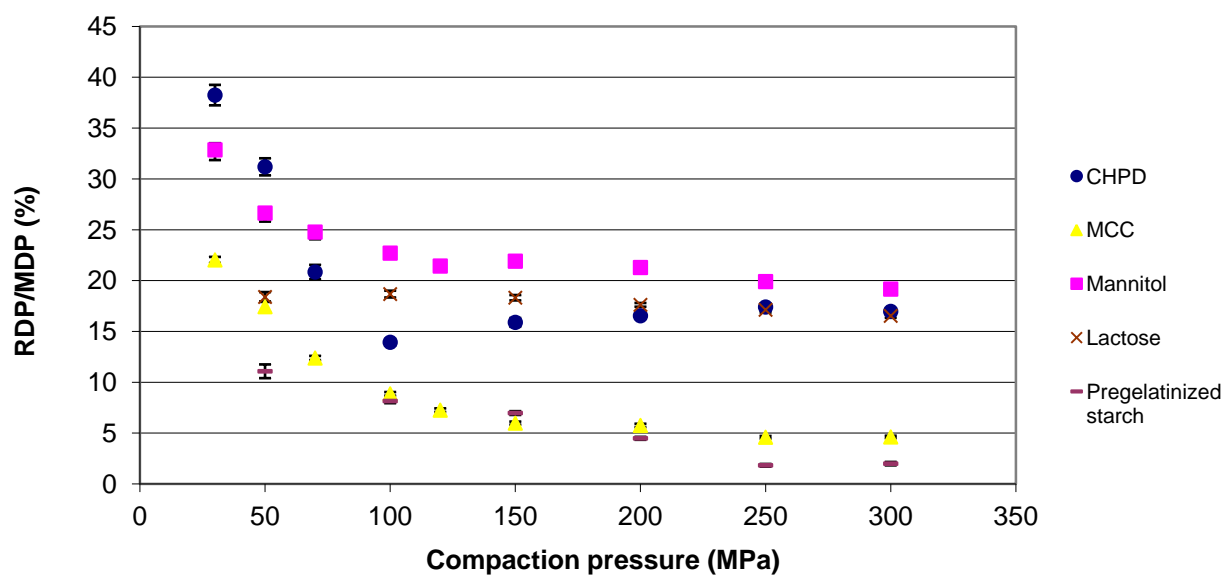


Figure 13 Effect of compaction pressure on RDP/MDP ratio at compaction speed 0.5 m/s

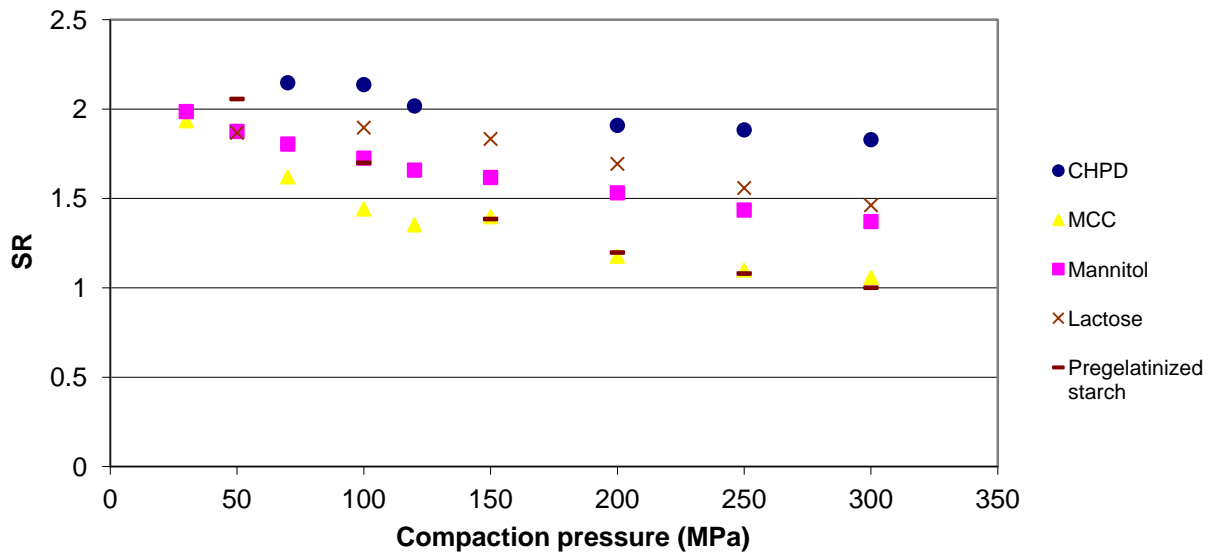


Figure 14 Effect of compaction pressure on axial to radial stresses ratio SR at compaction speed 0.5 m/s

Effect of precompression pressure on radial die wall parameters

Precompression had no effect on RDP and SR for MCC and pregelatinized starch as well as CHPD but for plastic materials (mannitol and lactose), RDP decreased, **Table 6**, and SR increased ($p < 0.05$). On the other hand, precompression had no effect on MDP and RDP/MDP ratio for all materials except for MCC (MDP decreased), **Table 6**. Precompression helped in particles rearrangement (powder densification), and hence ease of contact and bonding between particles leading to a cohesive mass with less tendency for radial deformation upon compression. This explains the decrease of MDP for MCC. Precompression also helps in removal of entrapped air and thus improves bonding between particles during the compaction

phase [34]. Precompression had the most significant effect on materials that showed the highest RDP (mainly plastic); where precompression decreased radial stress relative to axial during compaction (increased SR), and decreased radial relaxation after decompression (decreased RDP).

Effect of compaction speed on radial die wall parameters

Increasing speed decreased MDP for all materials, ($p < 0.05$). However, increasing speed led to the increase of RDP for mannitol ($p < 0.001$) and the decrease of RDP for MCC, lactose, and pregelatinized starch ($p < 0.05$), and no effect for CHPD, see **Table 6**. The decrease of dwell time (increase of speed) decreased the time of deformation for all types of materials during compaction and so led to a decrease in MDP. On the other hand, the increase of speed led to increase of radial recovery for mannitol like the same effect produced by speed on elastic recovery for materials with axial elastic component. All materials with elastic component showed a decrease in radial recovery (low RDP) as they experienced higher axial recovery (high elastic recovery). Finally, speed had no effect on the radial recovery of materials with brittle behavior due to the fracture of particles rather than deformation.

Effect of radial die wall pressure changes on compacts' physical properties

Materials with an elastic component (MCC and pregelatinized starch) during decompression showed highest elastic recovery ($p < 0.0001$) within the die at zero pressure ER_0 as well as the highest void volume change ($p < 0.0001$) with the least RDP values, see **Figure 15** and **16**. Thus, they had the greatest probability for capping. ER_0 would be more accurate to describe any tableting problem like capping and lamination on unloading in comparison to measuring elastic recovery like after 48 hrs as the problem would have been already occurred. Viscoelastic materials like MCC keep high energy in compacts [28], so on relaxation during deloading they would be liable for capping, especially at high speeds, unless they show strong bonding between particles. Moreover, high frictions between the die-wall and the compact may prevent the newly formed compact from relaxation and the relief of stored energy which would probably lead to capping or lamination [2]. MCC and pregelatinized starch showed the lowest RDP values and highest void volume change (lowest friction and highest porous structures during ejection) and thus fewer tendencies for capping or lamination. These were in accordance with the results of Sugimori et al. [35], where they stated that RDP depends on the elasticity and the use of powders with low RDP like MCC reduced capping tendency. Although MCC showed highest elastic recovery, but in comparison to pregelatinized starch and other materials, it showed the highest RTS, ($p < 0.0001$),

Figure 17. RTS indicates the force required to break bonds between particles. In case of MCC, the high bonding between particles limits the disruptive effect of elastic recovery [30]. However, materials with high elastic recovery at high compaction speeds during decompression would be still at high risk for capping [36-38]. Plastic materials (mannitol and lactose) showed the least values for ER_0 and void volume change ($p < 0.0001$) and the highest RDP values (higher tendencies for friction). This was practically observed where compaction of MCC and pregelatinized starch did not need any external lubrication (low ejection forces, did not exceed 200 N), while it was completely unavoidable to use external lubrication with mannitol and lactose (very high ejection forces more than 1500N). However, mannitol showed stronger compacts (higher RTS) than lactose due to the brittle component of the later. The brittle CHPD showed intermediate values between viscoelastic and plastic materials for ER_0 ; void volume change and low RTS which makes it highly liable for decompression defects like capping, lamination or chipping. **Table 8** summarizes the compaction parameters previously discussed in relation to materials deformation behavior.

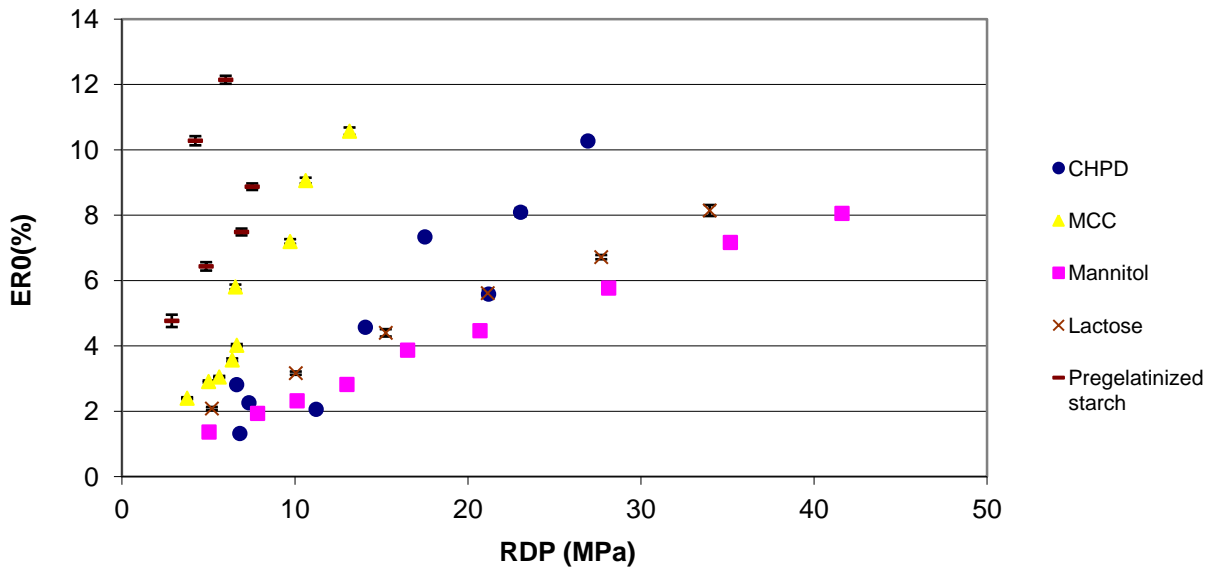


Figure 15 Change of RDP with ER_0 at compaction speed 0.5 m/s

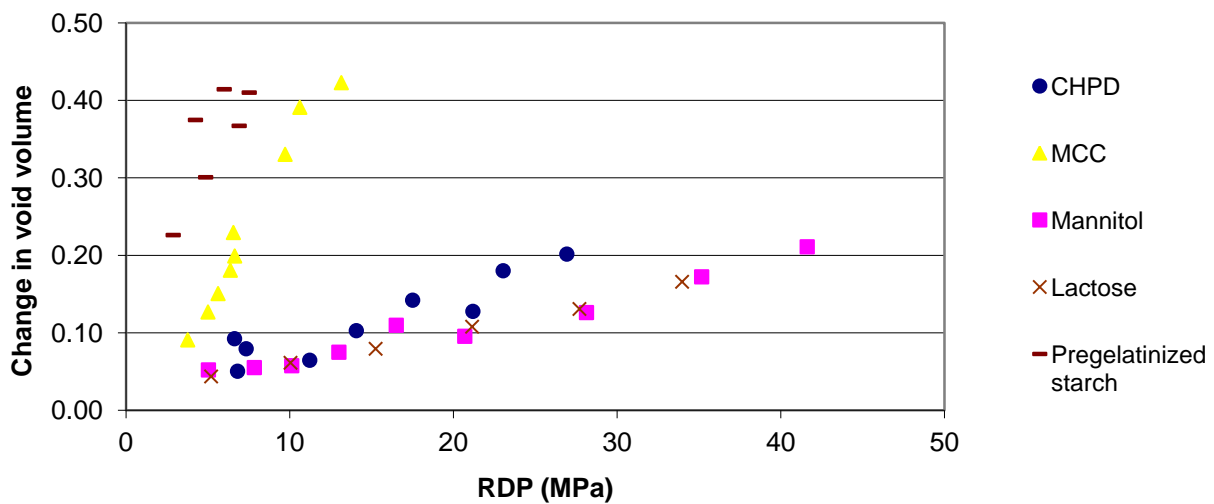


Figure 16 Change of RDP with void volume change at compaction speed 0.5 m/s

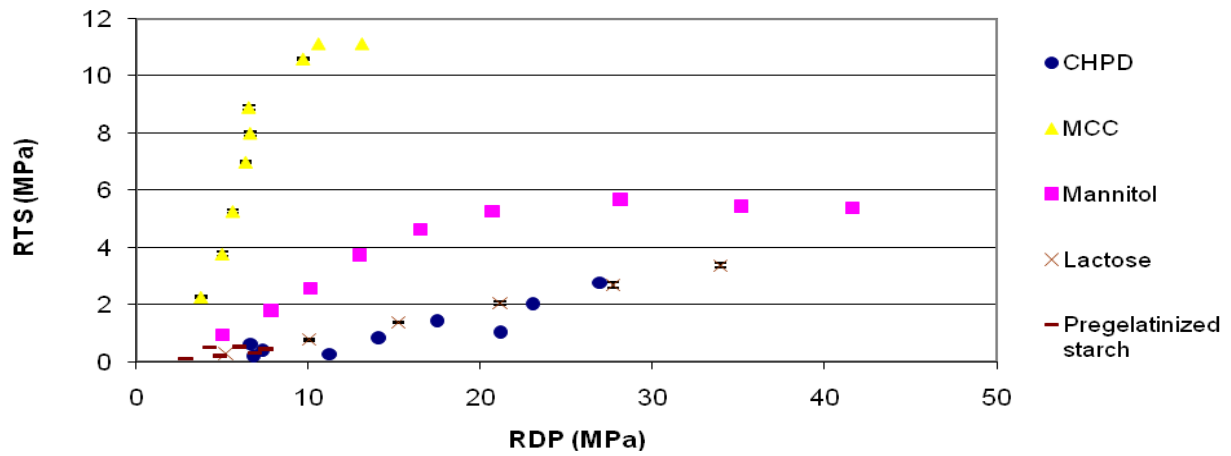


Figure 17 Change of RDP with RTS at compaction speed 0.5 m/s

Table 8 Different levels for compaction parameters in relation to materials' deformation behavior

Parameter	Materials		
	Elastic/Plastic	Plastic	Plastic/ Brittle
RDP	↑	↑↑↑	↑↑
MDP*	↑↑↑	↑↑	↑↑
RDP/MDP	↓↓↓	↓↓	↓↓
SR	↓↓↓	↓↓	↓/-
ER ₀	↑↑↑	↑	↑/↑↑
VC	↑↑↑	↑	↑/↑↑
RTS	↑↑↑ ^{**}	↑↑	↑

↑↑↑= High, ↑↑=Medium, ↑= Small, - = No Effect, ↑ = Increasing, ↓= Decreasing

* At high pressures > 200 MPa

** Only MCC as Pregelatinized starch showed very low values

Conclusion

Die-wall pressure investigation is of help to monitor compact formation at two critical steps; decompression (elastic recovery) and ejection phases (friction). Radial die-wall pressure reflects radial relaxation and so probability for friction. An increasing RDP value during compaction would indicate higher tendency for friction, while a high constant value of MDP would provide an evidence for plastic behavior; a character always desired in powder formulations. We highly recommend using radial die-wall pressures for setting limits for high-speed tableting machines to give a continuous control feedback for problems arising during manufacture, such as lamination and capping by detecting friction phenomena in early stages of development.

References

- [1] Humbert-Droz P, Gurny R, Mordier D, Doelker E. Densification behavior of drugs presenting availability problems. *Int J Pharm Tech Prod Mfr* 1983; 4: 29-35.
- [2] Van der voort maarschalk K, Zuurman K, Vromans H, Bolhuis GK, Lerk C.F. Stress relaxation of compacts produced from viscoelastic materials. *Int J Pharm* 1997; 151: 27-34.
- [3] Picker KM. Time dependence of elastic recovery for characterization of tableting materials. *Pharm Dev Technol* 2001; 6: 61-70.
- [4] Heckel RW. Density–pressure relationship in powder compaction. *Trans Metall Soc AIME* 1961; 221: 671-675.
- [5] Heckel RW. An analysis of powder compaction phenomena. *Trans Metall Soc AIME* 1961; 221: 1001-1008.
- [6] Kuny T, Leuenberger H. Compression behavior of the enzyme β -galactosidase and its mixture with microcrystalline cellulose. *Int J Pharm* 2003; 260: 137-147.

- [7] Kuentz M, Leuenberger H. Pressure susceptibility of polymer tablets as a critical property: a modified Heckel equation. *J Pharm Sci* 1999; 88: 174-179.
- [8] Sinka IC, Cunningham JC, Zavallangos A. Analysis of tablet compaction II. Finite element analysis of density distributions in convex tablets. *J Pharm Sci* 2004; 93: 2040-2053.
- [9] Sinka IC, Motazedian F, Cocks ACF, Pitt KG. The effect of processing parameters on pharmaceutical tablet properties. *Powder Technol* 2009; 189: 276-284.
- [10] Djemai A, Sinka, IC. NMR imaging of density distributions in tablets. *Int J Pharm* 2006; 319: 55-62.
- [11] Busignies V, Leclerc B, Porion P, Evesque P, Couarraze G, Tchoreloff P. Quantitative measurements of localized density variations in cylindrical tablets using X-ray microtomography. *Eur J Pharm Biopharm* 2006; 64: 38-50.
- [12] Han LH, Elliott JA, Bentham AC, Mills A, Amidon GE, Hancock BC. A modified Drucker-Prager Cap model for die compaction simulation for pharmaceutical powders. *Int J Solids Struct* 2008; 45: 3088-3106.

- [13] Long WM. Radial pressure in powder compaction. Powder Metall 1960; 6:73-86.
- [14] Leigh S, Carless JE, Burt BW. Compression characteristics of some pharmaceutical materials. J Pharm Sci 1967; 56: 888-892.
- [15] Obiorah BA, Shotton E. The effect of waxes, hydrolyzed gelatin and moisture on the compression characteristics of paracetamol and phenacetin. J Pharm Pharmacol 1976; 28: 629-632.
- [16] Obiorah BA. Possible prediction of compression characteristics from pressure cycle plots. Int J Pharm 1978; 1: 249-255.
- [17] Doelker E, Massuelle D. Benefits of die-wall instrumentation for research and development in tableting. Eur J Pharm Biopharm 2004; 58: 427-444.
- [18] Moe DV, Rippie EG. Nondestructive viscoelastic analysis of anisotropy in compressed tablets. J Pharm Sci 1997; 86: 26-32.
- [19] Rippie EG, Danielson DW. Viscoelastic stress/strain behavior of pharmaceutical tablets: analysis during unloading and post-compression periods. J Pharm Sci 1981; 70: 476-482.

- [20] Cocolas HG, Lordi NG. Axial to radial pressure transmission of tablet excipients using a novel instrumented die. *Drug Dev Ind Pharm* 1993; 19: 2473-2497.
- [21] Yeh C, Altaf SA, Hoag SW. Theory of force transducer design optimization for die wall stress measurement during tablet compaction: optimization and validation of split-web die using finite element analysis. *Pharm Res* 1997; 14: 1161-1170.
- [22] Carless JE, Leigh S, Pharmac JP. Compression characteristics of powders: radial die wall pressure transmission and density changes. *J Pharm Sci* 1974; 26: 289-297.
- [23] Sugimori K, Mori S. Characterization of die wall pressure to predict capping of flat- or convex-faced drug tablets of various sizes. *Powder Technol* 1989; 58: 259-264.
- [24] Fell JT, Newton JM. Determination of tablet strength by the diametrical-compression test. *J Pharm Sci* 1970; 59: 688-691.
- [25] Gohel MC, Jogani PD. A review of co-processed directly compressible excipients. *J Pharm Pharmaceut Sci* 2005; 8: 76-93.

- [26] Ilić I, Kása Jr P, Dreu R, Pintye-Hódi K, Srcic S. The compressibility and compactability of different types of lactose. *Drug Dev Ind Pharm* 2009; 35: 1271-1280.
- [27] Narayan P, Hancock BC. The relationship between the particle properties, mechanical behavior, and surface roughness of some pharmaceutical excipient compacts. *Mater Sci Eng* 2003; A355: 24-36.
- [28] Doelker E. Comparative compaction properties of various microcrystalline cellulose types and generic products. *Drug Dev Ind Pharm* 1993; 19: 2399-2471.
- [29] Rees JE, Rue PJ. Time-dependent deformation of some direct compression excipients. *J Pharm Pharmacol* 1978; 30: 601-607.
- [30] Krycer I, Pope DG, Hersey JA. An evaluation of the techniques employed to investigate powder compaction behavior. *Int J Pharm* 1982; 12: 113-134.
- [31] Doelker E, Shotton E. The effect of some binding agents on the mechanical properties of granules and their compression characteristics. *J Pharm Pharmacol* 1977; 29:193-198.

- [32] Sugimori K, Kawashima Y. Technical note: A new practical index to predict capping occurring during the tableting process. *Eur J Pharm Biopharm* 1997; 44: 323-326.
- [33] Takeuchi H, Nagira S, Yamamoto H, Kawashima Y. Die wall pressure measurement for evaluation of compaction property of pharmaceutical materials. *Int J Pharm* 2004; 274: 131-138.
- [34] Tanino T, Aoki Y, Furuya Y, Sato K, Takeda T, Mizuta T. Occurrence of capping due to insufficient air escape during tablet compression and a method to prevent it. *Chem Pharm Bull* 1995; 43: 1772-1779.
- [35] Sugimori K, Mori S, Kawashima Y. Application of a newly defined capping index in evaluation of the compressibility of pharmaceutical powders. *Adv Powder Technol* 1990; 1: 25-37.
- [36] Dwivedi SK, Oates RJ, Mitchell AG. Estimation of elastic recovery, work of decompression and Young's modulus using a rotary tablet press. *J Pharm Pharmacol* 1992; 44: 459-466.
- [37] Sugimori K, Mori S, Kawashima Y. Introduction of a new index for the prediction of capping tendency of tablets. *Chem Pharm Bull* 1989; 32: 452-458.

- [38] Casahoursat L, Lemagnen G, Larrouture D. The use of stress–relaxation trials to characterize tablet capping. *Drug Dev Ind Pharm* 1988; 14: 2179-2199.

Chapter 2: Study of radial die-wall pressure during high speed tableting: effect of formulation variables²

Abstract

Context: With high-speed compaction cycles as applied in pharmaceutical industrial presses, robust tools like radial die-wall pressure (RDWP) are required to monitor the deformation behavior of formulations under pressure and to avoid common problems such as capping. **Objective:** In this chapter the effects of common formulation factors such as lubricant, binder, and drug loading on RDWP were investigated. **Materials and Methods:** Compaction simulation using PressterTM was applied for five pharmaceutical fillers with different compaction behaviors. Two lubricants, two binders, and paracetamol as a model drug were used. Residual die-wall (RDP) and other compaction parameters were measured. **Results and Discussion:** Lubricant reduced RDP for fillers with plastic/ brittle behavior(s), ($p < 0.05$), while increased RDP for fillers with viscoelastic behavior, ($p < 0.05$), leading to higher tendency for capping in the later fillers. Binder reduced RDP for the fillers, ($p < 0.05$), hence decreased capping probability. By increasing drug

² "Reprinted from Drug Dev Ind Pharm, Vol./No., S. Abdel-Hamid, M. Koziolk, and G.Betz, Study of radial die-wall pressure during high speed tableting: effect of formulation variables, Pages 1-12, Copyright (2011), with permission from Informa Healthcare"

loading for fillers with viscoelastic behavior, RDP was increased, ($p=0.00001$), leading to capping, especially at high compaction pressure and speed. **Conclusion:** Die-wall instrumentation was useful in investigating formulation variables and detecting capping during high speed tableting.

Keywords: tableting, instrumentation, simulation, lubricant, binder, drug loading, capping

Introduction

Understanding the behavior of pharmaceutical powders during compaction would help in the improvement of the quality of the final compact. During compaction, powders undergo: particle rearrangement, bonding, and deformation. Ejection is the last step of powder compaction. It is a critical step during which some tableting problems such as capping, lamination, and sticking may occur. Ejection is the force required to overcome the adhesion of the compact to the die-wall or what is known as friction because there is always an irreversible pressure exerted by the compact contact to the die at zero compaction called the residual die wall pressure (RDP). Die-wall pressure monitoring through die-instrumentation is of great help to understand particle-die wall interaction during axial compaction [1]. Using a mechanical simulator for rotary tablet machines, like the Presster™, to match compression force, dwell time, and punch displacement profile of many industrial presses, would be of great help in product development.

Lubricants are excipients which decrease the adhesion forces or friction between the compact surface and the die-wall by forming a barrier that reduces the contact between the surfaces of the compact and the die-wall [2, 3]. In the pharmaceutical field, lubricants act by continuous fluid formation, or more commonly, boundary lubrication [4]. A lubricant should ideally have a high melting point, low moisture

content, low affinity of friction with metal surfaces, fine particle size, large specific area, and film-forming ability [5]. The type of lubricant, its concentration, as well as the method of lubrication, influences hardness, friability, disintegration, dissolution, and surface properties of tablets [6-8]. Binders are used to improve the compressibility of powders due to their plasticity and to produce compacts of reasonable tensile strength due to interparticle adhesion [9, 10]. Dry binders are known as “pressure binders” while those used for wet granulation are known as “solution binders” [11, 12]. Reducing the particle size of dry binders improves binding capacity [13]. Paracetamol is a very good model drug to study the effect of drug loading. Paracetamol compacts undergo capping usually at high speeds due to its poor tabletability and compressibility [14-17].

The aim of the present chapter was to investigate, by the aid of compaction simulation and RDWP monitoring, the effect of some commonly used formulation excipients such as binders and lubricants, as well as paracetamol drug loading on the compaction behavior of different direct-compressible fillers at high compaction speeds. Moreover, using RDWP as a tool to predict capping and lamination during high speed tableting was applied.

Materials and Methods

Materials

Microcrystalline cellulose MCC (Avicel[®] PH102, FMC Corporation, DE, US), directly compressible mannitol (Pardeck[®] M200, Merck KGaA, Darmstadt, Germany), calcium hydrogen phosphate dihydrate CHPD (Emcompress[®], JRS Pharma, Rosenberg, Germany), pregelatinized starch (Sta-Rx[®] 1500, Colorcon, Idstein, Germany), spray dried lactose monohydrate SDL (Flowlac[®] 100, Meggle, Wasserburg, Germany) was used for the effect of binder and effect of drug loading studies, direct compressible lactose monohydrate DCL (supplied by Novartis AG, Basel, Switzerland) was used in the study of lubricant effect. Magnesium stearate (Mg-stearate, supplied by Sandoz AG, Basel, Switzerland) and polyethylene glycol (PEG 6000, Clariant AG, Muttens, Switzerland) were used as lubricants in concentrations of 0, 1 and 2 % (w/w). Copovidone (Kollidon[®] VA 64, BASF, Hannover, Germany) and hydroxypropylcellulose medium substituted (NISSO-HPC M, Nippon-Soda Co. Ltd., Japan) in concentrations of 0, 5 and 10 % (w/w) were used as binders. Paracetamol (Rhodapap[®], Rhodia S.A., France) was used as a model active pharmaceutical ingredient at three different loadings; 20, 50 and 80 % (w/w).

Methods

Powder Characterization

True density

True density of powders was measured by AccuPyc 1330 helium pycnometer (Micrometrics, Norcross, GA, US). A known weight of the samples was placed into the sample cell. Values were expressed as the mean of five parallel measurements.

Particle-size distribution

The average particle size was determined by laser diffraction with a Malvern Mastersizer X (Malvern Instruments, Worcestershire, UK). The measurements were carried out three times for each sample. Obscuration value between 10 to 30% was got in all measurements. The function “polydisperse” was activated.

Morphological studies

Particle morphology was assessed by scanning electron microscopy (SEM) (Nova NanoSem 230, Eindhoven, Netherlands). Samples were mounted on aluminum stubs using double side adhesive carbon tape and sputter coated with gold 20 nm (BalTec MED 020 Coating System, Lichtenstein).

Preparation of mixtures

Mixtures of different fillers and an additive (lubricant or binder or drug) were prepared by mixing for two minutes at 100 rpm in a Turbula[®] mixer (Type T2A, Wilhelm A. Bachofen AG, Switzerland). Formulations for experiments of binder and drug loading effect had 1% (w/w) Mg stearate as a lubricant.

Powder compaction

Powder compaction was carried out using a compaction simulator (Presster[™], Metropolitan Computing Corp., NJ, US) simulating the tablet press Korsch PH336 (36 stations). The compaction rolls used were 300 mm in diameter. Accordingly, a flat-faced B-tooling with a diameter of 10 mm was used to make tablets of 250 mg in weight. Powder feed was manually done. Punches and dies were cleaned with ethanol after each compression cycle. For external lubrication, punches and dies were dusted with Mg stearate powder before each compaction cycle. In case of lubricant effect experiments, external lubrication was done for runs with zero percent lubricant to guarantee the feasibility of all experiments and the comparability of the powders. The machine was set to perform compaction pressures of 50, 150 and 300 MPa at the compaction speeds of 0.5 and 2 m/s corresponding to the following dwell times (19 and 4.8 ms), respectively. Six tablets were compressed at the same experimental conditions and the mean was

calculated. Residual die-wall pressure (RDP), maximum die-wall pressure (MDP), compressibility (compression force kN versus compact volume cm³), and ejection force (F_e) were measured. The die-wall pressure reaches a maximum value, MDP, just after the upper and lower punches show maximum compression values, and shows a constant residual value, RDP, after upper and lower punch forces become zero, **Figure 18**. RDP/MDP ratio as well as axial to radial stress ratio (SR) (MDP to the average of upper and lower compression pressures) was calculated. Moreover, friction coefficient during ejection FCE (μ_e) and friction coefficient during compression FCC (μ_c) were calculated according to equation 1 [18] and equation 2 [19]:

$$\mu_e = \frac{F_e}{F_{r0}} \quad (1)$$

Where F_e is the ejection force and F_{r0} is the residual die-wall force.

$$\mu_c = \frac{D}{4H} \frac{F_U}{MDF} \left(\frac{F_L}{F_U} \right)^{\frac{LPD}{H}} \ln \frac{F_L}{F_U} \quad (2)$$

Equation (2), developed by Cunningham and coworkers, was modified in this study to fit the dynamics of the PressterTM. F_U and F_L are the upper and lower compression

forces, MDF is the maximum die-wall force, LPD is the lower punch displacement, D is the die diameter, and H is the compaction height.

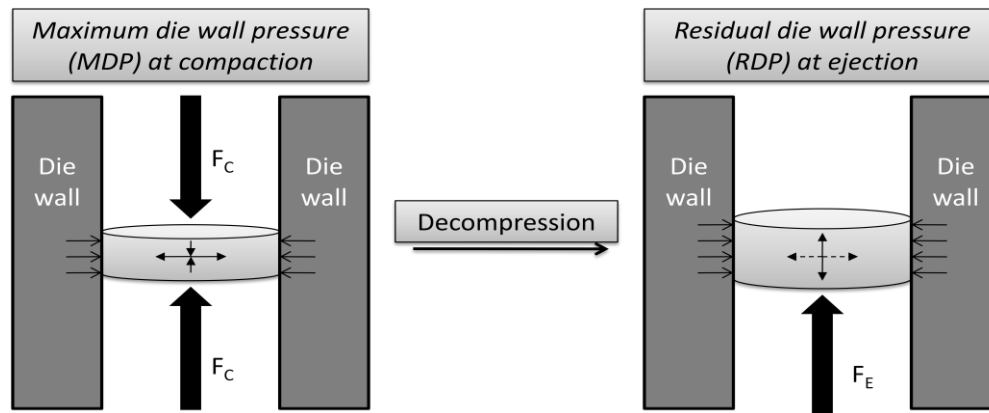


Figure 18 Schematic diagram for MDP and RDP [F_c - Compaction Force, F_e - Ejection Force]

Radial tensile strength (RTS)

Crushing strength of a compact was determined by pressing it diametrically [20] on a Pharmatron tablet tester (model 8D, Dr Schleuniger Pharmatron Inc., Solothurn, Switzerland). Radial tensile strength σ (MPa) was calculated according to:

$$\sigma = 2F/\pi dh \quad (3)$$

Where F is the force required to cause failure in tension (N), d is the compact diameter (mm), h is the compact thickness (mm), and π is a constant equals 3.1416.

Compacts dimensions were measured using a micrometer with a precision of 0.01mm (Mitutoyo, Japan).

Elastic recovery (% ER_0)

The % ER_0 for a compact was calculated from “zero pressure thickness” that could be seen from the force vs. thickness plot, and “minimum punch gap” (thickness at maximum compression), features of Presster[®] software.

Data interpretation

To study the effect of different compaction variables, runs were generated according to an experimental design using STAVEX[®] 5.0 (Aicos, Switzerland) applying a 3-level full-factorial design with 18 runs, optimization mode, **Table 9**. Factors were set as quantitative except for speed and in case of external versus no lubrication, they were set as qualitative. Compression pressure (3 levels), speed (2 levels), and an additive (lubricant or binder or drug loading) (3 levels) were the factors. RDP, MDP, SR, F_e , μ_c , μ_e and ER_0 , and RTS were the responses. Least squares analysis was applied for the fitted model of optimization. The model was evaluated in terms of statistical significance using analysis of variance (ANOVA) at a level of significance ($p < 0.05$). Graph Pad Prism v.5.00 software was used for Pearson's correlations.

Table 9 Different experimental designs generated by STAVEX[®] 5.0 to study the impact of lubricant, binder, and drug loading on RDWP

Run	Compression pressure (MPa)	Speed (m/s)	Additive (%)*		
			<i>I Lubricant</i>	<i>II Binder</i>	<i>III Drug loading</i>
1	50	0.5	0	0	20
2	50	2	0	0	20
3	50	0.5	1	5	50
4	50	2	1	5	50
5	50	0.5	2	10	80
6	50	2	2	10	80
7	150	0.5	0	0	20
8	150	2	0	0	20
9	150	0.5	1	5	50
10	150	2	1	5	50
11	150	0.5	2	10	80
12	150	2	2	10	80
13	300	0.5	0	0	20
14	300	2	0	0	20
15	300	0.5	1	5	50
16	300	2	1	5	50
17	300	0.5	2	10	80
18	300	2	2	10	80

* Effect of each additive (lubricant or binder or drug) was studied separately each time with increasing compression pressure and speed

Results and Discussion

True density and particle size distribution

Table 10 shows the true density, median and mean diameters, as well as the span (particle size distribution), and the specific surface area of the investigated powders. The true density values for all fillers were in the same range except for CHPD, which had the highest true density. All values corresponded with the ones reported in literature [21]. Mean particle size for all fillers was determined to be in the range of 95 -193 μm . Pregelatinized starch particles showed the widest particle size distribution while those of CHPD showed the narrowest. Particles of pre-gelatinized starch were the finest, and hence had the biggest specific surface area, while those of CHPD were the coarsest, and thus had the smallest specific surface area. Regarding lubricants, Mg stearate showed very fine particle size around 9 μm which would probably have a big influence on its efficiency as a lubricant. On the other hand, the mean particle size of the binder copovidone and HPC were almost the same (82 and 85 μm respectively) which would make the molecular weight as the more decisive factor. Paracetamol also showed fine particle size around 74 μm which led to some problems during compaction.

Table 10 Median, and mean diameters, span, specific surface area, and true density of the investigated powders

Powder	Median (μm) \pm SD	Mean (μm) \pm SD	Span * \pm SD	Specific Surface area (m^2/g) \pm SD	True density (g/cm^3) \pm SD
MCC	124.63 \pm 9.3 $\cdot 10^{-1}$	136.57 \pm 9.4 $\cdot 10^{-1}$	1.68 \pm 1 $\cdot 10^{-3}$	0.0454 \pm 2.08 $\cdot 10^{-4}$	1.5859 \pm 1.9 $\cdot 10^{-3}$
Mannitol	131.15 \pm 0.2 $\cdot 10$	149.22 \pm 0.25 $\cdot 10$	1.73 \pm 2.22 $\cdot 10^{-2}$	0.0425 \pm 4.56 $\cdot 10^{-4}$	1.5154 \pm 0.7 $\cdot 10^{-3}$
CHPD	181.71 \pm 0.3 $\cdot 10$	188.02 \pm 0.29 $\cdot 10$	0.86 \pm 1.38 $\cdot 10^{-2}$	0.0145 \pm 2.45 $\cdot 10^{-4}$	2.4818 \pm 1.6 $\cdot 10^{-3}$
Preg. Starch	86.51 \pm 1.6 $\cdot 10^{-1}$	94.90 \pm 3 $\cdot 10^{-2}$	1.87 \pm 8.72 $\cdot 10^{-3}$	0.0836 \pm 2.99 $\cdot 10^{-4}$	1.4964 \pm 0.6 $\cdot 10^{-3}$
DCL	182.06 \pm 0.14 $\cdot 10$	193.16 \pm 0.14 $\cdot 10$	1.20 \pm 2.22 $\cdot 10^{-2}$	0.0254 \pm 2.08 $\cdot 10^{-4}$	1.5384 \pm 0.7 $\cdot 10^{-3}$
SDL	124.87 \pm 0.11 $\cdot 10$	131.44 \pm 0.1 $\cdot 10$	1.43 \pm 6.66 $\cdot 10^{-3}$	0.0444 \pm 2.99 $\cdot 10^{-4}$	1.5419 \pm 1.2 $\cdot 10^{-3}$
Mg stearate	8.30 \pm 6 $\cdot 10^{-2}$	9.84 \pm 33 $\cdot 10^{-2}$	1.29 \pm 6 $\cdot 10^{-2}$	0.71 \pm 7 $\cdot 10^{-3}$	1.0744 \pm 1.1 $\cdot 10^{-3}$
PEG 6000	56.93 \pm 0.3 $\cdot 10$	62.42 \pm 0.46 $\cdot 10$	1.91 \pm 4 $\cdot 10^{-2}$	0.16 \pm 2 $\cdot 10^{-2}$	1.2719 \pm 0.4 $\cdot 10^{-3}$
Copovidone	70.01 \pm 0.11 $\cdot 10$	82.00 \pm 0.14 $\cdot 10$	1.97 \pm 1 $\cdot 10^{-2}$	0.11 \pm 1 $\cdot 10^{-3}$	1.2509 \pm 0.7 $\cdot 10^{-3}$
HPC	80.68 \pm 34 $\cdot 10^{-2}$	85.83 \pm 41 $\cdot 10^{-2}$	1.43 \pm 1 $\cdot 10^{-2}$	0.09 \pm 1 $\cdot 10^{-3}$	1.2261 \pm 0.3 $\cdot 10^{-3}$
Paracetamol	47.57 \pm 79 $\cdot 10^{-2}$	73.63 \pm 0.15 $\cdot 10$	3.41 \pm 7 $\cdot 10^{-2}$	0.19 \pm 1 $\cdot 10^{-3}$	1.2923 \pm 0.9 $\cdot 10^{-3}$

* Span is the measurement of the width of the distribution. The smaller the value, the narrower is the distribution. The width is calculated as: $d(0.9)-d(0.1)/d(0.5)$

Effect of lubricant on radial die-wall pressure and friction

Mg stearate

Materials with viscoelastic behavior such as pregelatinized starch showed an increase in RDP, **Figure 19a**, MDP, ER_0 and μ_c ($p < 0.05$), or no change in these parameters such as MCC. However, pregelatinized starch showed a decrease in μ_e and F_e ($p < 0.0001$). Deformation of powder under compression would lead to densification and so an increase in internal friction between particles. Moreover, it would lead also to increase of contact areas with the die-wall, so a higher probability of adhesion or friction.

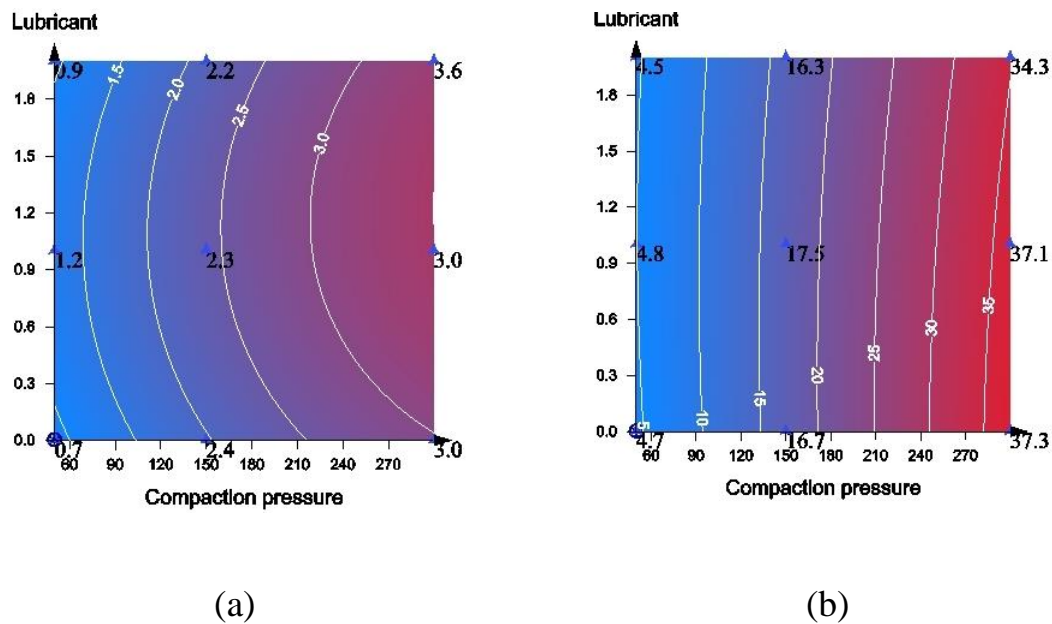


Figure 19 Contour plots showing the effect of the lubricant Mg stearate on RDP (values in black on the right) for (a) Pregelatinized starch, (b) Mannitol at compaction speed 2 m/s

Deformation mechanism of the pharmaceutical powders e.g. plastic or brittle would influence surface rugosity of individual particles and so would have an influence on the particle die-wall adhesive interactions [22]. Mg stearate is the most commonly used lubricant in tableting [23]. Mg stearate facilitates powder densification by the reduction of interparticulate friction [24, 25]. This led to an increase in RDP, MDP, SR, and μ_c for fillers with viscoelastic deformation behavior like pregelatinized starch. Moreover, Mg stearate enhanced the viscoelastic nature of these fillers [26]. Mg stearate showed no effect on MCC because the higher plastic nature of MCC, in comparison to pregelatinized starch, equalized the increase in elasticity induced by the lubricant. Although MCC compacts possessed high tensile strength, capping occurred for such compacts due to very high values of ER_0 . The presence of Mg-stearate had an adverse effect on bonding for MCC [27], and consequently, in this study we assume that this weak bonding was further broken by the high elastic recovery of MCC compacts. Regarding the effect of Mg stearate on pregelatinized starch, although F_e was reduced, RDP was increased. This could be explained by the increased ER_0 for pregelatinized starch which could produce more contact areas with the die-wall and hence increase RDP and simultaneously, its self lubricating property would reduce F_e . On the other hand, by increasing the concentration of Mg stearate, materials with plastic/brittle behavior(s) such as mannitol, lactose, and CHPD showed a decrease in RDP, ($p < 0.05$), **Figure 19b**, and only mannitol

showed an increase in MDP ($p < 0.0001$). Parameters like μ_e as well as F_e were decreased ($p < 0.05$) for mannitol and lactose, and no change in case of CHPD occurred. For such fillers, the decrease in friction between die-wall and compact was the dominant mechanism and led to a decrease in RDP, RDP/MDP, F_e , and μ_e . This is in accordance with what was reported about plastic materials like mannitol that they are highly sensitive to lubricant effect where adhesive forces between the particles and the die-wall are reduced [23, 28, 29]. The low lubricant sensitivity of CHPD regarding the friction forces was due to its brittle deformation behavior [30]. New, fresh surfaces were created by particle fragmentation during the compaction process and therefore, the appeared friction forces were not affected [31, 32]. RDP/MDP ratio decreased only in case of the plastic and/or brittle materials, like mannitol and lactose ($p < 0.0002$). Thus, it could not be taken generally as a sensitive parameter for the evaluation of lubricants as previously reported [28]. SR ratio was increased ($p < 0.001$) only in case of mannitol and pregelatinized starch whereas there was no change in SR for other fillers. SR was always directly related to MDP as it was reported that MDP could represent the transmission of axial pressure to the die-wall [33]. The increase of MDP in case of mannitol and pregelatinized starch can be explained by the reduction of interparticulate contact and bonding [25]. This resulted in a bigger contact area with the die-wall and hence an increased MDP.

Polyethylene glycol PEG 6000

For stability, compaction, and biopharmaceutical reasons, polymeric hydrophilic lubricants such as PEG 6000 could be used [34, 35]. MCC showed an increase of all parameters; RDP ($p < 0.002$), **Figure 20a**, μ_e ($p < 0.02$), μ_c ($p = 0.00001$), and F_e ($p < 0.002$), by increasing PEG 6000 concentration. PEG was reported to have a viscoelastic spring-like behavior [36]. This explains the increase of all compaction parameters like RDP and F_e with MCC. Moreover, for MCC and pregelatinized starch, MDP and SR were increased ($p < 0.05$) as PEG concentration increased. This is attributed to the enhancement of the densification behavior of MCC and pregelatinized starch by the presence of PEG due to decreased friction between the powder particles. On the other hand, for plastic and/or brittle fillers such as mannitol and lactose; RDP showed a decrease by increasing PEG concentration ($p < 0.006$), **Figure 20b**. This is explained by the increase of the filler cohesion due to the binding properties of PEG [37]. However, at high compaction pressure and speed, mannitol exhibited capping which could be explained by enhanced spring effect of PEG at these conditions where mannitol already exhibits high radial relaxation according to previous studies [38]. It could be also attributed to the lower lubricant effectiveness of PEG in comparison to Mg stearate [34]. Parameters like RDP/MDP ($p < 0.03$), μ_e ($p < 0.05$), μ_c ($p < 0.009$), and F_e ($p < 0.0006$) were also decreased for mannitol and lactose. By increasing PEG concentration in case of

pregelatinized starch and CHPD, RDP remained constant because F_e remained constant [39]. These fillers were hardly affected by PEG because CHPD undergoes mainly fragmentation during compaction and pregelatinized starch possesses self-lubricating properties [40].

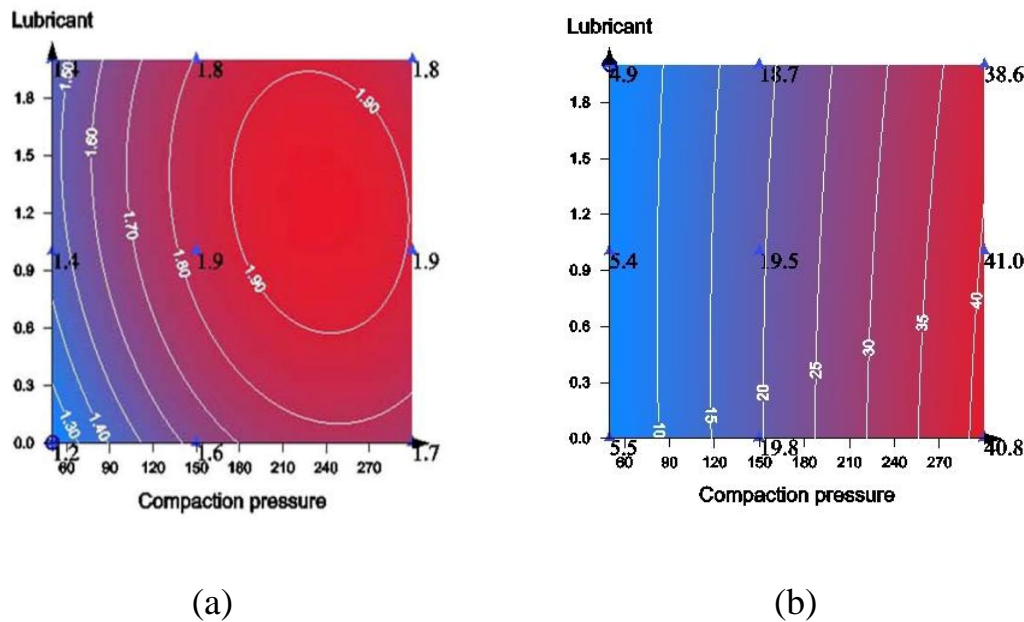


Figure 20 Contour plots showing the effect of the lubricant PEG 6000 on RDP (values in black on the right) for (a) MCC, (b) Mannitol at compaction speed 2 m/s

External lubrication

Experiments for external lubrication with Mg stearate versus no lubrication for the die was done only for MCC, pregelatinized starch, and lactose due to the highly abrasive character of the other fillers. The results showed no change in die-wall compaction parameters except for pregelatinized starch where MDP was decreased

($p = 0.0022$). However, F_e was reduced ($p < 0.03$) for all fillers; SR remained constant only for lactose, whereas it was increased for MCC and decreased in case of pregelatinized starch ($p < 0.05$). On the other hand, external lubrication with PEG 6000 (done only for MCC and pregelatinized starch) showed a decrease in RDP ($p = 0.03$), **Figure 21**, MDP ($p < 0.0005$), SR ($p < 0.03$), μ_e ($p < 0.05$), μ_c ($p < 0.01$), and, F_e ($p < 0.006$).

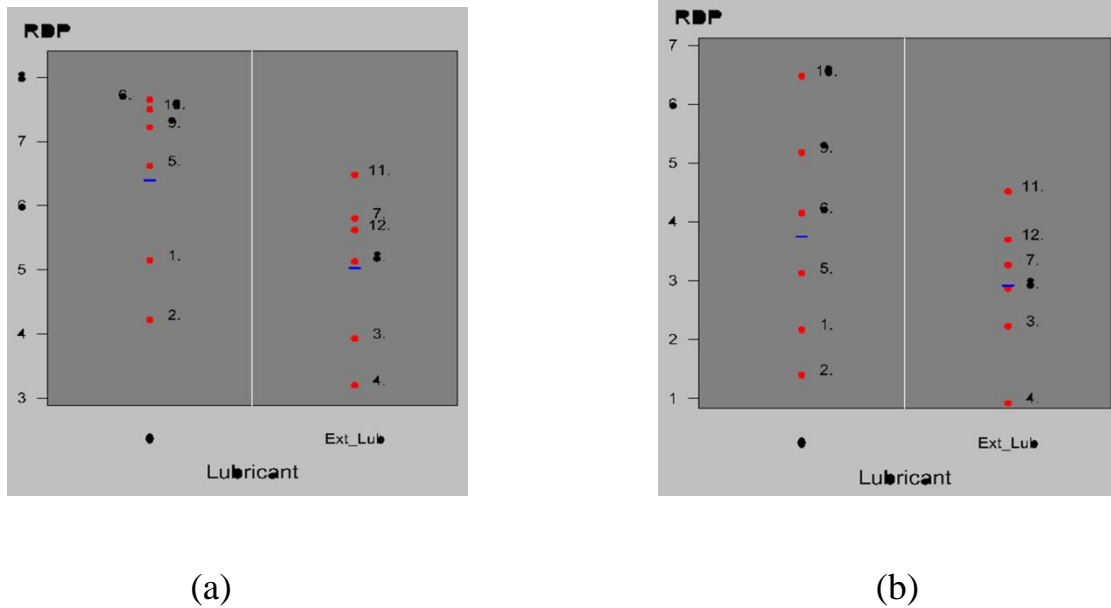


Figure 21 Plots for different runs comparing the effect on RDP of no lubrication (on the left) versus external lubrication with the lubricant PEG 6000 for (a) MCC, (b) Pregelatinized starch

External lubrication is the direct application of lubricant to the tablet machine tooling, without blending with powder [41]. External lubrication is usually applied to avoid the deleterious effects of lubricants on the tensile strength and the

disintegration time of the compacts [42, 43]. Generally as an external lubricant, PEG showed better lubrication effects on compaction parameters than Mg stearate which could be attributed to its asperity melting [44-46]. Hence, PEG acted as a fluid lubricant reducing friction between the tooling and distributing the stresses to die-wall more homogenously leading to the reduction of RDP, MDP, F_e , μ_e and μ_c . On the other hand, it was interesting to note that for pregelatinized starch, unlike internal lubrication with Mg stearate, SR was decreased with external lubrication. This can be explained by the less densification effect of Mg stearate when applied externally, leading to the reduction of axial pressure transmission to the die-wall.

Effect of binder on radial die wall pressure and friction

Copovidone

By increasing the concentration of copovidone, materials with plastic/brittle behavior(s) such as mannitol, lactose, and CHPD, showed a decrease in RDP, **Figure 22a**, and RDP/MDP ratio, ($p < 0.05$), and only mannitol and lactose showed an increase in MDP ($p < 0.023$) and SR ($p < 0.05$). On the other hand, materials with viscoelastic behavior such as MCC and pregelatinized starch showed an increase in RDP ($p < 0.05$), **Figure 22b**, and RDP/MDP ratio, ($p < 0.05$) and only MCC showed an increase in MDP ($p < 0.002$).

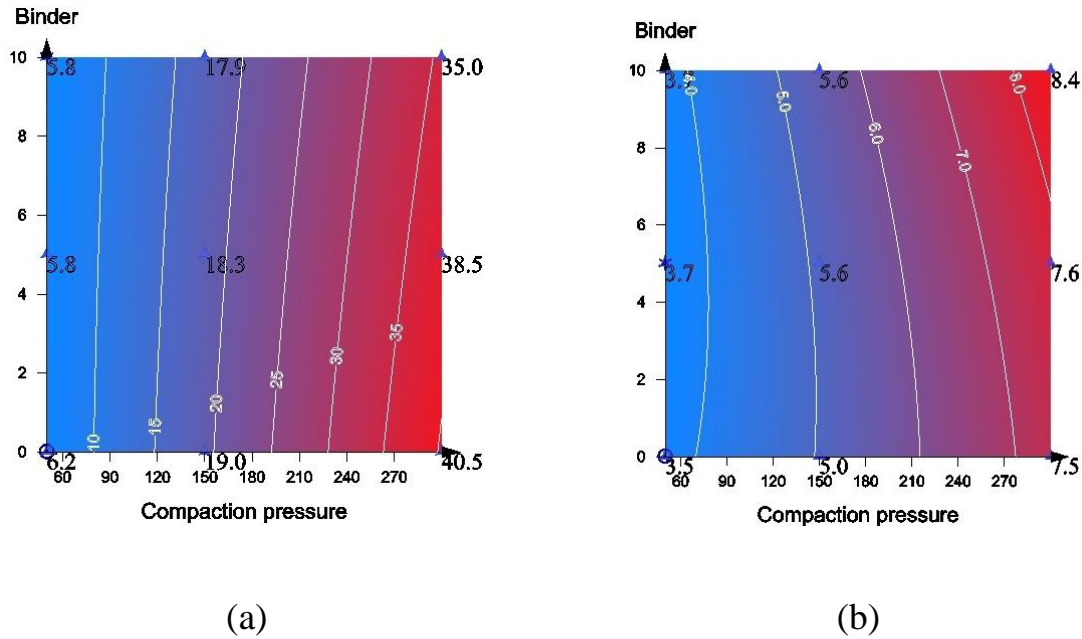


Figure 22 Contour plots showing the effect of the binder copovidone on RDP (values in black on the right) for (a) Mannitol, (b) MCC at compaction speed 2 m/s

Hydroxypropylcellulose HPC

All fillers showed a decrease in RDP and RDP/MDP ratio with HPC ($p < 0.0002$), except pregelatinized starch showed no change. Also, all the fillers (except for CHPD and pregelatinized starch) showed an increase of MDP ($p < 0.002$) and SR ($p < 0.05$). Unlike copovidone, the fillers MCC, mannitol, lactose, and CHPD showed an increase in ER_0 , ($p < 0.0008$), by increasing the concentration of HPC. Moreover, materials with a brittle behavior such as lactose, and CHPD showed a decrease in F_e and RTS directly after ejection ($p = 0.00001$), **Figure 23**.

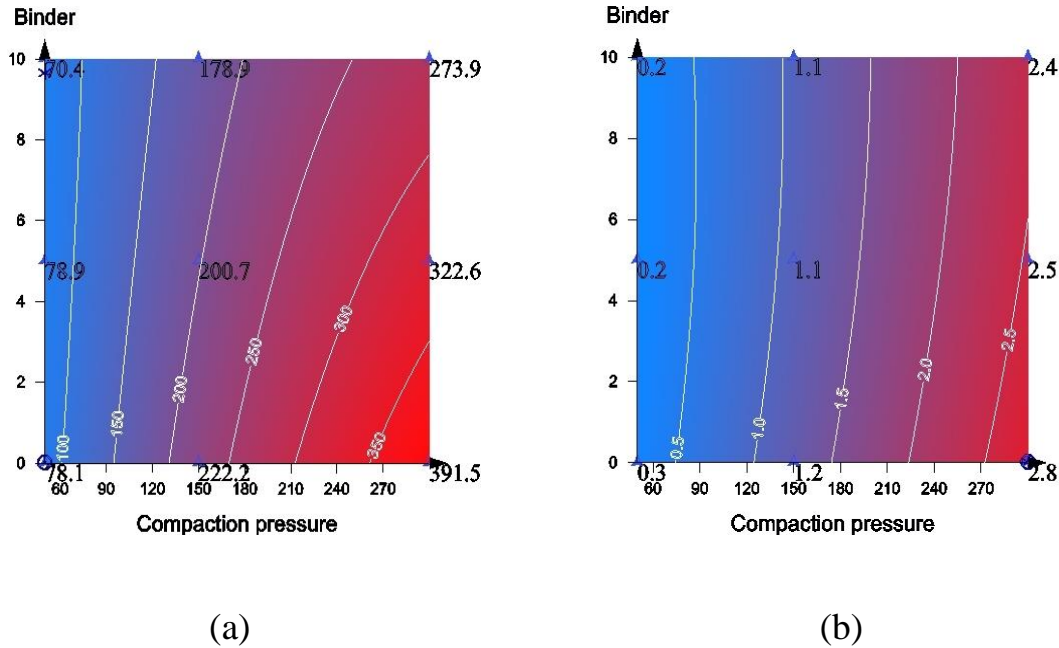
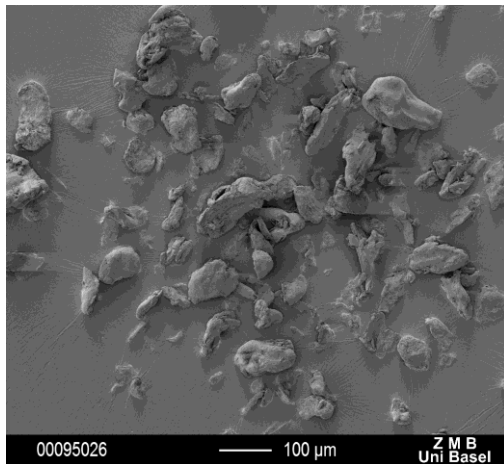


Figure 23 Contour plots showing the effect of the binder HPC on (a) F_e , (b) RTS, (values in black on the right) for lactose at compaction speed 2 m/s

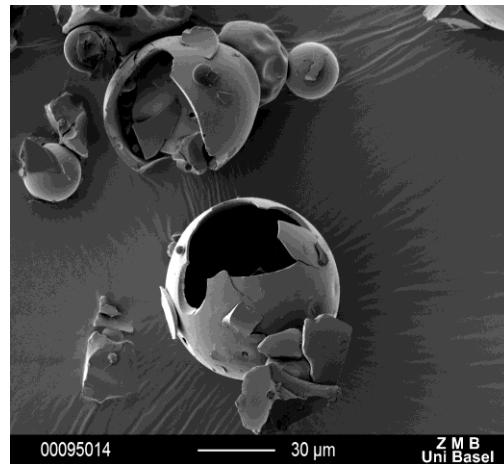
The use of copovidone and HPC conferred higher plasticity and also a certain degree of elasticity to the formulations [47]. However, the two binders showed different effects on compaction parameters. Copovidone showed an increase in RDP and RDP/MDP for MCC and pregelatinized starch, whereas HPC decreased RDP and RDP/MDP for all fillers except for pregelatinized starch. HPC as a binder was reported to act as an elastic body [48], and to reduce RDP and F_e as well [2]. By increasing the elasticity of the formulations, elastic recovery was more likely to occur during decompression phase. As a consequence, the compact contracted radially and expanded axially, which led to decreased values of RDP. The

increased plasticity conferred by HPC, which led to an increase in cohesive forces accompanied by decreased adhesive forces, was responsible for lower RDP values. Generally both binders lead to the increase of MDP for all materials (except for CHPD, no effect due to its brittle nature), which means increasing plasticity of the filler during compaction, a well known effect for binders [31, 49]. Both binders reduced F_e for plastic and/or brittle materials by enhancing axial over radial relaxation (high ER_0 values). It seemed also, that copovidone reduced the friction to the die-wall and acted as a lubricant due to its existence in spherical shaped particles [13]. Although ER_0 was increased by increasing HPC for different formulations, HPC increased MDP and reduced RDP (increased plasticity over elasticity), and thus the tendency for capping was decreased. Hence, cohesive forces within the powder were increased at the expense of adhesive forces. These findings are in accordance with those reported in previous studies [50, 51]. HPC showed greater binding capacity than copovidone by reducing RDP for all fillers; while in case of copovidone, RDP was reduced only with brittle/plastic materials. It was reported that both the small particle size and the molecular weight have an influence on the dry binding properties [13]. Moreover, fine particle sized HPC was reported to be commonly used as a “pressure binder” [48]. However, mean particle size was almost equal for the two binders, **Table 10**. Therefore, the superiority of HPC could be attributed to the higher molecular weight of HPC (ca 600 000) to that

of copovidone (45 000-70 000) which provide higher tendency for HPC to form bonding. Moreover, the shape also played an important role, where HPC exists as microfibrinous elongated particles while copovidone exists in form of spherical particles that offers less contact areas, **Figure 24**, so the former provides higher surface area. Also, HPC is highly plastic while copovidone consists of spherical particles which would undergo fracture to some extent [50].



(a)



(b)

Figure 24 SEM pictures showing the particles for (a) HPC, and (b) Copovidone

The increase of RDP for pregelatinized starch and MCC with copovidone could be attributed to the binder enhancement of the plastic component on the behalf of elastic component for these fillers, or due to the formation of liquid bridges with the die-wall due to its hygroscopicity [49]. The reduction of RTS for the brittle

fillers CHPD and lactose on the addition of HPC could be explained by the brittle deformation nature of these two fillers which lead to the continuous creation of new large number of clean sites without binder and hence weaker cohesion [9, 10, 48].

Effect of Drug loading on radial die wall pressure and compressibility

By increasing paracetamol loading for materials with viscoelastic behavior such as MCC and pregelatinized starch; RDP and RDP/MDP, ($p=0.00001$), as well as F_e ($p< 0.05$), and μ_e ($p< 0.03$) were increased by increasing paracetamol loading, **Figure 25a**, leading to higher tendency of capping and lamination. Capping tendency of paracetamol was quite reported [52-54]. The reason is mainly due to the increased elasticity of the formulation [15, 55, 56]. Although paracetamol has an elastic component like pregelatinized starch and MCC, unlike these fillers paracetamol shows higher RDP values [1]. Moreover, it was reported that paracetamol particles showed very high adhesion [57], consequently, the RDP values of pregelatinized starch and MCC were increased with higher paracetamol loadings. Hence, friction and F_e were increased for these fillers. On the contrary, by increasing paracetamol loading for materials with plastic/brittle behavior(s) such as mannitol, lactose, and CHPD; RDP and RDP/MDP ratio were decreased, ($p=0.00001$), **Figure 25b**, and this was accompanied by an increase in ER_0 ($p< 0.05$) and a decrease in F_e ($p< 0.05$), and μ_e ($p< 0.01$). This is attributed to the

fragmentation character of the drug as well as increasing axial over radial relaxation propensity for these fillers, especially at high speed [58].

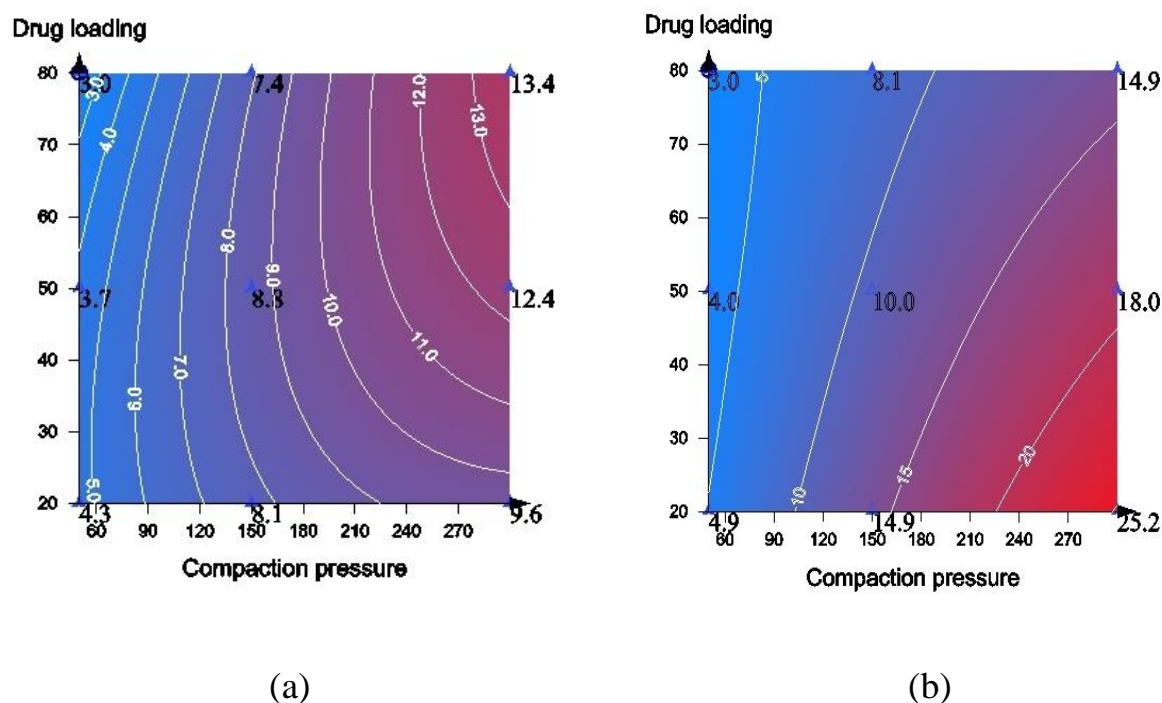


Figure 25 Contour plots showing the effect of drug loading on RDP (values in black on the right) for (a) MCC, (b) Lactose at compaction speed 2 m/s

Regarding formulations compressibility, the relation between compression force and compact volume followed the semi logarithmic pattern. Compressibility slopes for the five fillers with different drug loadings (20, 50, 80 % w/w) at low and high compaction speeds (0.5, 2 m/s) are shown in **Table 11**. Pregelatinized starch showed the highest slopes while CHPD showed the lowest due to elastic nature of the former and brittle behavior of the later. Also, mannitol showed the greatest

slope change by increasing drug loading and compaction speed due to its high plasticity, while CHPD showed almost no change. Compressibility of MCC, mannitol, and lactose showed lower values at high drug loading due to the poor compressibility of paracetamol caused by its irregular particle shape [59]. **Table 12** shows the degree of correlation between compact volume and MDP. Again, mannitol showed the strongest correlation and CHPD showed almost the weakest. This is again due to the high plastic and brittle behaviors of mannitol and CHPD, respectively. **Table 13** summarizes the effects of the all previously discussed formulation variables on RDWP and other compaction parameters.

Table 11 Compressibility slopes of different fillers at different paracetamol loadings (20, 50, 80 % w/w) at low and high compaction speeds (0.5, 2 m/s)

	MCC	Mannitol	SDL	Pregelatinized Starch	CHPD
0.5/20%	-0.028	-0.029	-0.02	-0.045	-0.019
R²	0.9835	0.9991	0.9948	0.9824	0.9987
0.5/50%	-0.026	-0.025	-0.018	-0.043	-0.019
R²	0.9895	0.9978	0.9916	0.986	0.9993
0.5/80%	-0.023	-0.021	-0.016	-0.044	-0.021
R²	0.9992	0.9744	0.9952	0.9836	0.997
2.0/20%	-0.031	-0.032	-0.021	-0.046	-0.021
R²	0.9821	0.999	0.9942	0.9785	0.9972
2.0/50%	-0.029	-0.026	-0.019	-0.045	-0.02
R²	0.9963	0.9985	0.9936	0.9783	0.9993
2.0/80%	-0.026	-0.022	-0.016	-0.046	-0.021
R²	0.999	0.9673	0.9986	0.9769	0.9999

Table 12 Pearson correlation between compact volume and MDP

Filler	Pearson correlation MDP/ compact volume
MCC	-0.865296022
Mannitol	-0.914985077
SDL	-0.828681748
Pregelatinized Starch	-0.883139632
CHPD	-0.608614118

Table 13 Effect of formulation variables on RDWP and other compaction parameters

Response	Lubricant		Binder		Drug Loading	
	plastic/elastic	plastic/brittle	plastic/elastic	plastic/brittle	plastic/elastic	plastic/brittle
RDP	↑	↓	↑	↓	↑	↓
MDP	↑	↑/-	↑/-	↑/-	-	-
RDP/MDP	-	↓	↑	↓	↑	↓
SR	↑/-	↑/-	↑	↑/-	-	-
F_e	↓	↓/-	-	↓	↑	↓
μ_e	↓	↓/-	-	↓	↑	↓
μ_c	↑	-	-	-	-	-
ER₀	↑	-	↑/-	↑/-	-	↑
RTS	NA	NA	NA	↓	NA	NA

- = No Effect, ↑ = Increasing, ↓ = Decreasing; NA = Not available data because of capping

Conclusion

Regarding the effects of lubricants and binders on the formulation, RDP was well correlated with F_e for materials with plastic and/or brittle behavior, whereas viscoelastic materials showed no correlation due to their elasticity, which reduced RDP during decompression. The RDP/MDP ratio was not suitable as a sensitive parameter for the evaluation of lubricants, since it only changed for plastic and/or brittle materials. Also, the MDP parameter was a good predictor for axial pressure transmission to the die-wall. External lubrication reduced the die-wall-compact friction without affecting the deformation behavior of the formulation. Not only would the continuous monitoring for the increase of RDP be a good indicator to predict capping but understanding of the deformation behavior of the compacted material is important as well. Additives enhancing the elasticity like HPC or weakening the bonds such as Mg stearate promoted the occurrence of capping and lamination. While, additives improving the mechanical strength of compacts such as copovidone, reduced capping tendency. High RDP values are not always responsible for capping, because MCC exhibited low RDP values and still showed capping, therefore, other parameters such ER_0 and tensile strength should also be considered. Moreover, high compaction force combined with high speed should be also avoided to prevent capping occurrence, especially at high drug loading.

References

- [1] Doelker E, Massuelle D. Benefits of die-wall instrumentation for research and development in tableting. *Eur J Pharm Biopharm* 2004; 58: 427-444.
- [2] Fukuda T, Fukumori Y, Wada S, Hanyu Y. Internal friction of compressed pharmaceutical powders observed in terms of the die wall pressure. *Chem Pharm Bull* 1980; 28: 393-400.
- [3] Hirai Y, Okada J. Effect of lubricant on die wall friction during compaction of pharmaceutical powders. *Chem Pharm Bull* 1982; 30: 684-694.
- [4] Staniforth JN, Cryer S, Ahmed HA, Davies SP. Aspects of pharmaceutical tribology. *Drug Dev Ind Pharm* 1989; 15: 2265-2294.
- [5] Wang J, Wen H, Desai D. Lubrication in tablet formulations. *Eur J Pharm Biopharm* 2010; 75: 1-15.
- [6] Lerk CF, Bolhuis GK, Smedema SS. Interaction of lubricants and colloidal silica during mixing with excipients I. Its effect on tableting. *Pharm Acta Helv* 1977; 52: 33-39.

- [7] Nicklasson M, Brodin A. The coating of disk surfaces by tablet lubricants, determined by an intrinsic rate of dissolution method. *Acta Pharm Suec* 1982; 19: 99-108.
- [8] Rowe RC. The coating of tablet surfaces by lubricants as determined by a film/tablet adhesion measurement. *Acta Pharm Suec* 1983; 20: 77-80.
- [9] Nyström C, Mazur J, Sjögren J. Studies on direct compression of tablets II. The influence of the particle size of a dry binder on the mechanical strength of tablets. *Int J Pharm* 1982; 10: 209-218.
- [10] Zhang Y, Law Y, Chakrabarti S. Physical properties and compact analysis of commonly used direct compression binders. *AAPS PharmSciTech* 2003; 4: 1-10.
- [11] Krycer I, Pope DG, Hersey JA. An evaluation of tablet binding agents part I. Solution binders. *Powder Technol* 1983; 34: 39-51.
- [12] Krycer I, Pope DG, Hersey JA. An evaluation of tablet binding agents part II. Pressure binders. *Powder Technol* 1983; 34: 53-56.
- [13] Kolter K, Flick D. Structure and dry binding activity of different polymers, including Kollidon VA 64. *Drug Dev Ind Pharm* 2000; 26:1159-1165.

- [14] Obiorah BA. Possible prediction of compression characteristics from pressure cycle plots. *Int J Pharm* 1978; 1: 249-255.
- [15] Garr JSM, Rubinstein MH. An investigation into the capping of paracetamol at increasing speeds of compression. *Int J Pharm* 1991; 72: 117-122.
- [16] Lin MC, Duncan-Hewitt WC. Deformation kinetics of acetaminophen crystals. *Int J Pharm* 1994; 106: 187-200.
- [17] Mollan Jr. MJ, Çelik M. Tableability of maltodextrins and acetaminophen mixtures. *Drug Dev Ind Pharm* 1994; 20: 3131-3149.
- [18] Hölzer AW, Sjögren J. Friction coefficients of tablet masses. *Int J Pharm* 1981; 7: 269-277.
- [19] Cunningham JC, Sinka IC, Zavaliangos A. Analysis of tablet compaction I. Characterization of mechanical behavior of powder and powder/tooling friction. *J Pharm Sci* 2004; 93: 2022-2039.
- [20] Fell JT, Newton JM. Determination of tablet strength by the diametrical-compression test. *J Pharm Sci* 1970; 59: 688-691.
- [21] Rowe RC, Sheskey PJ, Owen SC. Handbook of pharmaceutical excipients. 5th ed. Pharmaceutical Association and Pharmaceutical Press, London, United Kingdom, Washington, US; 2006 pp. 97, 132, 390, 450, 732.

- [22] Okada J, Matsuda Y, Fukumori Y. Measurement of the adhesive force of pharmaceutical powders by the centrifugal method II. Relation between the surface condition of substrates and the separation force-particle residue curves. *Yakugaku Zasshi* 1971; 91: 1207-1210.
- [23] Hölzer AW, Sjögren J. Evaluation of some lubricants by the comparison of friction coefficients and tablet properties. *Acta Pharm Suec* 1981; 18: 139-148.
- [24] Bolhuis GK, Lerk CF, Zijlstra HT, De Boer AH. Film formation by magnesium stearate during mixing and its effect on tableting. *Pharm Weekbl.* 1975; 110: 317-325.
- [25] Vromans H, Lerk CF. Densification properties and compactibility of mixtures of pharmaceutical excipients with and without magnesium stearate. *Int J Pharm* 1988; 46: 183-192.
- [26] Ebba F, Piccerelle P, Prinderre P, Opota D, Joachim J. Stress relaxation studies of granules as a function of different lubricants. *Eur J Pharm Biopharm* 2001; 52: 211-220.
- [27] Jarosz PJ, Parrott EL. Effect of lubricants on tensile strengths of tablets. *Drug Dev Ind Pharm* 1984; 10: 259-273.

- [28] Takeuchi H, Nagira S, Aikawa M, Yamamoto H, Kawashima Y. Effect of lubrication on the compaction properties of pharmaceutical excipients as measured by die wall pressure. *J Drug Deliv Sci Tec* 2005; 15: 177-182.
- [29] Kikuta J, Kitamori N. Evaluation of the die wall friction during tablet ejection. *Powder Technol* 1983; 35: 195-200.
- [30] Roberts RJ, Rowe RC. The young's modulus of pharmaceutical materials. *Int J Pharm* 1987; 37: 15-18.
- [31] De Boer AH, Bolhuis GK, Lerk CF. Bonding characteristics by scanning electron microscope of powders mixed with magnesium stearate. *Powder Technol* 1978; 20: 75-82.
- [32] Duberg M, Nyström C. Studies on direct compression of tablets XI: Evaluation of methods for the estimation of particle fragmentation during compaction. *Acta Pharm Suec* 1982; 19: 421-436.
- [33] Takeuchi H, Nagira S, Yamamoto H, Kawashima Y. Die wall pressure measurement for evaluation of compaction property of pharmaceutical materials. *Int J Pharm* 2004; 274: 131-138.

- [34] Delacourte A, Predella P, Leterme P. A Method for quantitative evaluation of the effectiveness of the lubricants used in tablet technology. *Drug Dev Ind Pharm* 1993;19:1047-1060.
- [35] Serwanis FS, Szabo-Revesz P, Pintye-Hódi K, Kása Jr P, Erös I. Surface treatment of acetylsalicylic acid with water-soluble lubricants in a fluid bed coater by the Wurster method. *Hung J Ind Chem* 1999; 27: 197-201.
- [36] Alvarez MC, Cuitino AM, Roddy MJ, Lordi NG. Comparison of the microstructure and mechanical behavior of visco-plastic and visco-elastic solids during compaction. *Pharm Sci* 1998; 1S: 179.
- [37] Rotthäuser B, Kraus G, Schmidt PC. Optimization of an effervescent tablet formulation containing spray dried L-leucine and polyethylene glycol 6000 as lubricants using a central composite design. *Eur J Pharm Biopharm* 1998; 46: 85-94.
- [38] Abdel-Hamid S, Betz G. Study of radial die-wall pressure changes during pharmaceutical powder compaction. *Drug Dev Ind Pharm* 2011; 37: 387-395.
- [39] Higuchi T, Shimamoto T, Eriksen SP, Yashiki T. Physics of tablet compression. XIV. Lateral die wall pressure during and after compression. *J Pharm Sci* 1965; 54: 111-118.

- [40] Gohel MC, Jogani PD. A review of co-processed directly compressible excipients. *J Pharm Pharmaceut Sci* 2005; 8: 76-93.
- [41] Gruber P, Glasel VI, Klingelholler W, Liske T. Direct lubrication of tablet tools, a contribution to the optimization of tablet manufacture. *Drugs Made Ger* 1991; 34: 24-30.
- [42] Otsuka M, Sato M, Matsuda M. Comparative evaluation of tableting compression behaviors by methods of internal and external lubricant addition: inhibition of enzymic activity of trypsin preparation by using external lubricant addition during the tableting compression process. *AAPS Pharm Sci* 2001; 3: 1-11.
- [43] Yamamura T, Ohta T, Taira T, Ogawa Y, Sakai Y, Moribe K, Yamamoto K. Effects of automated external lubrication on tablet properties and the stability of eprazinone hydrochloride. *Int J Pharm* 2009; 370: 1-7.
- [44] Fassihi AR. Consolidation behavior of polymeric substances in non disintegrating solid matrices. *Int J Pharm* 1988; 44: 249-256.
- [45] Larhrib H, Wells JI, Rubinstein MH. Compressing polyethylene glycols: the effect of compression pressure and speed. *Int J Pharm* 1997; 147:199-205.

- [46] Al-Nasassrah MA, Podczec F, Newton JM. The effect of an increase in chain length on the mechanical properties of polyethylene glycols. *Eur J Pharm Biopharm* 1998; 46: 31-38.
- [47] Herting MG, Klose K, Kleinebudde P. Comparison of different dry binders for roll compaction/dry granulation. *Pharm Dev Technol* 2007; 12: 525-532.
- [48] Picker-Freyer KM, Durig T. Physical mechanical and tablet formation properties of hydroxypropylcellulose: in pure form and in mixtures. *AAPS PharmSciTech* 2007; 8: E92.
- [49] Nyström C, Glazer M. Studies on direct compression of tablets. XIII. The effect of some dry binders on the tablet strength of compounds with different fragmentation propensity. *Int J Pharm* 1985; 23: 255-263.
- [50] Joneja SK, Harcum WW, Skinner GW, Barnum PE, Guo JH. Investigating the fundamental effects of binders on pharmaceutical tablet performance. *Drug Dev Ind Pharm* 1999; 25: 1129-1135.
- [51] Skinner GW, Harcum WW, Barnum PE, Guo JH. The evaluation of fine-particle hydroxypropylcellulose as a roller compaction binder in pharmaceutical applications. *Drug Dev Ind Pharm* 1999; 25: 1121-1128.

- [52] Alderborn G, Nyström C. Radial and axial tensile strength and strength variability of paracetamol tablets. *Acta Pharm Suec* 1984; 21: 1-8.
- [53] Malamataris S, Bin Baie S, Pilpel N. Plasto-elasticity and tableting of paracetamol, Avicel and other powders. *J Pharm Pharmacol* 1984; 36: 616-617.
- [54] Bangadu AB, Pilpel N. Effects of composition, moisture and stearic acid on the plasto-elasticity and tableting of paracetamol-microcrystalline cellulose mixtures. *J Pharm Pharmacol* 1985; 37: 289-293.
- [55] Carless JE, Leigh S. Compression characteristics of powders: radial die wall pressure transmission and density changes. *J Pharm Pharmacol* 1974; 26: 289-297.
- [56] Malamataris S, Hatjichristos T, Rees JE. Apparent compressive elastic modulus and strength isotropy compacts formed from binary powder mixes. *Int J Pharm* 1996; 141: 101-108.
- [57] Shimada Y, Yonezawa Y, Sunada H. Measurement and evaluation of the adhesive force between particles by the direct separation method. *J Pharm Sci* 2003; 92: 560-568.

- [58] Roberts RJ, Rowe RC. The effect of punch velocity on the compaction of a variety of materials. *J Pharm Pharmacol* 1985; 37: 377-384.
- [59] Garekani HA, Ford JL, Rubinstein MH, Rajabi-Siahboomi AR. Effect of compression force, compression speed, and particle size on the compression properties of paracetamol. *Drug Dev Ind Pharm* 2001; 27: 935-942.

Chapter 3: Investigating the effect of particle size and shape on high speed tableting through radial die-wall pressure monitoring³

Abstract

Context: Investigating particle properties such as shape and size is important in understanding the deformation behavior of the powder under compression during tableting. Particle shape and size control the pattern of powder rearrangement and interaction in the die and so the final properties of the compact. **Objective:** The aim of this chapter was to examine the effect of particle size and shape on compactability. Particle friction and adhesion were investigated through radial die-wall pressure (RDWP) monitoring. **Materials and Methods:** Powders and granules of different sizes and shapes of materials with different compaction behavior were used. Compaction simulation using the PressterTM with an instrumented die was applied. **Results and Discussion:** Small particle size increased residual die-wall pressure (RDP), and maximum die-wall pressure MDP ($p < 0.05$) for plastic and viscoelastic materials, respectively, while big particle size had an opposite effect. No effect was

³ "Reprinted from Int J Pharm, Vol.413 /No.1-2, S. Abdel-Hamid, F. Alshihabi, and G.Betz, Investigating the effect of particle size and shape on high speed tableting through radial die-wall pressure monitoring, Pages 29-35, Copyright (2011), with permission from Elsevier"

found on brittle material, however big particle size showed higher friction for such materials. Regarding morphology, fibrous elongated particles of microcrystalline cellulose had less friction tendency to the die-wall in comparison to rugged surface mannitol particles. **Conclusion:** RDWP monitoring is a useful tool to understand the compactability of particles on changing their size or shape.

Key words: particle size, shape, radial die-wall pressure, compaction, simulation

Introduction

Tablet formation depends on particles rearrangement or densification then interaction between these particles by bonding. The size of particles plays a role in this interaction regarding the available surface area and bonding propensity. There are international guidelines regarding acceptance of particle size distributions of new drug substances [1]. Particle size was reported to have an influence on the compression process during tableting [2, 3]. For direct compression, usually particle size in the range of 100-200 μm is used [4]. Granulation is often added as unit operation before the compaction step not only to enlarge particle size of the starting material but also to improve the mechanical properties under pressure [5, 6]. Particle size is related to deformation behavior like plastic/fragmentation transition, [7, 8]. Particle size influences the compact final porosity, tensile strength, and dissolution as well [9-12]. Studies on particle size in literature are mainly directed to the effect on tablet tensile strength and particle bonding [13-15]. Particle shape also plays an important role in the interparticulate as well as particle-die wall interaction [16]. Particle shape would determine the pattern of particles rearrangement in planes and consequently the type of bonding such as interlocking or solid bridges [17]. Particle shape and surface roughness could increase friction tendency and adhesion of the particles to the punch or die-wall leading to a well

known tableting problem which is sticking [18, 19]. It was even found that particle size and shape of powders control the efficiency of lubrication [20].

There is no previous work investigating the effect of particle size and shape on compaction through RDWP monitoring. Using a compaction simulator with an instrumented die, to match the compaction process in industrial presses is highly beneficial in early product development and scaling up [21]. The aim of this chapter was to investigate the effect of particle size and shape on compactability of powders and granules with different deformation behaviors through monitoring RDWP using a compaction simulator.

Materials and Methods

Materials

Microcrystalline cellulose MCC (Avicel[®] PH101, PH102, FMC Corporation, DE, US), directly compressible mannitol (Parteck[®] M200, M300 Merck KGaA, Darmstadt, Germany), calcium hydrogen phosphate dihydrate CHPD (Emcompress[®], JRS Pharma, Rosenberg, Germany), milled lactose monohydrate (SorboLac[®] 400, Meggle, Wasserburg, Germany), magnesium stearate (Mg-stearate, supplied by Sandoz AG, Basel, Switzerland), paracetamol (Rhodapap[®], Rhodia S.A., France), Kollidon[®] 30 (polyvinylpyrrolidone PVP, BASF, Burgbenheim, Germany).

Methods

Granulation

Granulation was done for size enlargement and forming many size ranges.

Granulation in fluidized bed granulator

The starting mixture for granulation was composed of paracetamol (64.82%), Avicel[®] PH101 (27.78%), and Kollidon[®] 30 (7.4%) as a binder. All granulations were carried in a Glatt GPCG-2 (Glatt, Binzen, Germany), top spray method. The binder solution (10 w/w % in aqueous solution) was sprayed onto the powder bed

using a nozzle assembled with 0.8 mm liquid insert and a 2 mm air cap with controlled atomizing air pressure (0.1 MPa) and spray rate (20 g/min). A constant inlet air temperature was chosen at 22°C. Batch size was 500 g.

Granulation in roller compactor

Dry granulation was done for Parateck[®] M200, and SorboLac[®] 400 with a Chilsonator IR220 and a FitzMill[®] LA1 (Fitzpatrick, Belgium), with a roll pressure 0.35 MPa, roll speed 2 rpm, milling speed 600 rpm, and screen sieve size 1mm.

Powder/Granules Characterization

True density

True density of powders was measured by AccuPyc 1330 helium pycnometer (Micrometrics, Norcross, GA, US). A known weight of the samples was placed into the sample cell. Values were expressed as the mean of five parallel measurements.

Particle-size distribution

Powders: The average particle size was determined by laser diffraction with a Malvern Mastersizer X (Malvern Instruments, Worcestershire, UK). The measurements were carried out three times for each sample. Obscuration value between 10 to 30% was got in all measurements. The function “polydisperse” was

activated. Mean and median particle size, span, and specific surface area were recorded.

Granules: The size distribution was evaluated by the sieve analysis method using a sieve shaker (Vibro, Retsch, Haan, Germany) at level 40 for 25 min with 710, 500, 355, 250, 180, 125, and 90 μm ISO-norm sieves. The fraction remaining on each sieve was determined by weighing.

Morphological studies

Particle morphology was assessed by scanning electron microscopy (SEM) (Nova NanoSem 230, Eindhoven, Netherlands). Samples were mounted on aluminum stubs using double side adhesive carbon tape and sputter coated with gold 20 nm (BalTec MED 020 Coating System, Lichtenstein).

Powder/ Granules compaction

Powder compaction was carried out using a compaction simulator (Presster[™], Metropolitan Computing Corp., NJ, US) simulating the tablet press Korsch PH336 (36 stations). The compaction rolls used were 300 mm in diameter. Accordingly, a flat-faced B-tooling with a diameter of 10 mm was used to make tablets of 250 mg in weight. Powder feed was manually done. All formulations had 1% (w/w) Mg stearate as a lubricant. The machine was set to perform compaction pressures of 50,

150, and 300 MPa at the compaction speeds of 0.5, 1.5 and 2 m/s corresponding to the following dwell times (19, 6.4, and 4.8 ms), respectively. Six tablets were compressed at the same experimental conditions and the mean was calculated. Residual die-wall pressure (RDP), maximum die-wall pressure (MDP), work of compaction (WC), and ejection force (EF) were measured.

Lubrication ratio (LR) (ratio of lower to upper compression force), and axial to radial stress ratio (SR) (MDP to the average of upper and lower compression pressures) was also calculated.

Compact characterization

Radial tensile strength (RTS)

Crushing strength of a compact was determined by pressing it diametrically on a Pharmatron tablet tester (model 8D, Dr Schleuniger Pharmatron Inc., Solothurn, Switzerland). Radial tensile strength σ (MPa) was calculated according to:

$$\sigma = 2F/\pi dh \quad (1)$$

Where F is the force required to cause failure in tension (N), d is the compact diameter (mm), h is the compact thickness (mm), and π is a constant equals 3.1416. Compacts dimensions were measured using a micrometer with a precision of 0.01mm (Mitutoyo, Japan).

Porosity

Compact porosity was calculated from compact apparent density and dimensions according to the following equation:

$$\varepsilon = 1 - \left[\left(m / \pi . r^2 . h \right) / \rho_T \right] \quad (2)$$

Where ε is the in-die porosity, m is the compact mass (mg), r is the compact radius (5 mm), h is the in-die compact height (mm), ρ_T is the true density (mg/mm³) of powders/granules.

Elastic recovery (% ER_0)

The % ER_0 for a compact was calculated from “zero pressure thickness” that could be seen from the force vs. thickness plot, and “minimum punch gap” (thickness at maximum compression), features of Presster[®] software.

$$ER_0(\%) = T_i - T_m / T_m . 100 \quad (3)$$

Where T_i is the compact thickness at zero pressure just before ejection, T_m is the minimum compact thickness at maximum compression force.

Data interpretation

To study the effect of different compaction variables, runs were generated according to an experimental design using STAVEX[®] 5.0 (Aicos, Switzerland), applying a vertex-centroid design quadratic, D-optimization mode, **Table 14**. Compaction pressure (3 levels), speed (3 levels), and granular particle size (6-8 levels) were the factors. RDP, MDP, SR, EF, LR, ER₀, WC, RTS, and porosity were the responses. Least squares analysis was applied for the fitted model of optimization. The model was evaluated in terms of statistical significance using analysis of variance (ANOVA) at a level of significance ($p < 0.05$).

Table 14 Experimental design generated by STAVEX[®] 5.0 to study the impact of particle size on radial die-wall pressure and friction tendency

Run	Compression Pressure (MPa)	Compression Speed (m/s)	Particle Size		
			G1	G2	G3
1	50	0.5	1	2	1
2	50	2	1	2	1
3	50	0.5	2	3	3
4	50	2	2	3	3
5	50	0.5	3	4	4
6	50	0.5	4	4	4
7	50	2	4	5	5
8	50	0.5	5	5	5
9	50	2	5	6	6
10	50	0.5	6	6	6
11	50	2	6	7	7
12	50	1.5	3	7	7
13	150	2	3	1	8
14	150	1.5	4	1	2
15	300	0.5	1	1	2
16	300	2	1	7	2
17	300	0.5	2	2	8
18	300	2	2	2	1
19	300	0.5	3	3	1
20	300	0.5	4	3	3
21	300	2	4	4	3
22	300	0.5	5	4	4
23	300	2	5	5	4
24	300	0.5	6	5	5
25	300	2	6	6	5
26	300	1.5/2/0.5 ^a	3	6	6
27	300	0.5/2 ^b		7	6
28	300	2/0.5 ^b		7	7
29	300	1.5/2 ^b		1	7
30	300	0.5			8
31	300	2			8
32	300	1.5			2

G1 granules of mixture: Paracetamol (64.82%), Avicel[®] PH101 (27.78%), and Kollidon[®] 30 (7.4%)

G2 granules of SorboLac[®] 400, G3 granules of Parteck[®] M200; ^a G1/G2/G3, ^b G2/G3

Particle size (μm) (1) <90 (2) 90 (3) 125 (4) 180 (5) 250 (6) 355 (7) 500 (8) 710

Results and Discussion

True density and particle size distribution

Table 15 shows the true density, median and mean diameters, as well as the span (particle size distribution), and the specific surface area of the investigated powders.

Table 15 Median, and mean diameters, span, specific surface area, and true density of the investigated powders

Powder	Median [μm] \pm SD	Mean [μm] \pm SD	Span \pm SD	Specific Surface area [m^2/g] \pm SD	True density [g/cm^3] \pm SD
MCC PH 101	44.37 \pm 0.63	64.6 \pm 2.31	2.87 \pm $14 \cdot 10^{-2}$	0.14 \pm $3 \cdot 10^{-3}$	1.4383 \pm $0.2 \cdot 10^{-2}$
MCC PH 102	124.63 \pm 0.93	136.57 \pm 0.94	1.68 \pm $1 \cdot 10^{-3}$	0.0454 \pm $2.08 \cdot 10^{-4}$	1.5859 \pm $1.9 \cdot 10^{-3}$
ParateckM200	131.15 \pm 1.99	149.22 \pm 2.55	1.73 \pm $2.22 \cdot 10^{-2}$	0.0425 \pm $4.56 \cdot 10^{-4}$	1.5154 \pm $0.7 \cdot 10^{-3}$
ParateckM300	179.04 \pm 5.38	248.70 \pm 5.49	2.24 \pm $6 \cdot 10^{-2}$	0.05 \pm $0.2 \cdot 10^{-2}$	1.3868 \pm $0.1 \cdot 10^{-2}$
Emcompress	181.71 \pm 3.02	188.02 \pm 2.90	0.86 \pm $1.38 \cdot 10^{-2}$	0.0145 \pm $2.45 \cdot 10^{-4}$	2.4818 \pm $1.6 \cdot 10^{-3}$

Emcompress showed the highest density while Parateck M300 showed the lowest. MCC PH101 showed the lowest mean particle size (highest surface area) while Parateck M300 showed the largest particle size. However, Emcompress showed the lowest surface area due to the narrowest particle size distribution. MCC PH102 showed almost double the mean particle size of MCC PH101 and a narrower

distribution as well. Parateck M300 showed around 40% more bigger size than Parateck M200 and wider distribution. Particle size distribution was reported to be non critical for tablet porosity [22], so deeper investigation for size and shape was carried out in this chapter.

Particle shape

MCC PH101 and 102 are elongated fibrous particles with rough surface while Parateck M200 and 300 are almost spherical particles with rug surface, and Emcompress particles show bumpy fibrous surface, **Figure 26**. Regarding granules, MCC PH101/Paracetamol granules were fibrous in shape, while Parateck M200 and SorboLac 400 granules were irregular in shape; however SorboLac 400 granules had a smoother surface compared to the rug surface of Parateck M200 granules, **Figure 27**.

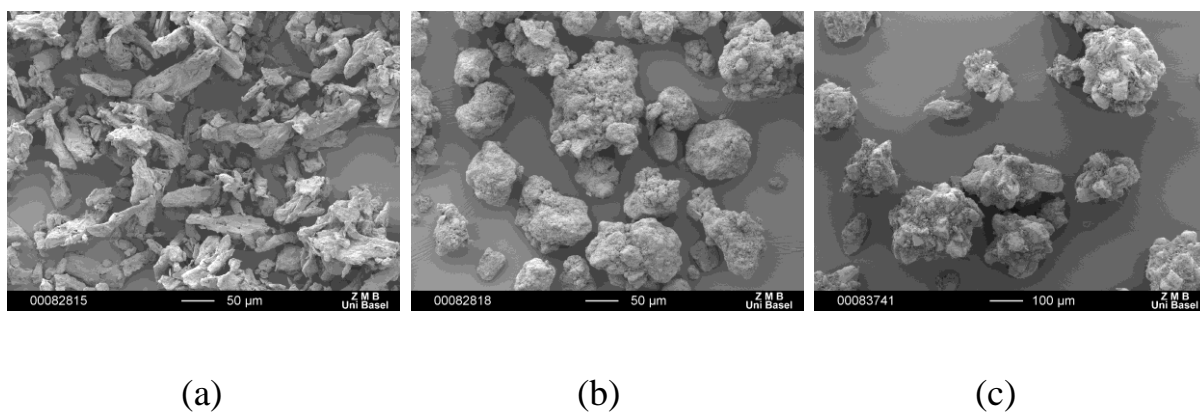


Figure 26 SEM pictures of the particles of (a) MCC PH101, (b) Parateck M200, and (c) Emcompress

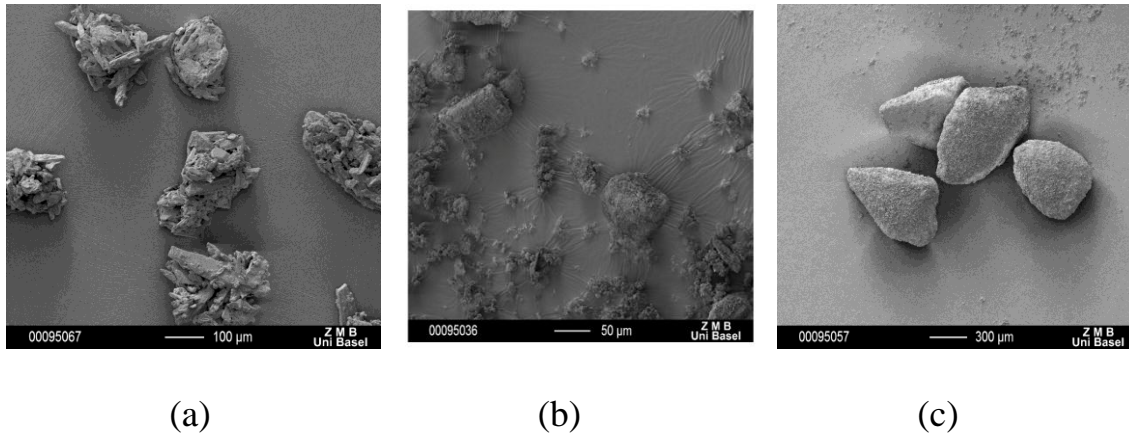


Figure 27 SEM pictures of the granules of (a) MCC PH101/Paracetamol, (b) Parateck M200, and (c) SorboLac 400

Corrugated or rough particles have more surface area than smooth particles that occupy the same volume. This contributes to higher ability of bonding with other particles or to the die-wall. Surface roughness could lead to increased tendency of friction and sticking [23, 24]. Irregular particle shape and surface roughness help in powder interlocking and hence ease of bonding [17]. Fibrous materials have higher surface area and so more potential bonding points [25]. For plastically deforming materials, a large surface area and surface roughness generally gives a greater bonding surface area, and hence stronger compacts [26].

Effect of particle size and shape on radial die-wall pressure

Powders

By increasing compaction pressure, there was no difference between the powders of MCC PH101 and 102 regarding the effect of particle size on RDP and MDP, the same result was found also for Parateck M200 and 300, **Figures 28** and **29**. This is in accordance with what was reported that there was no difference in compressibility for two particle sizes of MCC [27]. However, Parateck (mannitol) showed higher RDP values than MCC, while Emcompress had values in between. This was due to the higher axial ER_0 for MCC, **Figure 30**. Regarding MDP, there was no significant difference between powders until 150 MPa but by increasing compaction pressure further, MCC showed higher values emphasizing their superiority in plasticity. Regarding shape, Parateck particles showed more surface rugosity than those of Avicel. This resulted in higher radial stress transmission, hence higher RDP values for Parateck and higher friction tendency. The elongated MCC particles aligned themselves parallel to the punch face, forming a layered structure that exhibited low radial stress and a higher axial one i.e. higher elastic recovery.

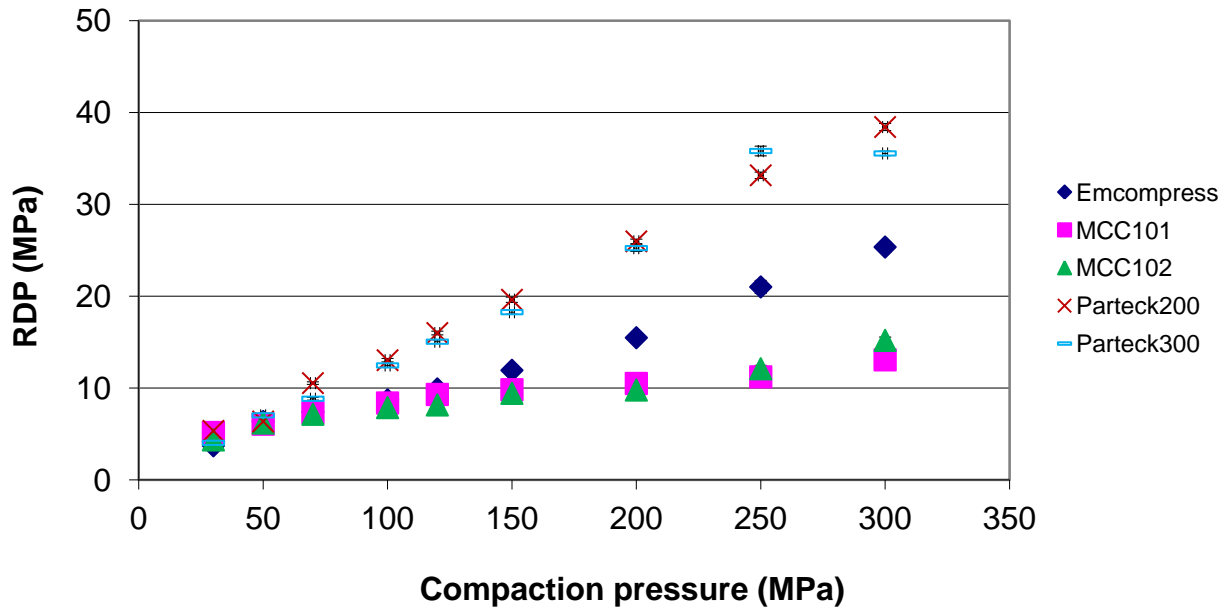


Figure 28 Effect of powders with different mean particle size on RDP

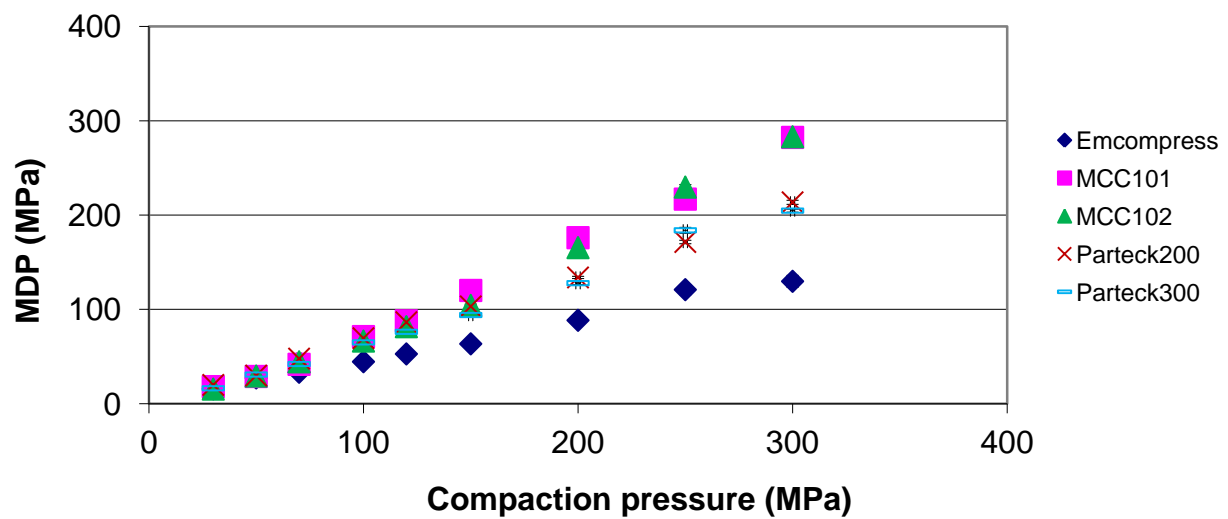


Figure 29 Effect of powders with different mean particle size on MDP

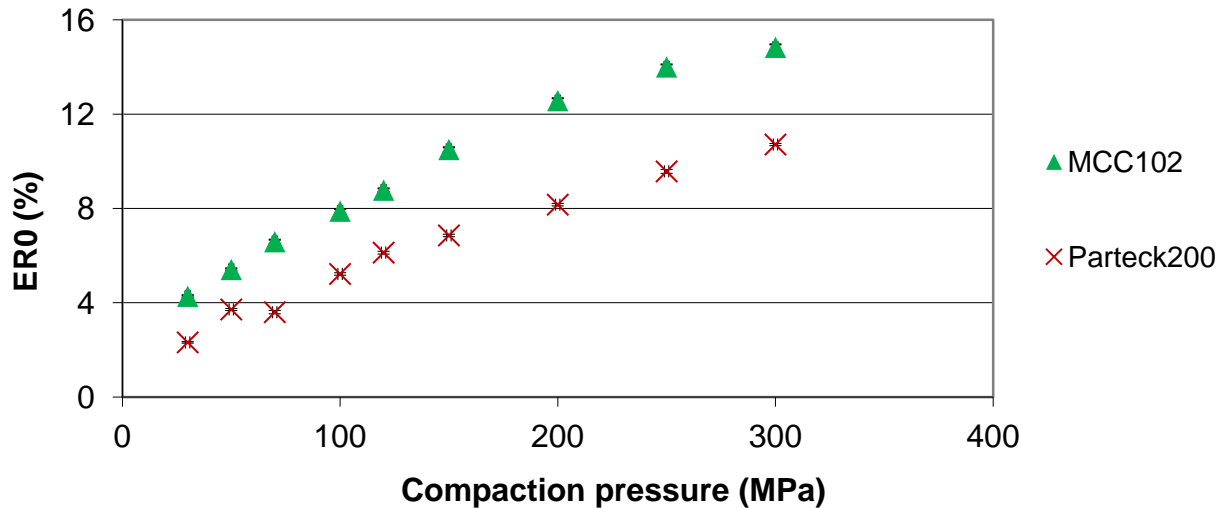


Figure 30 ER_0 of MCC PH102 and Parateck M200

Granules

Regarding models' diagnostics, the fit for all models for the different responses was very good (0.9920- 0.9999). There was no evidence for non-normality of model deviations (except for EF and ER_0 , there was a weak evidence for non-normality of model deviations; for RDP and MDP in case of Parateck M200 granules, there was a strong evidence for non-normality of model deviations for the former and weak evidence for the later. Means were independent on factor level.

Effect of size and shape on RDP and EF

Regarding granules, by increasing compression pressure, Parateck M200 granules less than 125 μm showed an increase in RDP while larger granules showed a decrease in RDP ($p < 0.05$), **Figure 31**. This was further confirmed by high EF for the small granules and low EF for the large granules, ($p < 0.0001$). This could be attributed to the higher interaction of small granules with the die-wall. It was also reported that larger particles exhibited higher degree of densification [28, 29], hence less particle-die interaction or friction. Small particles have higher tendency for friction which results in higher capability of bonding due to surface activation [30].

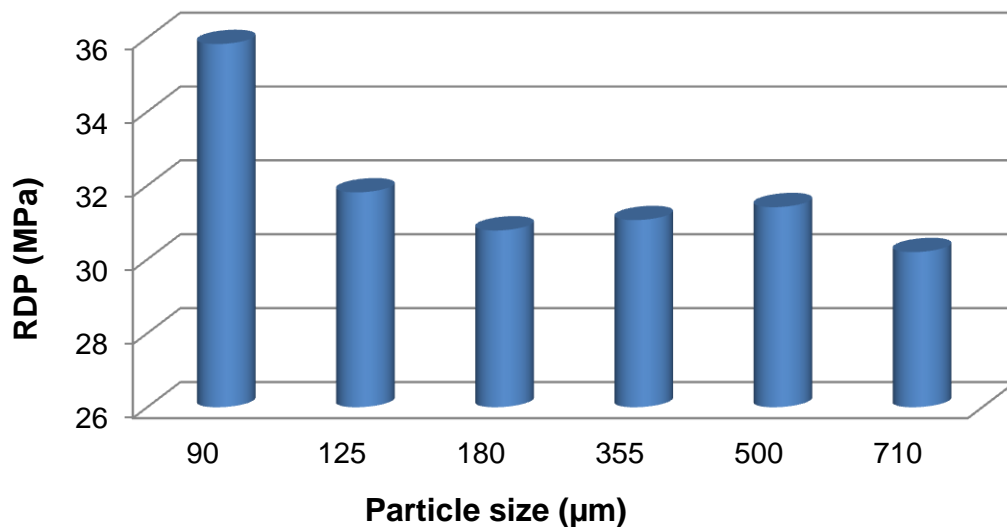


Figure 31 Effect of particle size of Parateck M200 granules on RDP at high compression pressure (300MPa) and speed (2 m/s) (RSE= 0.4)

On the other hand, MCC PH101/Paracetamol granules showed a decrease in RDP at high compaction pressure for granules below 125 μm , while larger granules showed an increase in RDP, ($p < 0.05$). This effect was confirmed by lower friction (low EF and high LR) for small granules; and higher friction (high EF and low LR) for large granules, ($p < 0.005$). This result could be explained by the presence of paracetamol as a major component in these granules, where for smaller granules; the effect of plastic MCC was more dominant on that of paracetamol, while in case of larger granules, the effect of paracetamol was more dominant due to high elastic recovery at high compression pressure. This is in accordance with the results of Patel and coworkers [29], who reported that large particles of paracetamol deformed mainly elastically while smaller particles deformed rather plastically. It was also reported that a change in particle size resulted in a different material deformation behavior [31]. Particle size of SorboLac 400 granules did not have any effect on RDP. This is due to fragmentation behavior of lactose [32, 33] where new contact points are continuously created by increasing compression, which leads to failure in bonding. Also, as shown previously lactose granules showed a smooth surface. Adolfsson and coworkers [15] reported that particle size had no effect on the bonding structure of lactose. Materials deforming by fragmentation show less ER_0 due to formation of numerous contact points between particles [24]. However, granules of SorboLac 400 less than 180 μm , showed low EF, while larger granules

showed high EF, ($p < 0.002$), **Figure 32**. This could be attributed to the decreased fragmentation propensity by increasing the particle size of lactose and due to the increase of irregularity by increasing particle size. This would lead to more friction for the large granules with the die-wall on ejection. This is in accordance with what was reported previously in literature [34-36].

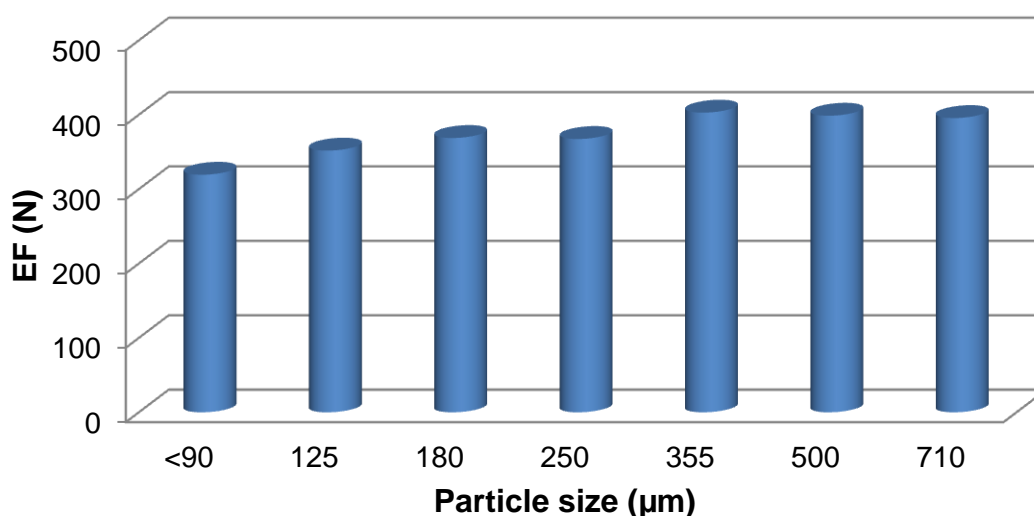


Figure 32 Effect of particle size of SorboLac 400 granules on EF at high compression pressure (300MPa) and speed (2 m/s) (RSE= 3.06)

Effect of size and shape on MDP and SR

Small granules behave more plastic [16]. That is why granules less than 125 μm of MCC PH101/Paracetamol, showed higher MDP ($p < 0.03$), **Figure 33**. This could be also attributed to the dominant effect of MCC PH101 in case of small granules while in case of large granules; the effect of fragmenting paracetamol was more

prominent. There was no difference between small and large granules of Parateck M200 and SorboLac 400 on MDP. However, the axial pressure transmission through granular bed SR was higher for granules less than 125 and 250 μm for Parateck M200 and SorboLac 400, respectively, than larger granules, ($p < 0.03$). This result could be explained by the smaller void volume and close particle packing in case of small particles while in case of larger particles, some of the compression force is spent in particle rearrangement and packing. On the other hand regarding Parateck M200 granules, speed reduced SR for granules less than 355 μm , ($p < 0.05$). Larger granules have better densification as mentioned before so the reduced dwell time was less influential on large than for smaller granules.

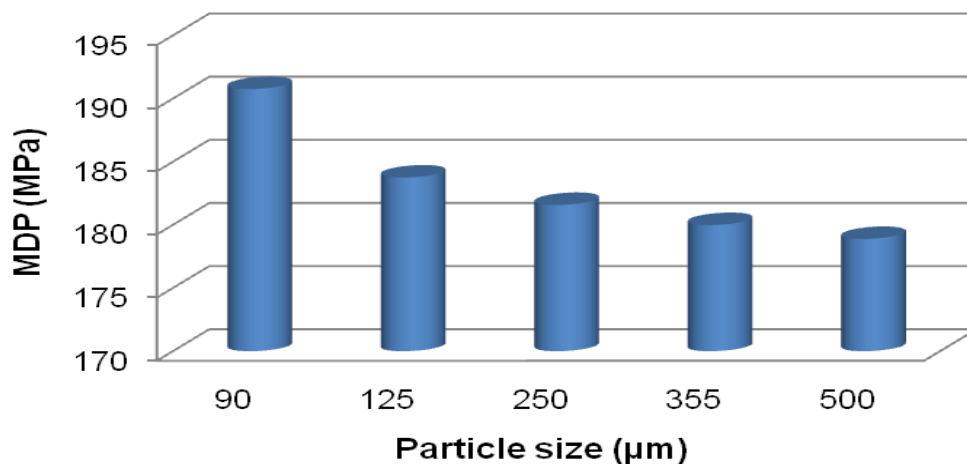


Figure 33 Effect of particle size of MCC PH101/ Paracetamol granules on MDP at high compression pressure (300MPa) and speed (2 m/s) (RSE= 1.13)

Effect of particle size and shape on ER_0 , WC, RTS, and Porosity

In this study, granules particle size had no effect on ER_0 , although literature was contradictory regarding this point where Patel and coworkers [29] reported that higher elastic recovery was observed for larger than smaller size particles, however Garekani and coworkers [37] reported an opposite result. Regarding the effect of particle size on WC, granules less than 180 and 125 μm for MCC PH101/Paracetamol and SorboLac 400, respectively, showed higher WC than larger granules ($p < 0.03$), which indicates more plastic behavior as mentioned before. This is attributed to the increased interparticulate interaction due to the numerous contact points per unit area for smaller particles. Similar results were reported by Garekani and coworkers [37]. By increasing compaction pressure, granules less than 355 μm were more porous than large ones ($p < 0.005$), for MCC PH101/Paracetamol and SorboLac 400. This could be explained by the higher degree of densification for larger particles and the higher interparticulate friction between small particles which hinders densification [38, 39]. Moreover, larger particles undergo continuous fragmentation by increasing pressure so as the smaller particles produced fill the voids [36, 40]. Regarding RTS, granules less than 125 μm of MCC PH101/Paracetamol formed stronger tablets ($p < 0.05$). This effect was reported previously where the van der Waal's forces increase when particle size decreases [15, 41, 42]. This is due to the intimate contact as well as the friction and

interaction between small granules which make them more ready for bond formation. This effect was only prominent in MCC PH101/Paracetamol granules due to the rough irregular surface which helped bonding [16].

Conclusion

Particle size and shape could completely change the compaction behavior of materials, which would finally affect the physical characters of the final compact. Particle size and shape play a big role in powder densification, cohesion, and adhesion during compaction. Small/irregular particles acted more plastically at high compression pressure and speed, showed better axial pressure transmission, more porous and stronger compacts, and had higher tendency for friction and sticking. The application of RDWP monitoring was very useful to understand these phenomena and was well correlated with other compaction parameters where RDP was well correlated to EF and MDP to SR.

References

- [1] International Conference on Harmonization (ICH). ICH 6QA- Specifications: Test procedures and acceptance criteria for new drug substances and new drug products: Chemical substances, 1999.
- [2] McKenna A, McCafferty DE. Effect of particle-size on the compaction mechanism and tensile- strength of tablets. J Pharm Pharmacol 1982; 34: 347-351.
- [3] Yajima T, Itai S, Hayashi H, Takayama K, Nagai T. Optimization of size distribution of granules for tablet compression. Chem Pharm Bull 1996; 44: 1056-1060.
- [4] Shekunov BY, Chattopadhyay P, Tong HHY, Chow AHL. Particle size analysis in pharmaceuticals: Principles, methods and applications. Pharm Res 2007; 24: 203-227.
- [5] Betz G, Junker-Bürgin P, Leuenberger H. Batch and continuous processing in the production of pharmaceutical granules. Pharm Dev Technol 2003; 8: 289-297.
- [6] Leuenberger H, Puchkov M, Krausbauer E, Betz G. Manufacturing pharmaceutical granules: is the granulation end-point a myth? Powder Technol 2009; 189: 141-148.

- [7] Roberts RJ, Rowe RC, Kendall K. Brittle-ductile transitions in the compaction of sodium chloride. *Chem Eng Sci* 1989; 44: 1647-1651.
- [8] Sebhatu T, Alderborn G. Relationships between the effective interparticulate contact area and the tensile strength of tablets of amorphous and crystalline lactose of varying particle size. *Eur J Pharm Sci* 1999; 8: 235-242.
- [9] Caraballo I, Millan M, Rabasco AM. Relationship between drug percolation threshold and particle size in matrix tablets. *Pharm Res* 1996; 13: 387-390.
- [10] Olsson H, Nyström C. Assessing tablet bond types from structural features that affect tablet tensile strength. *Pharm Res* 2001; 18: 203-210.
- [11] Sadeghi F, Garekani HA, Goli F. Tableting of Eudragit RS and propranolol hydrochloride solid dispersion: Effect of particle size, compaction force, and plasticizer addition on drug release. *Drug Dev Ind Pharm* 2004; 30: 759-766.
- [12] Siepmann J, Kranz H, Peppas NA, Bodmeier R. Calculation of the required size and shape of hydroxypropylmethylcellulose matrices to achieve desired drug release profiles. *Int J Pharm* 2000; 201: 151-164.
- [13] Sheikh-Salem M, Fell JT. The tensile strength of tablets of lactose, sodium chloride, and their mixtures. *Acta Pharm Suec* 1982; 19: 391-396.
- [14] Nokhodchi A, Rubinstein MH, Ford JL. The effect of particle size and viscosity grade on the compaction properties of hydroxypropylmethylcellulose 2208. *Int J Pharm* 1995; 126: 189-197.

- [15] Adolfsson A, Olsson H, Nyström C. Effect of particle size and compaction load on interparticulate bonding structure for some pharmaceutical materials studied by compaction and strength characterization in butanol. *Eur J Pharm Biopharm* 1997; 44: 243-251.
- [16] Sun C, Grant DJW. Effects of initial particle size on the tableting properties of L-lysine monohydrochloride dihydrate powder. *Int J Pharm* 2001; 215: 221-228.
- [17] Karehill PG, Glazer M, Nyström C. Studies on direct compression of tablets. XXIII. The importance of surface roughness for the compactability of some directly compressible materials with different bonding and volume reduction properties. *Int J Pharm* 1990; 64: 35-43.
- [18] Jones R, Pollocka HM, Geldartb D, Verlinden A. Inter-particle forces in cohesive powders studied by AFM: Effects of relative humidity, particle size and wall adhesion. *Powder Tech* 2003; 132: 196-210.
- [19] Jones R, Pollocka HM, Geldartb D, Verlinden-Luts A. Frictional forces between cohesive powder particles studied by AFM. *Ultramicroscopy* 2004; 100: 59-78.
- [20] Vromans H, Lerk CF. Densification properties and compactability of mixtures of pharmaceutical excipients with and without magnesium stearate. *Int J Pharm* 1988; 46: 183-192.

- [21] Abdel-Hamid S, Betz G. Study of radial die-wall pressure changes during pharmaceutical powder compaction. *Drug Dev Ind Pharm* 2011; 37: 387-395.
- [22] Fichtner F, Rasmuson A, Alderborn G. Particle size distribution and evolution in tablet structure during and after compaction. *Int J Pharm* 2005; 292: 211-225.
- [23] Pesonen T, Paronen P. The effect of particle and powder properties on the mechanical properties of directly compressed cellulose tablets. *Drug Dev Ind Pharm* 1990; 16: 31-54.
- [24] Nyström C, Alderborn G, Duberg M, Karehill PG. Bonding surface area and bonding mechanism – two important factors for the understanding of powder compactability. *Drug Dev Ind Pharm* 1993; 19: 2143-2196.
- [25] Gustafsson C, Bonferoni MC, Caramella C, Lennholm H, Nyström C. Characterization of particle properties and compaction behavior of hydroxypropylmethylcellulose with different degrees of methoxy/hydroxypropyl substitution. *Eur J Pharm Sci* 1999; 9: 171-184.
- [26] Alderborn G, Nyström C. Studies on direct compression of tablets IV. The effect of particle size on the mechanical strength of tablets. *Acta Pharm Suec* 1982; 19: 381-390.

- [27] Patel NK, Upadhyay AH, Bergum JS, Reier GE. An evaluation of microcrystalline cellulose and lactose excipients using an instrumented single station tablet press. *Int J Pharm* 1994; 110: 203-210.
- [28] Vromans H, Bolhuis GK, Lerk CF, Van de Biggelaar H, Bosch H. Studies on tableting properties of lactose 7: the effect of variations in primary particle size and percentage of amorphous lactose in spray dried lactose products. *Int J Pharm* 1987; 35: 29-37.
- [29] Patel S, Kaushal AM, Bansal AK. Effect of particle size and compression force on compaction behavior and derived mathematical parameters of compressibility. *Pharm Res* 2007; 24: 111-124.
- [30] Hüttenrauch R, Fricke S, Zielke P. Mechanical activation of pharmaceutical systems. *Pharm Res* 1985; 2: 302-306.
- [31] Alderborn G, Boryesson E, Glazer M, Nyström C. Studies on direct compression of tablets. XIX The effect of particle size and shape on the mechanical strength of sodium bicarbonate tablets. *Acta Pharm Suec* 1988; 25: 31-40.
- [32] Duberg M, Nyström C. Studies on direct compression of tablets VI. Evaluation of methods for the estimation of particle fragmentation during compaction. *Acta Pharm Suec* 1982; 19: 421-436.

- [33] Riepma KA, Veenstra J, De Boer AH, Bolhuis GK, Zuurman K, Lerk CF, Vromans H. Consolidation and compaction of powder mixtures: II. Binary mixtures of different particle size fractions of α -lactose monohydrate. *Int J Pharm* 1991; 76: 9-15.
- [34] Shotton E, Obiorah BA. Effect of physical properties on compression characteristics. *J Pharm Sci* 1975; 64: 1213-1215.
- [35] Alderborn G, Pasanen K, Nyström C. Studies on direct compression of tablets XI. Characterization of particle fragmentation during compaction by permeametry measurements of tablets. *Int J Pharm* 1985; 23: 79-86.
- [36] De Boer AH, Vromans H, Lerk CF, Bolhuis GK, Kussendrager KD, Bosch H. Studies on tableting properties of lactose III. The consolidation behavior of sieve fractions of crystalline α -lactose monohydrate. *Pharm Weekbl Sci* 1986; 8: 145-150.
- [37] Garekani HA, Ford JL, Rubinstein MH, Rajabi-Siahboomi AR. Effect of compression force, compression speed, and particle size on the compression properties of paracetamol. *Drug Dev Ind Pharm* 2001; 27: 935-942.
- [38] York P. Particle slippage and rearrangement during compression of pharmaceutical powders. *J Pharm Pharmacol* 1978; 30: 6-10.

- [39] Roberts RJ, Rowe RC. The effect of the relationship between punch velocity and particle size on the compaction behavior of materials with varying deformation mechanisms. *J Pharm Pharmacol* 1986; 38: 567-571.
- [40] Narayan P, Hancock BC. The relationship between the particle properties, mechanical behavior, and surface roughness of some pharmaceutical excipients compacts. *Mater Sci Eng* 2003; A355: 24-36.
- [41] Van der Watt JG. The effect of the particle size of microcrystalline cellulose on tablet properties in mixtures with magnesium stearate. *Int J Pharm* 1987; 36: 51-54.
- [42] Vromans H, De Boer AH, Bolhuis GK, Lerk CF, Kussendrager KD. Studies on tableting properties of lactose, Part 1. The effect of initial particle size on binding properties and dehydration characteristics of lactose. *Acta Pharm Suec* 1985; 22: 163-172.

Chapter 4: Radial die-wall pressure as a reliable tool for studying the effect of powder water activity on high speed tableting⁴

Abstract

Context: The effect of moisture as a function of water activity (A_w) on the compaction process is important to understand particle/water interaction and deformation. Studying powder /moisture interaction under pressure with radial die-wall pressure (RDWP) tool was never done. **Objective:** The aim of this chapter was to use this tool to study this interaction at high compression pressure and speed. Moreover, the effect of changing machine ejection cam angle (EA) on ejection force (EF) was investigated. Also, a new tool for prediction of tablet sticking was proposed. **Materials and Methods:** Materials with different deformation behaviors stored at low and high moisture conditions were used. Compaction simulation guided by modeling was applied. **Results and Discussion:** High A_w resulted in a low residual die-wall pressure (RDP) for all materials, and a high maximum die-wall pressure (MDP) for plastic materials, ($p < 0.05$). This was due to the

⁴ "Reprinted from Int J Pharm, Vol.411 /No.1-2, S. Abdel-Hamid and G.Betz, Radial die-wall pressure as a reliable tool for studying the effect of powder water activity on high speed tableting, Pages 152-161, Copyright (2011), with permission from Elsevier"

lubricating and plasticizing effects of water, respectively. However, microcrystalline cellulose showed capping at high A_w and compression pressure. By increasing compression pressure at high A_w for all materials, effective fall time (EFT) was increased, ($p < 0.05$), showing tendency for sticking. Increasing EA caused an increase of friction and EF for powders, ($p < 0.05$). **Conclusion:** RDWP was a useful tool to understand particle/moisture interaction under pressure.

Key words: water activity, radial die-wall pressure, ejection angle, sticking

Introduction

Water activity (A_w) is the active or free part of powder moisture content. By definition, A_w is the relative humidity which is reached at equilibrium for a product in a sealed container and is expressed on a scale of zero to one. A_w is also known as equilibrium relative humidity. Stubberud and coworkers [1] recommend studying the effect of moisture as a function of A_w if the degree of powder crystallinity is unknown. They suggest that the presence of moisture in powder during tableting may lead to phase transitions at high temperatures generated by the press machine. Generally moisture affects many powder characteristics like flowability and compact hardness and could later alter the compact disintegration or dissolution profile [2]. Moisture changes the cohesive/adhesive behavior of powder [3]. Moreover, moisture content could change the deformation behavior, bonding type, and area of particles [4, 5]. Effect of moisture on tableting compression cycles was previously reported by Touré and coworkers [6]. The presence of moisture in powder for a certain limit is important for compression and consolidation [7-13]. Water is reported to act as a plasticizer for polymers and amorphous powders, increasing molecular mobility, and lowers the glass transition temperature turning the material from a hard to a soft rubbery state [14-16]. Application of fully instrumented compaction simulators is helpful in

understanding the compaction cycle at early stages of development and in monitoring tablet production process as well [17]. Among the forces that could be measured by the sensors in the simulator, the adhesive force radially transmitted to the die-wall. Controlling such a tool is very beneficial to understand particles deformation and interaction with moisture under pressure and speed. Moreover, this parameter was rarely used in compaction research, and data regarding this issue are quite old and controversial. Another interesting feature of this chapter was the capability to change ejection cam angle (EA) by the aid of compaction simulation. No studies at all are found regarding the effect of changing ejection angle on ejection force. A major advantage of the simulator used in this study; the Presster, that this angle could be changed to investigate friction and ejection forces. In rotary machines, this angle is fixed to different values, e.g. Korsch: 13°; Fette: 12°. The aim of this chapter was to investigate the effect of A_w on compaction of powders through RDWP monitoring. Tools for early prediction of powder sticking were also applied. Moreover, the effect of ejection angle change on ejection was studied. Finally these tools were discussed and evaluated for a real application.

Materials and Methods

Materials

Microcrystalline cellulose MCC (Avicel[®] PH102, FMC Corporation, DE, US), directly compressible mannitol (Pardeck[®] M200, Merck KGaA, Darmstadt, Germany), calcium hydrogen phosphate dihydrate CHPD (Emcompress[®], JRS Pharma, Rosenberg, Germany), pregelatinized starch (Sta-Rx[®] 1500, Colorcon, Idstein, Germany), spray dried lactose monohydrate (Flowlac[®] 100, Meggle, Wasserburg, Germany), and magnesium stearate (Mg stearate, supplied by Sandoz AG, Basel, Switzerland).

Methods

Powder storage

Powders were stored for six weeks to ensure complete equilibrium in desiccators with two extreme conditions of relative humidity; (0% RH, temperature 19-20°C), and (90% RH, temperature 21-22°C) created by a saturated solutions of phosphorus pentoxide and potassium nitrate, respectively (analytical grade, Merck KGaA, Darmstadt, Germany).

Powder Characterization

Water activity (A_w)

Powder water activity as well as temperature were checked regularly with HygroPalm AW1 and HygroClip water activity station (Rotronic AG, Bassersdorf, Switzerland) before, during, and after compaction, see **Table 16**.

Table 16 Average water activity (A_w) values of powders before, during, and after compaction

Material	% RH	A_w	Temperature °C
MCC	0	0.042 ± 0.01	28.30 ± 1.63
	90	0.879 ± 0.02	29.00 ± 0.90
Pregelatinized starch	0	0.058 ± 0.01	28.90 ± 1.56
	90	0.882 ± 0.01	28.95 ± 1.06
Mannitol	0	0.305 ± 0.07	29.10 ± 1.14
	90	0.864 ± 0.02	29.50 ± 0.66
Lactose	0	0.234 ± 0.13	30.00 ± 2.12
	90	0.566 ± 0.23	30.35 ± 1.48
CHPD	0	0.285 ± 0.17	28.10 ± 0.99
	90	0.583 ± 0.23	28.40 ± 0.71

True density

True density of powders was measured by AccuPyc 1330 helium pycnometer (Micrometrics, Norcross, GA, US). A known weight of the samples was placed into the sample cell. Values were expressed as the mean of five parallel measurements.

Differential scanning calorimetry (DSC)

DSC was done to check any phase transitions after the storage of powders at the two different relative humidity conditions (Perkin Elmer DSC 4000, MA, US). Samples (4 to 8 mg) were encapsulated in aluminum pans with holes and heated in a temperature range of 0 to 250°C with a heating rate 10°C/min in a nitrogen atmosphere.

Powder compaction

Powder compaction was carried out using a compaction simulator (PressterTM, Metropolitan Computing Corp., NJ, US) simulating the tablet press Korsch PH336 (36 stations). The compaction rolls used were 300 mm in diameter. Accordingly, a flat-faced B-tooling with a diameter of 10 mm was used to make tablets of 250 mg in weight. Powder feed was manually done. All formulations had 1% (w/w) Mg-stearate as a lubricant. The machine was set to perform compaction pressures of 50 and 300 MPa at the compaction speeds of 0.5 and 2 m/s corresponding to the following dwell times (19, and 4.8 ms), respectively, and at the ejection angles of 5

and 15 degrees. Six tablets were compressed at the same experimental conditions and the mean was calculated. Residual die-wall pressure (RDP), maximum die-wall pressure (MDP), work of compaction (WC), ejection force (EF), take-off force (TO, force required to scrape the formed compact from the lower punch after ejection), and effective fall time (EFT, Time interval between 90% and 10% of the peak on the down slope for force/time compression curve) were measured. Moreover, axial to radial stress ratio (SR) (MDP to the average of upper and lower compression pressures), friction coefficient during compression FCC (μ_c), and friction coefficient during ejection FCE (μ_e) were calculated. Friction coefficients were calculated according to equation 1 [18] and equation 2 [19]:

$$\mu_e = \frac{F_e}{F_{r0}} \quad (1)$$

Where F_e is the ejection force and F_{r0} is the residual die-wall force.

$$\mu_c = \frac{D}{4H} \frac{F_U}{MDF} \left(\frac{F_L}{F_U} \right)^{\frac{LPD}{H}} \ln \frac{F_L}{F_U} \quad (2)$$

Equation (2), developed by Cunningham and coworkers, was modified in this study to fit the dynamics of the PressterTM. F_U and F_L are the upper and lower compression

forces, MDF is the maximum die-wall force, LPD is the lower punch displacement, D is the die diameter, and H is the compaction height.

Compact characterization

Radial tensile strength (RTS)

Crushing strength of a compact was determined by pressing it diametrically on a Pharmatron tablet tester (model 8D, Dr Schleuniger Pharmatron Inc., Solothurn, Switzerland). Radial tensile strength σ (MPa) was calculated according to:

$$\sigma = 2F/\pi dh \quad (3)$$

Where F is the force required to cause failure in tension (N), d is the compact diameter (mm), h is the compact thickness (mm), and π is a constant equals 3.1416. Compacts dimensions were measured using a micrometer with a precision of 0.01mm (Mitutoyo, Japan).

Porosity

Compact porosity was calculated from compact's apparent density and dimensions according to the following equation:

$$\varepsilon = 1 - \left[(m / \pi . r^2 . h) / \rho_T \right] \quad (4)$$

Where ε is the in-die porosity, m is the compact mass (mg), r is the compact radius (5 mm), h is the in-die compact height (mm), ρ_T is the true density (mg/mm³) of powders.

Elastic recovery (% ER_0)

The % ER_0 for a compact was calculated from “zero pressure thickness” that could be seen from the force vs. thickness plot, and “minimum punch gap” (thickness at maximum compression), features of Presster[®] software.

$$ER_0(\%) = T_i - T_m / T_m \cdot 100 \quad (5)$$

Where T_i is the compact thickness at zero pressure just before ejection, T_m is the minimum compact thickness at maximum compression force.

Differential scanning calorimetry (DSC)

A mass from the compact was snatched by a spatula and measured after compaction as mentioned above.

Data interpretation

To study the effect of different compaction variables, runs were generated according to an experimental design using STAVEX[®] 5.0 (Aicos, Switzerland), applying a 2-level full-factorial design, two blocks, unforced, modeling mode,

Table 17. Compaction pressure, speed, Aw, and EA (2- Level) were the factors. RDP, MDP, SR, EF, FCE, FCC, TO, EFT, WC, RTS, ER₀, and porosity were the responses. Least squares analysis was applied for the fitted model. The model was evaluated in terms of statistical significance using analysis of variance (ANOVA) at a level of significance ($p < 0.05$).

Table 17 Experimental design generated by STAVEX[®] 5.0 to study the effect of powder water activity (Aw) and machine's ejection cam angle (EA) on radial die-wall pressure at high/low compression pressures and speeds

Run	Compression Pressure (MPa)	Compression Speed (m/s)	Aw (%)	EA (degrees)
1	50	0.5	0	5
2	50	2	90	5
3	50	2	0	15
4	50	0.5	90	15
5	300	2	0	5
6	300	0.5	90	5
7	300	0.5	0	15
8	300	2	90	15
9	300	0.5	0	5
10	300	2	90	5
11	300	2	0	15
12	300	0.5	90	15
13	50	2	0	5
14	50	0.5	90	5
15	50	0.5	0	15
16	50	2	90	15

Results and Discussion

True density and Differential Scanning Calorimetry (DSC)

Table 18 shows the values of true density for powders used and DSC parameters.

Table 18 True density and DSC parameters of the investigated powders

Powder	True density \pm SD	RH (%)	Peak Temperature ($^{\circ}$ C) \pm SD	Delta H (J/g) \pm SD
MCC	$1.5859 \pm 1.9 \cdot 10^{-3}$	0	76.58 ± 1.65	168.08 ± 13.22
		90	76.68 ± 4.8	193.72 ± 16.9
Pregelatinized starch	$1.4964 \pm 0.6 \cdot 10^{-3}$	0	89.48 ± 3.01	237.05 ± 0.00
		90	83.73 ± 0.00	247.81 ± 0.00
Mannitol	$1.5154 \pm 0.7 \cdot 10^{-3}$	0	168.73 ± 0.36	249.67 ± 6.49
		90	168.49 ± 0.1	243.41 ± 1.07
Lactose	$1.5419 \pm 1.2 \cdot 10^{-3}$	0	145.63 ± 0.43	166.56 ± 24.59
		90	146.86 ± 0.11	175.79 ± 29.43
CHPD	$2.4818 \pm 1.6 \cdot 10^{-3}$	0	192.9 ± 1.32	392.79 ± 9.29
		90	194.54 ± 1.67	388.73 ± 21.55

The true density values for all powders were in the same range except for CHPD, which had the highest true density. Regarding DSC, powders showed almost the same thermograms at 0 and 90 % RH where peak temperature and Delta H did not significantly change. Also for compacts, the same result was found at low/high

speeds and compression pressures (results not shown). These results indicated no phase change due to moisture. Mannitol, lactose, and CHPD powders showed relatively high A_w before, during, and after compaction regarding to powder storage at 0% RH. Previous study showed that these powders were the least sensitive to moisture [20].

Effect of A_w on Residual Die-wall Pressure (RDP)

By increasing compression pressure and A_w , RDP was reduced for all powders, ($p < 0.00001$), except for pregelatinized starch where increasing compression pressure/speed at high A_w caused an increase in RDP, ($p < 0.003$). **Figure 34** shows the effect of A_w on RDP for MCC, where RDP was significantly reduced by increasing A_w .

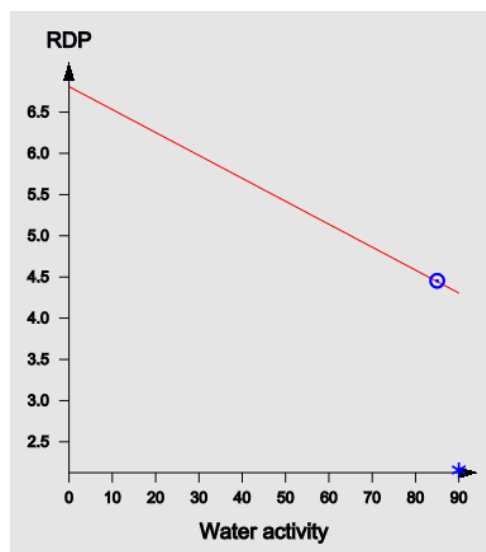


Figure 34 Effect of A_w on RDP for MCC

The reduction of RDP could be attributed to lubrication effect of water where adsorbed moisture reduces particle surface energy, hence adhesion to die-wall. Similar results were reported before [21-24]. However for pregelatinized starch, the increase of RDP at high speed /compression pressure is related to the increase in radial relaxation for pregelatinized starch compacts at these conditions by increasing A_w due to reduced interparticulate friction and interaction.

Effect of A_w on Maximum Die-wall Pressure (MDP)

By increasing compression pressure and A_w , MDP was increased for plastic powders MCC, pregelatinized starch, and mannitol, ($p < 0.007$). **Figure 35** shows the increase of MDP for MCC by increasing A_w .

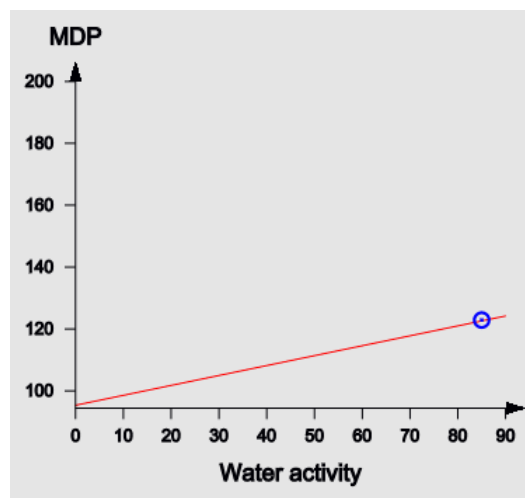


Figure 35 Effect of A_w on MDP for MCC

Regarding brittle powders; MDP was reduced for lactose, ($p < 0.05$), and no effect in case of CHPD. The increase of MDP was due to the increased plasticity of the powders by moisture. At high A_w , compression pressure caused an increase in MDP for MCC and pregelatinized starch, ($p < 0.00001$), due to plasticity enhancement and a decrease in MDP for lactose, ($p < 0.002$), due to the prevalence of its brittle nature and creation of new surfaces continuously that fail to adhere to the die-wall. On the other hand, increasing speed at high A_w led to the increase of MDP for pregelatinized starch which could be explained similar to the effect on RDP. Obiorah and Shotton [25] reported that moisture caused a slight increase of MDP for paracetamol and phenacetin. Nokhodchi and coworkers [26] reported that moisture improves plastic deformation for ibuprofen compacts. It was found that water acts as a plasticizer that increases molecular mobility and increases compressibility of powders [1, 27-33]. Moisture was reported to facilitate powder compression by reduction of interparticulate friction [24, 34]. Moreover, moisture was also reported to increase the rearrangement and slippage of particles and reducing interparticulate interactions [12, 35, 36]. In this study, CHPD and mannitol are crystalline in nature, while pregelatinized starch, MCC, and lactose have both crystalline and amorphous fractions [10, 31, 37-39]. Moisture increased the fluidity and molecular mobility of crystalline powders and changed hard, glassy, amorphous powders to a soft, rubbery

state, so the net result was an improvement in compressibility and high radial relaxation in response to applied axial pressure.

Effect of A_w on Stress Ratio (SR)

By increasing compaction pressure and A_w , stress transmission through powder bed was increased for all powders (except CHPD, no effect), ($p < 0.01$), which was attributed to the increase of plasticity for these powders as mentioned for MDP.

Figure 36 shows the effect of A_w on SR for pregelatinized starch where SR significantly increases by increasing A_w .

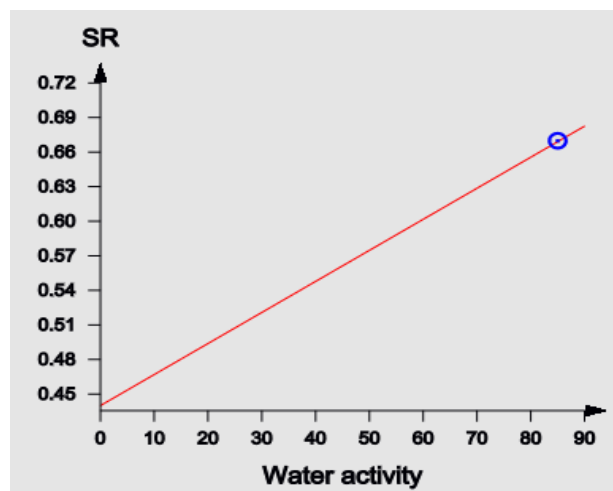


Figure 36 Effect of A_w on SR for pregelatinized starch

Increasing compression pressure at high A_w increased SR for MCC, ($p < 0.0001$), and reduced SR for lactose and pregelatinized starch, ($p < 0.0003$), because of the increase of fragmentation for the first and limited MDP increase relative for the

applied high axial pressure for the later. However at high A_w , speed increased SR for pregelatinized starch, ($p < 0.0001$), due to enhancing the plastic component over the elastic component where elastic recovery was reduced, as would be mentioned later. Moisture content within powder was reported to improve axial pressure transmission through powder bed due to improvement of densification [40, 41] and due to hydrodynamic lubrication [12].

Effect of A_w on Ejection Force (EF)

By increasing compaction pressure and A_w , EF was reduced for MCC, lactose, and CHPD, ($p < 0.0005$), due to lubrication effect as mentioned with RDP. No effect was found for pregelatinized starch, and mannitol. Increasing compression pressure at high A_w reduced EF for mannitol and CHPD due to the lubrication effect of moisture, ($p < 0.003$). Nokhodchi and coworkers [23] reported that an increase in moisture resulted in reduction of EF for ibuprofen compacts. This was due to reduction of particle adhesion to die-wall by the water film on the particle surface.

Effect of A_w on Friction Coefficient during Compaction (FCC) and Friction Coefficient during Ejection (FCE)

By increasing A_w , friction coefficient during compaction FCC was reduced for MCC, **Figure 37**, and pregelatinized starch, ($p < 0.0001$), due to die-lubrication effect by moisture and reduction of particulate friction. However, in case of

mannitol; FCC was increased. This could be due to the low sensitivity of mannitol to moisture [42]. No effect was found on lactose and CHPD due to their brittle nature.

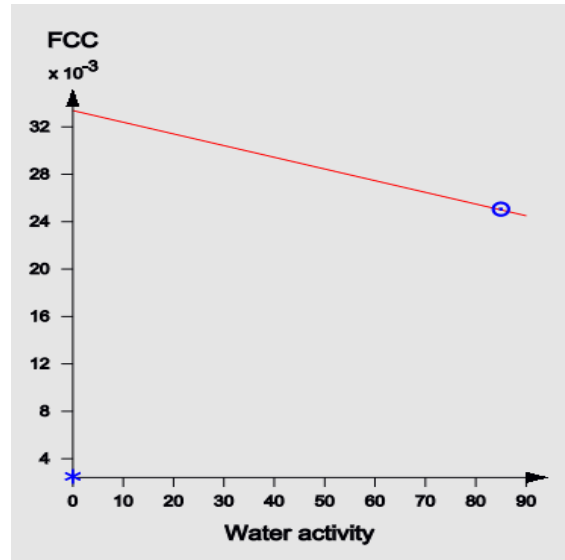


Figure 37 Effect of A_w on FCC for MCC

Regarding friction during ejection, by increasing A_w ; FCE was reduced for MCC, lactose, and CHPD, ($p < 0.02$), but increased in case of mannitol, ($p < 0.008$), **Figure 38**. This is explained similar to the effect of A_w on FCC. Similar results were reported by Shotton and Rees [43].

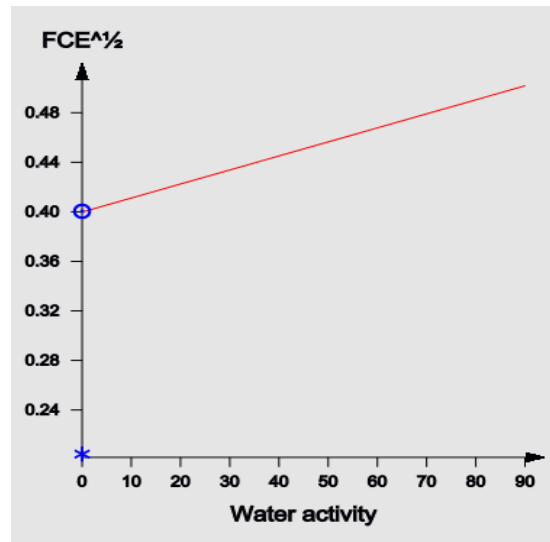


Figure 38 Effect of A_w on FCE for mannitol

Effect of A_w on Take-off force (TO) and Effective Fall Time (EFT) (sticking prediction tools)

By increasing A_w , TO force was enhanced only for pregelatinized starch, **Figure 39**, and CHPD, ($p < 0.008$), leading to higher tendency of sticking while TO force was reduced for lactose, ($p < 0.03$).

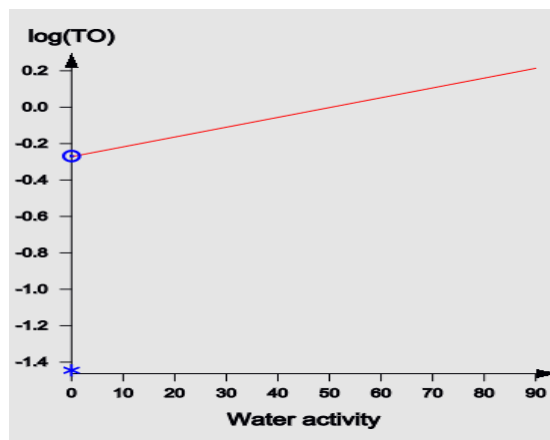


Figure 39 Effect of A_w on TO for pregelatinized starch

Moisture could act as a triggering agent to activate the surface of particles for adhesion. On the other hand, lactose showed a reduced TO force by increasing moisture due to smoother surface in comparison to CHPD [44]. TO force has been previously used as a prediction tool for sticking, however not sensitive enough to differentiate between the powders quantitatively [45]. Moisture was reported to be directly related to sticking [46, 47]. Pregelatinized starch was reported to show inherent sticking tendency by increasing moisture [48]. In this chapter, a new sticking prediction tool was proposed; EFT which is derived from the decompression time. A delay or an increase in EFT means upper punch sticking to the compact surface which requires more time for separation during decompression phase. It was found that by increasing compression pressure at high A_w ; all the powders showed an increase in EFT, ($p < 0.01$), showing tendency for sticking at these extreme conditions. **Figure 40** shows the effect of increasing A_w and compression pressure on pregelatinized starch where EFT was significantly increased. However by increasing A_w at low pressure, EFT was decreased for MCC, pregelatinized starch, and CHPD, ($p < 0.002$), due to water lubrication effect. Generally, speed decreases decompression time, however, interaction of speed and A_w increased EFT for pregelatinized starch, ($p < 0.007$) showing sticking tendency for this excipient and decreased EFT for lactose, ($p < 0.01$), due to its weak sensitivity for moisture and smooth surface as mentioned before.

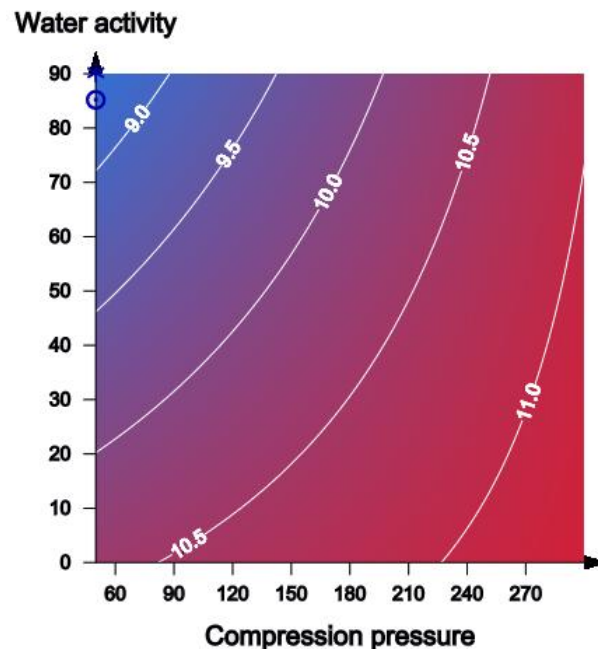


Figure 40 Effect of A_w on EFT for pregelatinized starch

Effect of A_w on Elastic Recovery (ER_0) and Radial Tensile Strength (RTS)

By increasing A_w , elastic recovery was reduced in case of MCC and pregelatinized starch, ($p < 0.001$), **Figure 41**. The presence of moisture led to the formation of strong hydrogen bonds for plastic materials and reduced ER_0 . This is in accordance with the results previously reported in literature [8, 12]. Nokhodchi and coworkers [23] reported that moisture reduced elastic energy for ibuprofen compacts by increasing Van der Waal's forces and reducing separation between particles. On the other hand, elastic recovery was increased for lactose by increasing A_w , ($p < 0.0001$), due to water multilayer formation on particle surface leading to an increase of the distance between particles and to a reduction of particles attraction

or bonding. This was further confirmed by the reduced RTS for lactose compacts, ($p < 0.0001$), **Figure 42**.

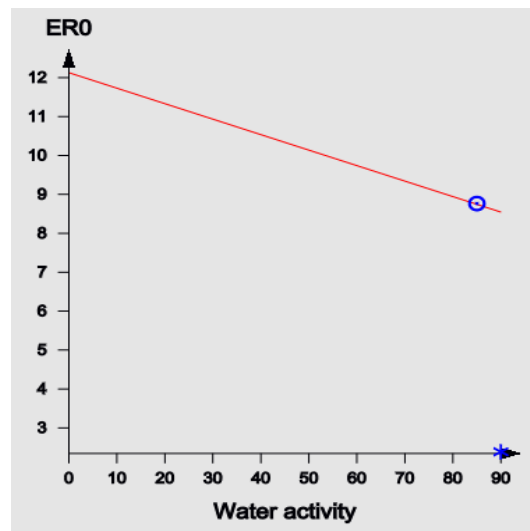


Figure 41 Effect of A_w on ER_0 for pregelatinized starch

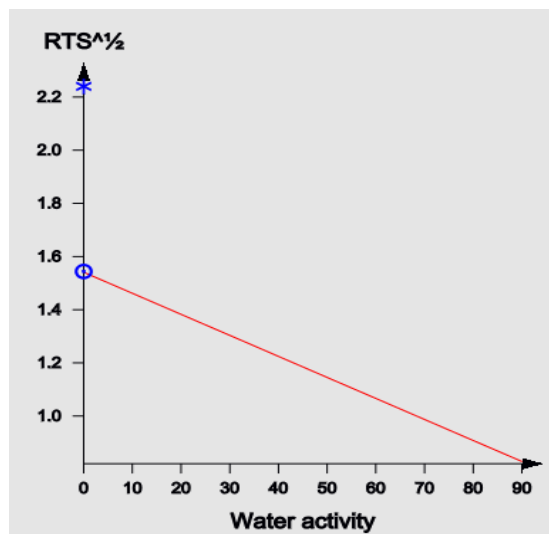


Figure 42 Effect of A_w on RTS for lactose

Lerk and coworkers [49] reported that removal of water of crystallization from α -lactose monohydrate resulted in higher tablet strength. Shukla and Price [50] reported a reduced RTS on increasing water content for lactose. Moisture was reported to reduce bonding between paracetamol particles [8, 51, 52]. By increasing compression pressure/speed at high A_w , ER_0 was increased for MCC. At these conditions, MCC compacts showed capping and lamination. Increasing speed caused shorter dwell time available for particle bonding, hence higher elastic recovery. These results are in accordance with those reported previously in literature [12, 23, 53]. In this study pregelatinized starch failed to form compacts at low A_w and low pressure which indicated the importance of moisture up to certain limits for successful compaction. This is in accordance with Zografi and Kontny [54] who reported that poor starch compacts were formed because of low moisture.

Effect of A_w on Work of Compaction (WC)

By increasing A_w , WC was reduced for all powders, ($p < 0.0001$), due to plasticizing effect of water by reduction of interparticulate friction and ease of particles slippage and arrangement, hence facilitated compressibility. Moisture content was reported to decrease plastic energy of compaction [11, 23, 31, 35, 55].

Effect of A_w on Porosity

By increasing A_w , porosity of the compacts was reduced for mannitol, lactose, and CHPD, ($p < 0.005$), and no effect was found for other powders. This could be explained by the condensation of water in the capillary region of powder bed at the area of contact between particles increasing the cohesion by liquid bridges. Such phenomenon was explained previously by Hiestand [56]. Armstrong and coworkers [57] reported reduction in porosity by increasing moisture for CHPD tablets. Garr and Rubinstein [12] reported that moisture increases the relative density of powder bed under compaction and Ahlneck and Alderborn [24] reported that high moisture reduced porosity. However at high compression pressures, porosity was increased for mannitol and lactose, ($p < 0.0003$), due to pressure effect where water is squeezed off the pores creating a porous structure. On the other hand, porosity was reduced for CHPD by increasing compression pressure at high A_w , ($p < 0.007$), due to its brittle nature and creation of new particles occupying the pores.

Effect of A_w on Ejection Angle (EA)

Not ever studied before, increasing the angle of ejection cam, enhanced the values of EF and FCE, ($p < 0.0001$), for all the powders (except mannitol, showed no effect). Thus, it is advised to adjust the EA to a minimum during compaction.

Figure 43 shows the effect of changing EA from 5 to 15 degrees on FCE for MCC

powder at high speed/ A_w and both low and high compression pressures where friction was increased.

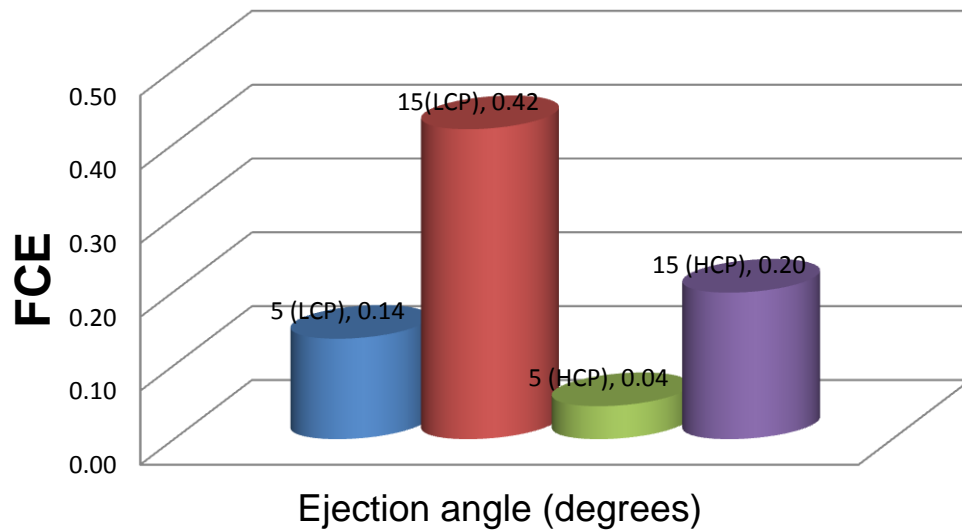


Figure 43 Effect of ejection angle change on FCE for MCC at high speed and A_w (LCP= Low compression pressure; HCP= High compression pressure) (RSE=0.01)

Conclusion

Aw or free moisture could give an estimate of the bound water in powder. Moisture could change the deformation behavior of particles. Radial die-wall monitoring was a useful tool to investigate particle/moisture interaction regarding cohesion and adhesion. Low RDP values induced by moisture showed low tendency for the particles to adhere to die-wall due to lubrication which was further confirmed by reduced other related compaction parameters like EF and friction coefficients. High MDP values induced by moisture plasticizing effects showed the ease of compressibility and good axial pressure transmission through powder bed. Moisture reduced elastic recovery due to decreased interparticulate interaction, reduced porosity due to filling of pores by water, and reduced tensile strength due to weakening of bonding. Moisture increased TO force due to activation of particle surface for bonding and reduced EFT due to lubrication effect. As a new reliable tool to detect sticking, EFT showed an increased value (delay in decompression) at high moisture and compression pressure. Regarding ejection, it is advised to keep the angle of ejection to a minimum during compaction in order to avoid the increase of EF and friction which could shorten the tablet machine and tooling life span.

References

- [1] Stubberud L, Arwidsson HG, Larsson A, Graffner C. Water–Solid interactions: II. Effect of moisture sorption and glass transition temperature on compactability of microcrystalline cellulose alone or in binary mixtures with Polyvinylpyrrolidone. *Int J Pharm* 1996; 134: 79-88.
- [2] Dawoodbahai S, Rhodes CT. The effect of moisture on powder flow and on compaction and physical stability of tablets. *Drug Dev Ind Pharm* 1989; 15: 1577-1600.
- [3] Maggi L, Bruni R, Conte U. Influence of the moisture on the performance of a new dry powder inhaler. *Int J Pharm* 1999; 177: 83-91.
- [4] Mollan MJ, Çelik M. The effects of humidity and storage time on the behavior of maltodextrins for direct compression. *Int J Pharm* 1995; 114: 23-32.
- [5] Sebhatu T, Elamin A, Ahlneck C. Effect of moisture sorption on tableting characteristics of spray dried (15% amorphous) lactose. *Pharm Res* 1994; 11: 1233-1238.
- [6] Touré P, Puisieux F, Duchene D, Carstensen JT. Energy terms in tablet compression cycles. *Powder Technol* 1980; 26: 213-216.

- [7] Rees JE. The use of compression modulus to describe compaction behavior. *J Pharm Pharmacol* 1970; 22: 245-246.
- [8] Khan KA, Musikabhumma P, Warr JP. The effect of moisture contents of microcrystalline cellulose on the compressional properties of some formulations. *Drug Dev Ind Pharm* 1981; 7: 525-528.
- [9] Armstrong NA, Patel A. The compressional properties of dextrose monohydrate and anhydrous dextrose of varying water content. *Drug Dev Ind Pharm* 1986; 12: 1885-1901.
- [10] Pilpel N, Ingham S. The Effect of moisture on the density, compaction and tensile strength of microcrystalline cellulose. *Powder Technol* 1988; 54: 161–164.
- [11] Shukla AJ, Price JC. Effect of moisture content on compression properties of two dextrose-based directly compressible diluents. *Pharm Res* 1991; 8: 336-340.
- [12] Garr JSM, Rubinstein MH. The influence of moisture on consolidation and compaction properties of paracetamol. *Int J Pharm* 1992; 81: 187-192.
- [13] Pande GS, Shangraw RF. Characterization of α -cyclodextrin for direct compression tableting: II. The role of moisture in the compactability of α – cyclodextrin. *Int J Pharm* 1995; 124: 231-239.

- [14] Oksanen CA, Zografi G. The relationship between the glass transition temperature and water vapor absorption of Polyvinylpyrrolidone. *Pharm Res* 1990; 7: 654- 657.
- [15] Slade L, Levine H. Beyond water activity: Recent advances based on an alternative approach to the assessment of food quality and safety. *Crit Rev Fd Sci Nutr* 1991; 30: 115-360.
- [16] Picker-Freyer KM, Durig T. Physical mechanical and tablet formation properties of hydroxypropylcellulose: in pure form and in mixtures. *AAPS PharmSciTech* 2007; 8: E92.
- [17] Doelker E, Massuelle D. Benefits of die-wall instrumentation for research and development in tableting. *Eur J Pharm Biopharm* 2004; 58: 427-444.
- [18] Hölzer AW, Sjögren J. Friction coefficients of tablet masses. *Int J Pharm* 1981; 7: 269-277.
- [19] Cunningham JC, Sinka IC, Zavaliangos A. Analysis of tablet compaction I. Characterization of mechanical behavior of powder and powder/tooling friction. *J Pharm Sci* 2004; 93: 2022-2039.
- [20] Sangekar SA, Sarli M, Sheth PR. Effect of moisture on physical characteristics of tablets prepared from direct compression excipients. *J Pharm Sci* 1972; 61: 939-944.

- [21] Rees JE, Shotton E. Effect of moisture in compaction of particulate material. *J Pharm Sci* 1971; 60: 1704-1708.
- [22] Staniforth JN, Baichwal AR, Hart JP, Heng PWS. Effect of addition of water on the rheological and mechanical properties of microcrystalline cellulose. *Int J Pharm* 1988; 41: 231-236.
- [23] Nokhodchi A, Rubinstein MH, Larhrib H, Guyot JC. The effect of moisture content on the energies involved in the compaction of ibuprofen. *Int J Pharm* 1995; 120: 13-20.
- [24] Ahlneck C, Alderborn G. Moisture adsorption and tableting: I. Effect on volume reduction properties and tablet strength for some crystalline materials. *Int J Pharm* 1989; 54: 131-141.
- [25] Obiorah BA, Shotton, E. The effect of waxes, hydrolyzed gelatin and moisture on the compression characteristics of paracetamol and Phenacetin. *J Pharm Pharmacol* 1976; 28: 629-632.
- [26] Nokhodchi A, Rubinstein MH, Larhrib H, Guyot JC. The effect of moisture on the properties of ibuprofen tablets. *Int J Pharm* 1995; 118: 191-197.
- [27] Khan F, Pilpel N. An investigation of moisture sorption in microcrystalline cellulose using sorption isotherms and dielectric response. *Powder Technol* 1987; 50: 237-241.

- [28] Lemagnen CG, Larrouture D. The use of stress relaxation trials to characterize tablet capping. *Drug Dev Ind Pharm* 1988; 14: 2179-2199.
- [29] Slade L, Levine H. Water relationships in starch transitions. *Carbohydr Polym* 1993; 21: 105-131.
- [30] Sebhatu T, Ahlneck C, Alderborn G. The effect of moisture content on the compression and bond-formation properties of amorphous lactose particle. *Int J Pharm* 1997; 146: 101-114.
- [31] Van der Voort Maarschalk K, Vromans H, Groenendijk W, Bolhuis GK, Lerk CF. Effect of water on deformation and bonding of pregelatinized starch compacts. *Eur J Pharm Biopharm* 1997; 44: 253-260.
- [32] Steendam R, Frijlink HW, Lerk CF. Plasticisation of amyloextrin by moisture: Consequences for compaction behavior and tablet properties. *Eur J Pharm Sci* 2001; 14: 245-254.
- [33] Zhang Y, Law Y, Chakrabarti S. Physical properties and compact analysis of commonly used direct compression binders. *AAPS PharmSciTech* 2003; 4: 1-10.
- [34] Coelho MC, Harnby N. Moisture bonding in powders. *Powder Technol* 1978; 20: 201-205.

- [35] Nokhodchi A, Ford J, Rowe P, Rubinstein M. The effect of moisture on the Heckel and energy analyses of hydroxypropylmethylcellulose 2208. *J Pharm Pharmacol* 1996; 48: 1121-1127.
- [36] Malamataris S, Karidas T, Goidas P. Effect of particle size and sorbed moisture on the compression behavior of some hydroxypropylmethylcellulose (HPMC) polymers. *Int J Pharm* 1994; 103: 205-215.
- [37] Günsel WC, Lachman L. Comparative evaluation of tablet formulations prepared from conventionally processed and spray-dried lactose. *J Pharm Sci* 1963; 52: 178-182.
- [38] Ahlneck C, Alderborn G. Moisture adsorption and tableting: II. The effect on tensile strength and air permeability of the relative humidity during storage of tablets of three crystalline materials. *Int J Pharm* 1989; 56: 143-150.
- [39] Salameh AK, Taylor LS. Physical stability of crystal hydrates and their anhydrides in the presence of excipients. *J Pharm Sci* 2006; 95: 446-461.
- [40] Jaffe J, Foss NE. Compression of crystalline substances. *J Amer Pharm Ass Sci* 1959; 48: 26-29.
- [41] Rees JE, Hersey JA. The strength of compacts containing moisture. *Pharm Acta Helv* 1972; 47: 235-243.

- [42] Yoshinari T, Forbes RT, York P, Kawashima Y. Improved compaction properties of mannitol after a moisture induced polymorphic transition. *Int J Pharm* 2003; 258: 121-131.
- [43] Shotton E, Rees E. The compaction properties of sodium chloride in the presence of moisture. *J Pharm Pharmacol* 1966; 18: 160S-167S.
- [44] Rowe RC, Sheskey PJ, Owen SC. Handbook of pharmaceutical excipients. 5th ed. Pharmaceutical Association and Pharmaceutical Press, London, United Kingdom, Washington, US; 2006, pp. 97, 396.
- [45] Wang JJ, Guillot MA, Bateman SD, Morris KR. Modeling of adhesion in tablet compression II. Compaction studies using a compaction simulator and an instrumented tablet press. *J Pharm Sci* 2004; 93: 407- 417.
- [46] Otsuka A. Adhesive properties and related phenomena for powdered pharmaceuticals. *Yakugaku Zasshi* 1998; 118: 127-142.
- [47] Shimada Y, Yonezawa Y, Sunada H. Measurement and evaluation of the adhesive force between particles by the direct separation method. *J Pharm Sci* 2003; 92: 560-568.
- [48] Waimer F, Krumme M, Danz P, Tenter U, Schmidt PC. A novel method for the detection of sticking of tablets. *Pharm Dev Technol* 1999; 4: 359-367.

- [49] Lerk CF, Andreae AC, De Boer AH, Bolhuis GK, Zuurman K, De Hoog P, Kussendrager KD, Van Leverink J. Increased binding capacity and flowability of α -Lactose monohydrate after dehydration. *J Pharm Pharmacol* 1983; 35: 747-748.
- [50] Shukla AJ, Price JC. Effect of moisture content on compression properties of directly compressible high beta-content anhydrous lactose. *Drug Dev Ind Pharm* 1991; 17: 2067-2081.
- [51] Malamataris S, Goidas P, Dimitriou A. Moisture sorption and tensile strength of some tableted direct compression excipients. *Int J Pharm* 1991; 68: 51-60.
- [52] Li LC, Peck GE. The effect of moisture content on the compression properties of maltodextrins. *J Pharm Pharmacol* 1990; 42: 272-275.
- [53] McKenna A, McCafferty DE. Effect of particle-size on the compaction mechanism and tensile- strength of tablets. *J Pharm Pharmacol* 1982; 34: 347-351.
- [54] Zografi G, Kontny MJ. The interactions of water with cellulose and starch-derived pharmaceutical excipients. *Pharm Res* 1986; 3: 187-194.
- [55] Esezobo S, Pilpel N. Moisture and gelatin effects on the interparticle attractive forces and compression behavior of oxytetracycline formulations. *J Pharm Pharmacol* 1976; 28: 75-81.

- [56] Hiestand EN. Powders: Particle–Particle Interactions. *J Pharm Sci* 1966; 55: 1325-1344.
- [57] Armstrong NA, Patel A, Jones TM. Relationship between porosity and water content of dicalcium phosphate tablets. *Int J Pharm* 1988; 48: 173-177.

Chapter 5: Investigating the effect of punch geometry on high speed tableting through radial die-wall pressure monitoring⁵

Abstract

Context: Dwell time mainly depends on punch geometry, so some tableting problems such as capping and lamination could occur at high speed compaction. Robust tools are required to monitor the interaction of punch tip and powder bed at these high speeds. **Objective:** The aim was to investigate the effect of punch geometry (flat and standard concave) on high speed compaction using radial die-wall pressure (RDWP) as a monitoring tool. **Materials and Methods:** Instrumented die guided by compaction simulation was applied for five materials with different compaction behaviors. **Results and Discussion:** Flat-faced punch showed higher residual, maximum die-wall pressures, and axial stress transmission than concave punches, ($p < 0.003$). Moreover, flat-faced punches showed less friction upon ejection, ($p < 0.003$). Flat compacts showed higher elastic recovery, tensile strength, and required less work of compaction than convex compacts, ($p < 0.05$). **Conclusion:**

⁵ "Reprinted from Pharm Dev Tech, Vol./No., S. Abdel-Hamid and G.Betz, Investigating the effect of punch geometry on high speed tableting through radial die-wall pressure monitoring, Pages 1-8, Copyright (2011), with permission from Informa Healthcare"

RDWP monitoring was a useful tool to prove that flat-faced punch induced higher radial stresses and particle/particle interactions in comparison to concave punch.

Key words: tooling geometry, radial die-wall pressure, high speed compaction, compaction simulation, density distribution, capping

Introduction

Tooling is important for effective pharmaceutical compaction and for the quality of the final compact. Tooling is referred to the set of punches and dies of a tablet press. The upper punch function is mainly compression and can be controlled by the adjustment of the penetration depth into the die. On the other hand, the lower punch has more functions in rotary presses such as die overfilling, moving up to allow excess powder scraping, compression, and finally ejection of compacts out of the die. Tooling is classified according to EU, TSM, and Japanese standards relative to the punch length and head dimensions. And for each design there are B and D types depending on punch barrel diameter. Tablet manufacture productivity highly depends on tooling, where some compaction problems such as capping, lamination, and sticking could arise regarding tooling geometry. The interaction between tooling and powder under pressure determines density distribution for this powder, so tooling geometry plays a key role in the compaction process [1]. The production of round surface tablets is usually not desired because this may lead to punch-to-die binding or self locking [2]. In comparison to flat-faced punches, higher compression forces are required for concave or cup-faced punches to compress the same powder mass or volume [3]. Sometimes, tooling helps to correct formulation defects by controlling tooling size and shape. Capping could occur whatever was

the tooling geometry where the development of a capping shear band for lactose compacts was reported to occur for both flat and convex compacts [4]. Understanding pressure distribution on punch tip surface is important for optimizing tooling design [5]. Punch geometry was reported to affect density distribution within compacts [6]. Although having more resistance against edge chipping, convex compacts are more liable to capping than flat-faced compacts [7]. Effect of punch geometry on powder compaction was never investigated before under conditions similar to real compaction (i.e. dwell time), where the studies were done at low speeds and at only single sided compaction. Nowadays the application of compaction simulation in pharmaceutical industry is no more an accessory. Simulation helps to deeply understand the process and fastens the scaling up process without problems, which saves money and time [8]. The Presster used in this study is a mechanical compaction replicator which allows mimicking production presses without any application of hydraulic control and hence, works under conditions close to production. RDWP monitoring was beneficial to investigate the compaction behavior of powders and detecting friction at early stage of development [9]. The aim was to use RDWP aided by compaction simulation for the first time to investigate the effect of flat and concave punch geometries on high speed tableting to be applied at development as well as during production.

Materials and Methods

Materials

Microcrystalline cellulose MCC (Avicel[®] PH102, FMC Corporation, DE, US), directly compressible mannitol (Pardeck[®] M200, Merck KGaA, Darmstadt, Germany), calcium hydrogen phosphate dihydrate CHPD (Emcompress[®], JRS Pharma, Rosenberg, Germany), pregelatinized starch (Sta-Rx[®] 1500, Colorcon, Idstein, Germany), spray dried lactose monohydrate (Flowlac[®] 100, Meggle, Wasserburg, Germany), magnesium stearate (Mg stearate, supplied by Sandoz AG, Basel, Switzerland). For basic studies, these materials cover the different deformation behaviors that could be shown by any formulation. MCC and pregelatinized starch are viscoelastic, mannitol is plastic, spray dried lactose is plastic/brittle, and CHPD is brittle [10-14].

Methods

Powder Characterization

True density

True density of powders was measured by AccuPyc 1330 helium pycnometer (Micrometrics, Norcross, GA, US). A known weight of the samples was placed into the sample cell. Values were expressed as the mean of five parallel measurements.

Particle-size distribution

The average particle size was determined by laser diffraction with a Malvern Mastersizer X (Malvern Instruments, Worcestershire, UK). The measurements were carried out three times for each sample. Obscuration value between 10 to 30% was got in all measurements. The function “polydisperse” was activated. Mean, median particle size, and span (particle size distribution) were recorded.

Powder compaction

Powder compaction was carried out using a compaction simulator (PressterTM, Metropolitan Computing Corp., NJ, US) simulating the tablet press Korsch PH336 (36 stations). The compaction rolls used were 300 mm in diameter. Accordingly, flat and standard cup B-tooling with a diameter of 10 mm was used to make tablets of 250 mg (350 mg for CHPD) in weight. Powder feed was manually done. The machine was set to perform compaction pressures of 50, 100, 150, 250, and 300 MPa at the compaction speeds of 0.5, 1, 1.5, and 2 m/s corresponding to the following dwell times (19, 9.5, 6.4, and 4.8 ms), respectively. The Presster carriage moves in a linear trend, so the speed was horizontal. Six tablets were compressed at the same experimental conditions and the mean was calculated. Residual die-wall pressure (RDP), maximum die-wall pressure (MDP), and work of compaction (WC) were measured. The die-wall pressure reaches a maximum value, MDP, just after

the upper and lower punches show maximum compression values, and shows a constant residual value, RDP, after upper and lower punch forces become zero. Axial to radial stress ratio (SR) (MDP to the average of upper and lower compression pressures) and friction coefficient during ejection FCE (μ_e) were also calculated. FCE (μ_e) was calculated according to the following equation [15]:

$$\mu_e = \frac{F_e}{F_{r0}} \quad (1)$$

Where F_e is the ejection force and F_{r0} is the residual die-wall force.

Compact characterization

Radial tensile strength (RTS)

Crushing strength of a compact was determined by pressing it diametrically on a Pharmatron tablet tester (model 8D, Dr Schleuniger Pharmatron Inc., Solothurn, Switzerland). Radial tensile strength σ (MPa) was calculated according to the equation [16]:

$$\sigma = 2F/\pi dh \quad (2)$$

Where F is the force required to cause failure in tension (N), d is the compact diameter (mm), h is the compact thickness (mm), and π is a constant equals 3.1416.

Compacts dimensions were measured using a micrometer with a precision of 0.01mm (Mitutoyo, Japan).

Porosity

Compact porosity was calculated from compact apparent density and dimensions according to the following equations:

For flat compacts:

$$\varepsilon = 1 - \left[\left(m / \pi . r^2 . h \right) / \rho_T \right] \quad (3)$$

For convex compacts:

$$\varepsilon = 1 - \left[\left(m / \left(80.16 + \left(\pi . r^2 . (h - 2.092) \right) \right) \right) / \rho_T \right] \quad (4)$$

Where ε is the in-die porosity, m is the compact mass (mg), r is the compact radius (5 mm), h is the in-die compact height (mm), 80.16 mm³ is the upper and lower cups' volume, 2.092 mm is the upper and lower cups' depth, and ρ_T is the true density (mg/mm³) of powders.

Elastic recovery (% ER_0)

The % ER_0 for a compact was calculated from “zero pressure thickness” that could be seen from the force vs. thickness plot, and “minimum punch gap” (thickness at maximum compression), features of Presster[®] software.

$$ER_0(\%) = T_i - T_m / T_m \cdot 100 \quad (5)$$

Where T_i is the compact thickness at zero pressure just before ejection, T_m is the minimum compact thickness at maximum compression force.

Data interpretation

To study the effect of different compaction variables, runs were generated according to an experimental design using STAVEX[®] 5.0 (Aicos, Switzerland) applying an external factorial design, linear/interaction; D-optimization, modeling mode, see **Table 19**. Compaction pressure (5 levels), speed (4 levels), and tooling shape (2 levels) were the factors. RDP, MDP, SR, FCE, ER_0 , RTS, WC, and porosity were the responses. Least squares analysis was applied for the fitted model. The model was evaluated in terms of statistical significance using analysis of variance (ANOVA) at a level of significance ($p < 0.05$).

Table 19 Experimental design generated by STAVEX[®] 5.0 to study the effect of tooling shape on radial die-wall pressure

Run	Compression Pressure (MPa)	Compression Speed (m/s)	Tooling Shape*
1	50	1.5	F
2	50	1.5	C
3	100	0.5	C
4	100	0.5	F
5	150	2	F
6	150	1	F
7	150	2	C
8	150	1	C
9	250	0.5	C
10	250	0.5	F
11	300	1.5	F
12	300	1.5	C

* (F) Flat-Face, (C) Standard Concave

Results and Discussion

True density and particle size distribution

Table 20 shows the median and mean diameters, and span (particle size distribution), as well as the true density of the investigated powders. Mean particle size of MCC, lactose, and mannitol were nearly equal, CHPD showed the largest mean particle size and narrowest particle size distribution while pregelatinized starch showed the smallest particle size and the widest particle size distribution. CHPD showed the highest density while densities of the other powders were almost the same.

Table 20 Median, and mean diameters, span, and true density of the investigated powders

Powder	Median [μm] \pm SD	Mean [μm] \pm SD	Span \pm SD	True density [g/cm^3] \pm SD
MCC	124.63 \pm 0.93	136.57 \pm 0.94	1.68 \pm $1 \cdot 10^{-3}$	1.5859 \pm $1.9 \cdot 10^{-3}$
Mannitol	131.15 \pm 1.99	149.22 \pm 2.55	1.73 \pm $2.22 \cdot 10^{-2}$	1.5154 \pm $0.7 \cdot 10^{-3}$
Lactose	124.87 \pm 1.10	131.44 \pm 1.01	1.43 \pm $6.66 \cdot 10^{-3}$	1.5419 \pm $1.2 \cdot 10^{-3}$
Pregelatinized starch	86.51 \pm 0.16	94.90 \pm 0.03	1.87 \pm $8.72 \cdot 10^{-3}$	1.4964 \pm $0.6 \cdot 10^{-3}$
CHPD	181.71 \pm 3.02	188.02 \pm 2.90	0.86 \pm $1.38 \cdot 10^{-2}$	2.4818 \pm $1.6 \cdot 10^{-3}$

Effect of punch geometry on Residual Die-wall Pressure (RDP), Maximum Die-wall Pressure (MDP), and Stress Ratio (SR)

For all materials both RDP and MDP were increased, ($p < 0.003$), by flat-faced punch in comparison to concave punch. **Figures 44-46** show the effect of punch geometry on radial die-wall pressure for MCC, lactose, and CHPD. It could be seen that both RDP and MDP were significantly increased (change from blue to red zones) by increasing both compression pressure and speed using flat-faced punch in comparison to concave punch. Moreover, flat-faced punch showed higher axial pressure transmission, ($p < 0.0001$). **Figure 47** shows the higher stress transmission through pregelatinized starch induced by flat punch in comparison to concave (change from blue to red zones).

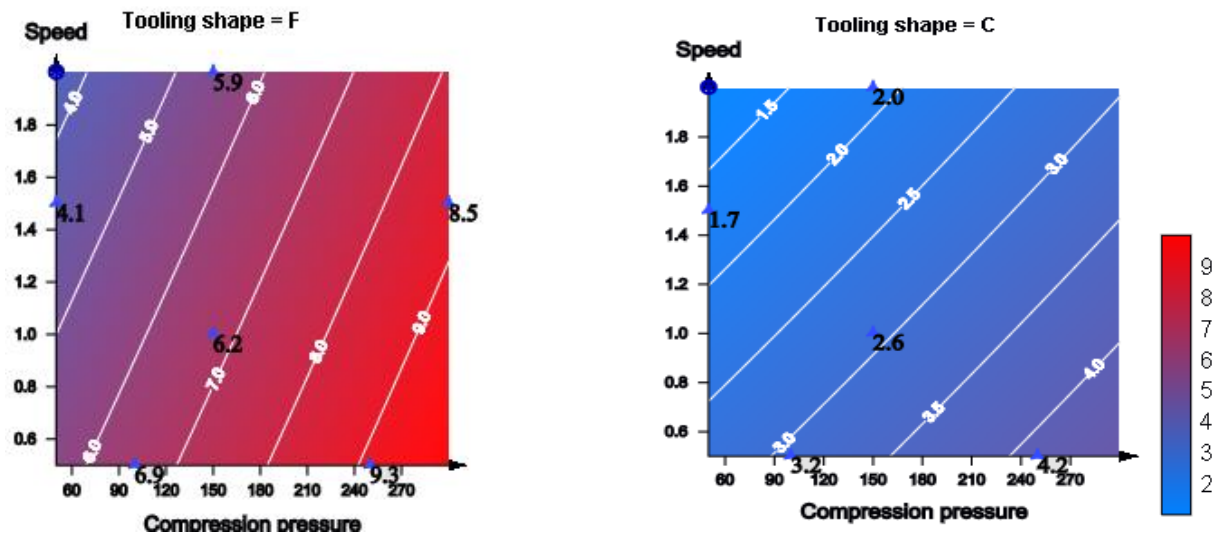


Figure 44 Contour plots showing the effect of flat (F) and concave (C) punch shapes on RDP for MCC

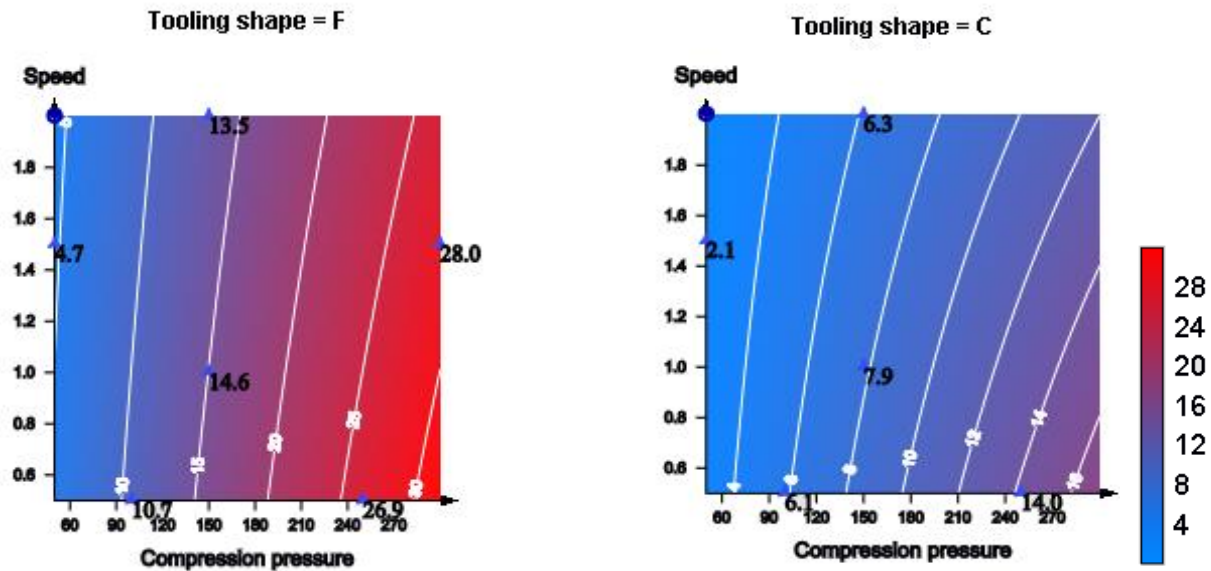


Figure 45 Contour plots showing the effect of flat (F) and concave (C) punch shapes on RDP for lactose

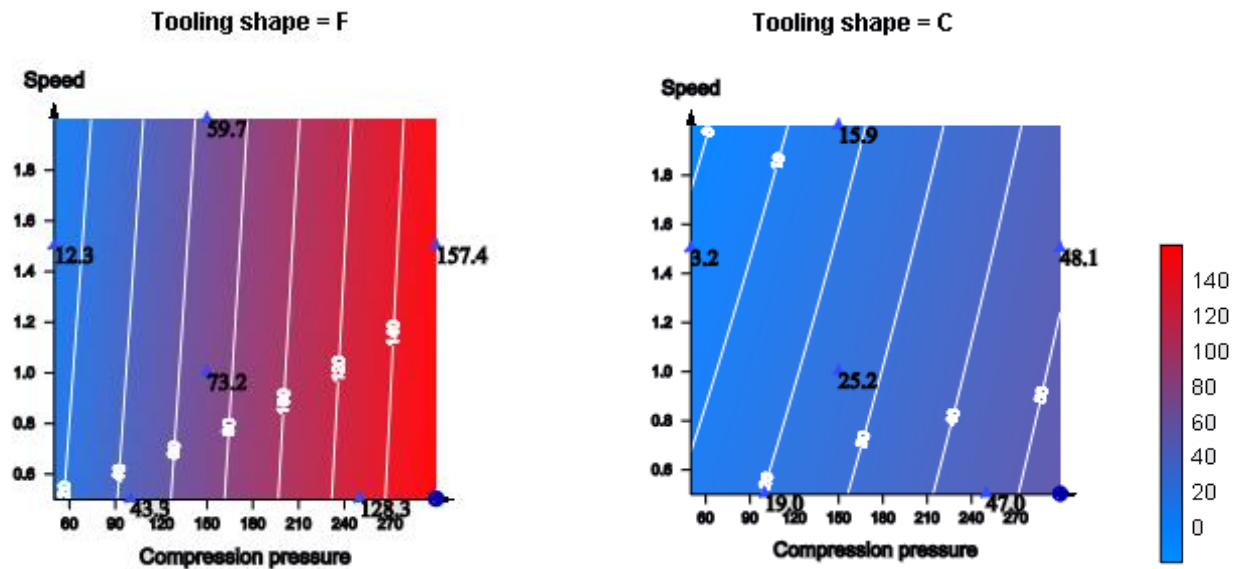


Figure 46 Contour plots showing the effect of flat (F) and concave (C) punch shapes on MDP for CHPD

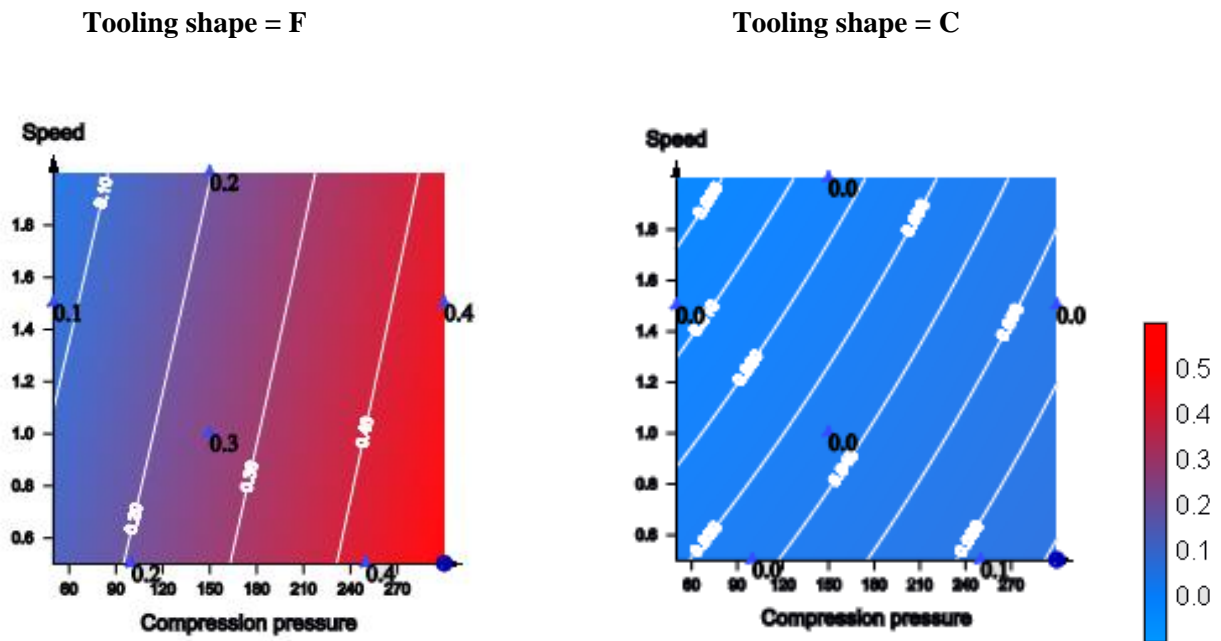


Figure 47 Contour plots showing the effect of flat (F) and concave (C) punch shapes on SR for pregelatinized starch

The increase of RDP and MDP for flat compacts in comparison to convex compacts was due to higher area of contact to die-wall and the higher axial-radial stress transmission. This could be explained regarding the punch tip design, where concave punches induced more radial powder movement due to its geometry in comparison to flat-faced punches, so denser zones would be found at the edges rather than the core. Flat-faced punch showed homogenous stress transmission on powder bed, which led to more uniformity in density distribution in comparison to concave punches, and hence higher axial-radial stress transmission. However, opposite results were reported that convex tablets have higher RDP than flat-faced

[17, 18]. The reason is the lack of good simulation technology at that time where the radial die-wall sensor was not covering the whole area for compaction. Moreover, Sugimori and coworkers reported extrapolated rather than directly measured values for RDP. The accurate reason why usually convex compacts experience higher capping tendency in comparison to flat compacts is not RDP values but rather the density distribution where for the former the distribution is more non uniform [19]. It was reported that skewed punch geometries led to higher stress gradients across powder bed during compaction [20], and hence big difference in densities.

Effect of punch geometry on Friction Coefficient during Ejection (FCE)

In comparison to concave punch, flat-faced punch showed lower friction during ejection for all powders, ($p < 0.003$), except for starch (no effect). **Figure 48** shows the effect of punch geometry on FCE for MCC where compaction with flat-punch showed less friction in comparison to concave punch. The geometry of concave punch caused more radial movement for powder, so higher density zones were expected at the edges in comparison to the core of the compact. This caused higher particle/die-wall interaction for convex compacts. These results are in accordance with Djemai and Sinka [21]. It was also reported that convex shaped MCC compacts developed high radial elastic recovery at the top corners which led to high friction at

these zones and hence capping occurred more frequently than with flat-faced compacts [7].

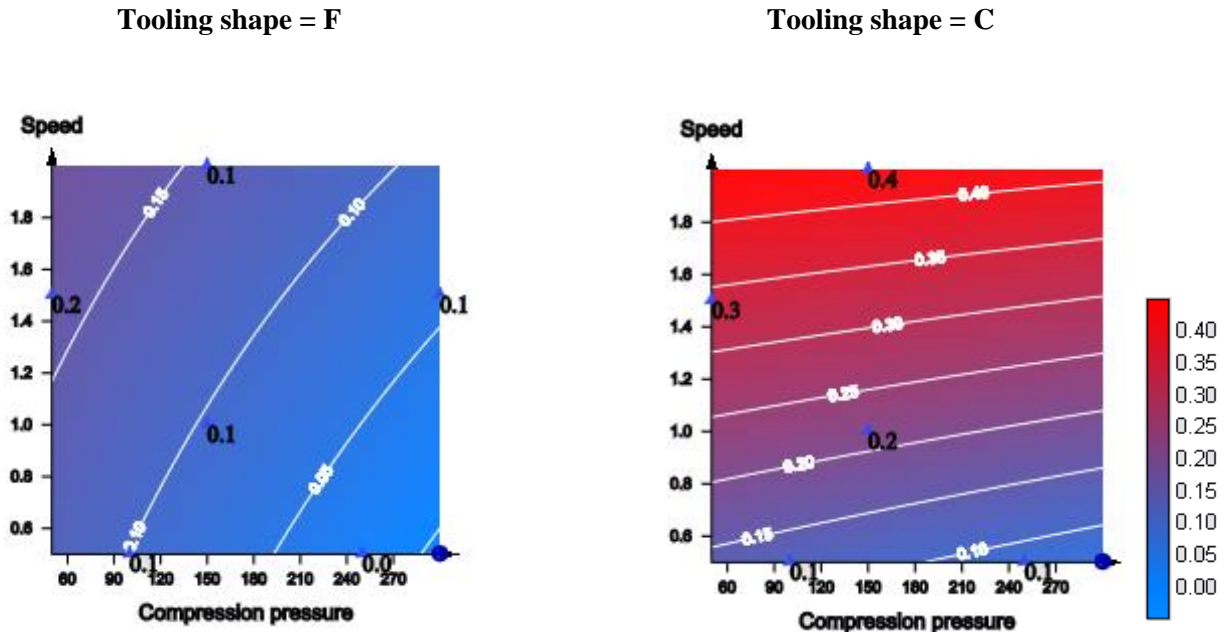


Figure 48 Contour plots showing the effect of flat (F) and concave (C) punch shapes on FCE for MCC

Effect of punch geometry on Elastic Recovery (ER_0) and Radial Tensile Strength (RTS)

Flat compacts showed higher elastic recovery for all materials in comparison to convex compacts, ($p < 0.002$), **Figure 49**. This was due to the design of concave punch tip where the edges come into the closest contact to the powder bed, and the center had the greatest separation during compression. Therefore, lower density zones for convex compacts were expected at the center, so they showed lower axial recovery in comparison to flat compacts. On the other hand, flat compacts showed

an increase in RTS for MCC, mannitol, **Figure 50**, and lactose in comparison to convex compacts, ($p < 0.02$). Convex compacts showed more radial powder movement, with expected high density for particles at the edges, hence more liability for interaction with the die-wall. Particle/die wall interaction (friction) impeded powder movement [22], and this led to high density gradient across convex compacts which resulted later for low tensile strength due to fewer contact points per unit area and hence weakening of interparticulate bonding. It was reported that lamination usually occurs at the boundaries between high and low density regions [23].

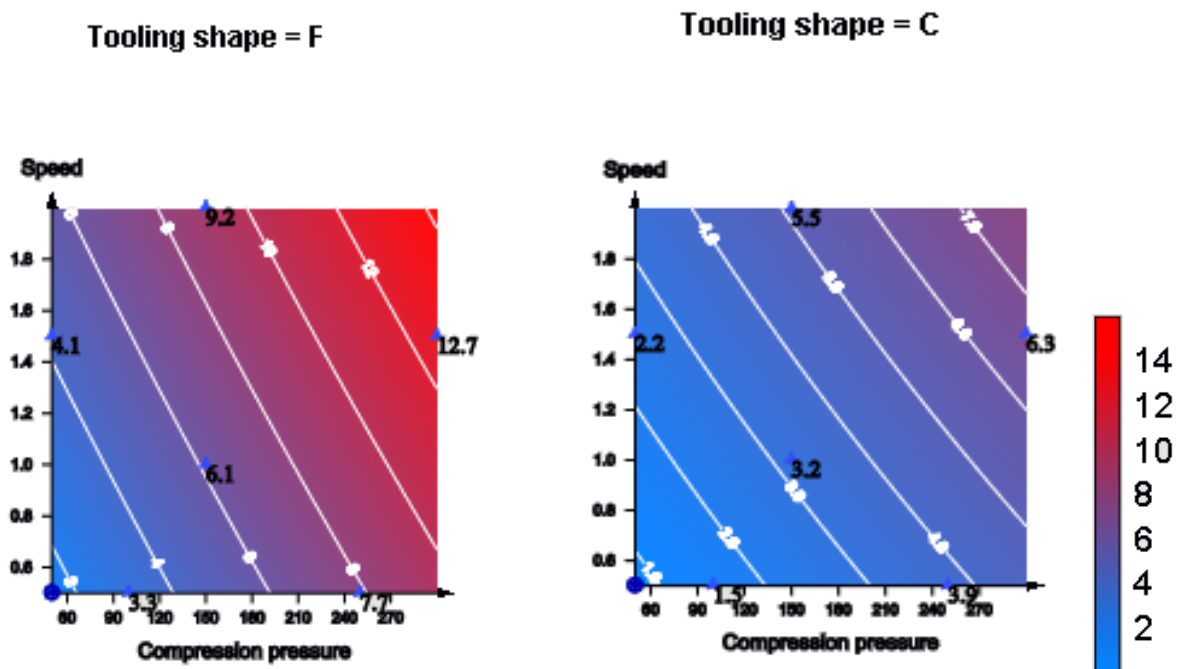


Figure 49 Contour plots showing the effect of flat (F) and concave (C) punch shapes on ER_0 for CHPD

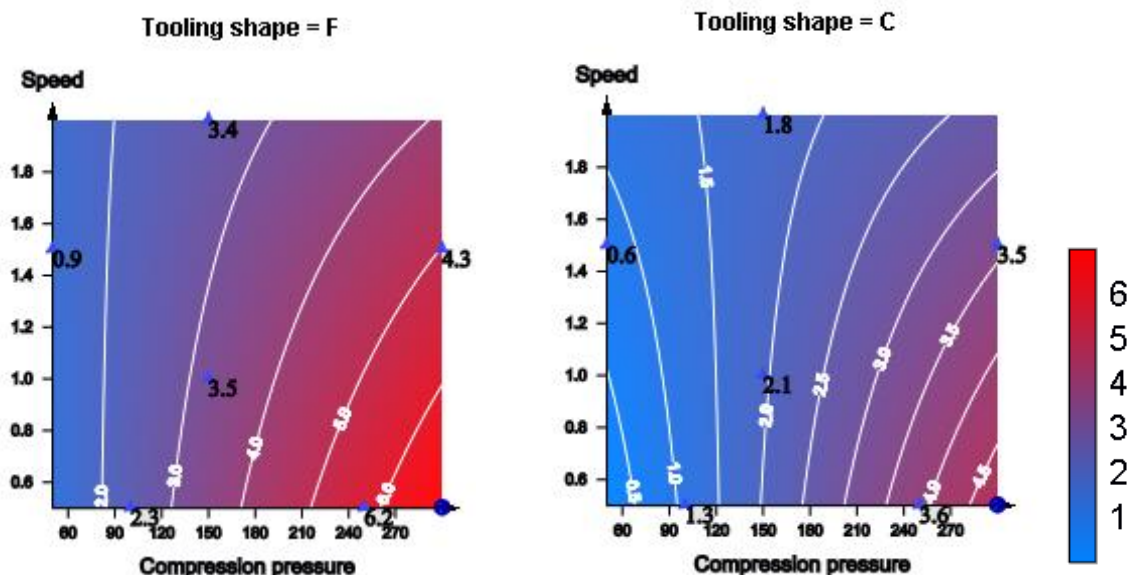


Figure 50 Contour plots showing the effect of flat (F) and concave (C) punch shapes on RTS for mannitol

Effect of punch geometry on Work of Compaction (WC) and porosity

Work of compaction was increased for mannitol, lactose, and CHPD, **Figure 51**, by concave punch in comparison to flat-faced punch, ($p < 0.02$). The reason was the big density gradient across powder bed created by concave punch geometry. This required more work of compaction for powder rearrangement and filling the low density core to bring particles in contact. The increase of work of compaction was reported to decrease trypsin tablet enzyme activity [24]. This shows how punch geometry could affect the final quality of tablet. On the other hand, porosity was also higher for mannitol, **Figure 52**, and lactose convex compacts in comparison to flat compacts, ($p < 0.005$). This was attributed again to creation of low density

zones by concave punch across the powder bed due to uneven distribution of the stress applied. Horikoshi and coworkers [25] reported that stress distribution inside the tablet was dependant on the geometry of the tablet and affected porosity distribution. **Table 21** summarizes all the previous results comparing flat and concave punches.

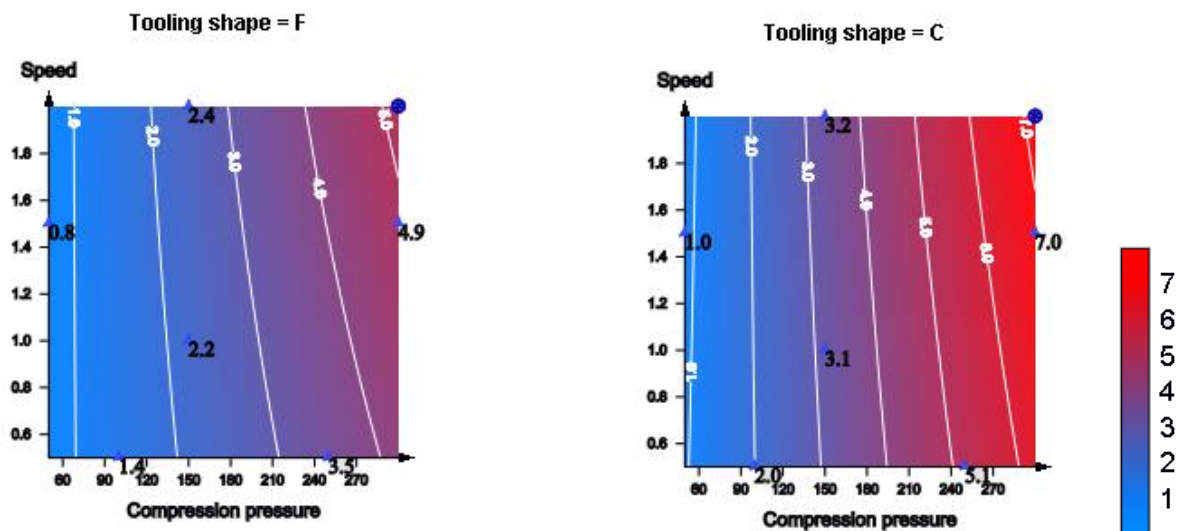


Figure 51 Contour plots showing the effect of flat (F) and concave (C) punch shapes on WC for CHPD

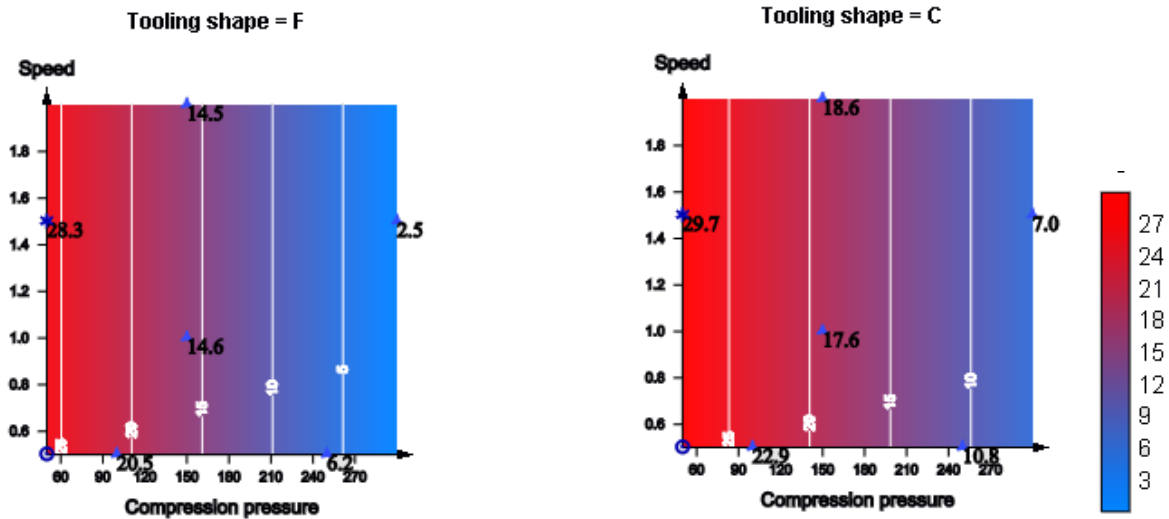


Figure 52 Contour plots showing the effect of flat (F) and concave (C) punch shapes on porosity for mannitol

Table 21 Comparison between the effect of flat-faced and standard concave punches on compaction parameters

Parameter	Flat Punch	Concave Punch
RDP	+	-
MDP	+	-
SR	+	-
FCE	-	+
ER ₀	+	-
RTS	+	-
WC	-	+
Porosity	-	+

+ Increase, - Decrease

Conclusion

With the continuous development of pharmaceutical press machines, where nowadays we have machines that produce million tablets per hour; studying the effect of tooling geometry as a key factor is very important to understand the compaction process. In this study we found that, both RDP and MDP were higher in case of flat-faced punches in comparison to concave or cup shaped punches due to more uniformity in density distribution caused by punch shape and higher contact area to the die-wall. The homogeneity in density for the powder bed due to flat shape resulted in even and higher axial-radial stress transmission to the die wall. Concave punch induced more radial movement for the powder, which led to higher densification at the edges in comparison to flat punch. This caused more particle/die-wall interaction or higher friction tendency. Flat compacts showed higher tensile strength, lower porosity, and work of compaction due to low density gradients for powder bed in comparison to convex compacts. On the other hand, convex compacts showed lower elastic recovery due to low density core. Radial die-wall monitoring was of great help to understand density changes of powder bed under compression regarding particle interaction to punch geometry.

References

- [1] Sinka IC, Cunningham JC, Zavaliangos A. The effect of wall friction in the compaction of pharmaceutical tablets with curved faces: a validation study of the Drucker-Prager Cap model. *Powder Technol* 2003; 133: 33-43.
- [2] Natoli, D. Tooling for pharmaceutical processing. In: Augsburger LL, Hoag SW, eds. *Pharmaceutical dosage forms: Tablets*, vol. 3: *Manufacture and process control*, 3rd ed. New York: Informa Healthcare; 2008: 1-48.
- [3] Ritschel W, Bauer-Brandl A. In *Die Tablette*, 2nd Ed.; Edition Cantor Verlag: Aulendorf, Germany, 2002.
- [4] Wu CY, Hancock BC, Mills A, Bentham AC, Best SM, Elliott JA. Numerical and experimental investigation of capping mechanisms during pharmaceutical tablet compaction. *Powder Technol* 2008; 181: 121-129.
- [5] Sinka IC, Cunningham JC, Zavallangos A. Analysis of tablet compaction II. Finite element analysis of density distributions in convex tablets. *J Pharm Sci* 2004; 93: 2040-2053.
- [6] Eiliazadeh B, Briscoe BJ, Sheng Y, Pitt K. Investigating density distributions for tablets of different geometry during the compaction of pharmaceuticals. *Particul Sci Technol* 2003; 21: 303-316.

- [7] Han LH, Elliott JA, Bentham AC, Mills A, Amidon GE, Hancock BC. A modified Drucker-Prager Cap model for die compaction simulation for pharmaceutical powders. *Int J Solids Struct* 2008; 45: 3088-3106.
- [8] Doelker E, Massuelle D. Benefits of die-wall instrumentation for research and development in tableting. *Eur J Pharm Biopharm* 2004; 58: 427-444.
- [9] Abdel-Hamid S, Betz G. Study of radial die-wall pressure changes during pharmaceutical powder compaction. *Drug Dev Ind Pharm* 2011; 37: 387-395.
- [10] Doelker E. Comparative compaction properties of various microcrystalline cellulose types and generic products. *Drug Dev Ind Pharm* 1993; 19: 2399-2471.
- [11] Van der Voort Maarschalk K, Vromans H, Groenendijk W, Bolhuis GK, Lerk CF. Effect of water on deformation and bonding of pregelatinized starch compacts. *Eur J Pharm Biopharm* 1997; 44: 253-260.
- [12] Narayan P, Hancock BC. The relationship between the particle properties, mechanical behavior, and surface roughness of some pharmaceutical excipient compacts. *Mater Sci Eng* 2003; A355: 24-36.
- [13] Ilić I, Kása Jr P, Dreu R, Pintye-Hódi K, Srcic S. The compressibility and compactibility of different types of lactose. *Drug Dev Ind Pharm* 2009; 35: 1271-1280.

- [14] Gohel MC, Jogani PD. A review of co-processed directly compressible excipients. *J Pharm Pharmaceut Sci* 2005; 8: 76-93.
- [15] Hölzer AW, Sjögren J. Friction coefficients of tablet masses. *Int J Pharm* 1981; 7: 269-277.
- [16] Fell JT, Newton JM. Determination of tablet strength by the diametrical-compression test. *J Pharm Sci* 1970; 59: 688-691.
- [17] Sugimori K, Mori S, Kawashima Y. Introduction of a new index for the prediction of capping tendency of tablets. *Chem Pharm Bull* 1989; 37: 458-462.
- [18] Sugimori K, Mori S, Kawashima Y. Characterization of die wall pressure to predict capping of flat- or convex-faced drug tablets of various sizes. *Powder Technol* 1989; 58: 259-264.
- [19] Eiliadzadeh B, Pitt K, Briscoe, B. Effects of punch geometry on powder movement during pharmaceutical tableting processes. *Int J Solids Struct* 2004; 41: 5967-5977.
- [20] Andersson DC, Larsson PL, Cadario A, Lindskog P. On the influence from punch geometry on the stress distribution at powder compaction. *Powder Technol* 2010; 202: 78-88.
- [21] Djemai A, Sinka IC. NMR imaging of density distributions in tablets. *Int J Pharm* 2006; 319: 55-62.

- [22] Ozkan N, Briscoe, BJ. The surface topography of compacted agglomerates; a means to optimize compaction conditions. *Powder Technol* 1996; 86: 201-207.
- [23] Sixsmith D, McCluskey D. The effect of punch tip geometry on powder movement during the tableting process. *J Pharm Pharmacol* 1981; 33: 79-81.
- [24] Otsuka M, Sato M, Matsuda M. Comparative evaluation of tableting compression behaviors by methods of internal and external lubricant addition: inhibition of enzymic activity of trypsin preparation by using external lubricant addition during the tableting compression process. *AAPS PharmSci* 2001; 3: 1-11.
- [25] Horikoshi I, Takeguchi N, Morii M. Estimation of stress distribution in the convex type tablet using specific enzyme activity as parameter. *Chem Pharm Bull* 1973; 21: 2136-2140.

Chapter 6: A novel tool for the prediction of tablet sticking during high speed compaction⁶

Abstract

Context: During tableting, capping is a problem of cohesion while sticking is a problem of adhesion. Sticking is a multi-composite problem; causes are either material or machine related. Nowadays detecting such a problem is a pre-requisite in the early stages of development. **Objective:** The aim of this chapter was to investigate sticking by radial die-wall pressure monitoring guided by compaction simulation. **Materials and Methods:** This was done by using the highly sticking drug; mefenamic acid (MA) at different drug loadings with different fillers that were compacted at different pressures and speeds. **Results and Discussion:** By increasing MA loading, viscoelastic fillers showed high residual radial pressure after compaction (RDP) while plastic/ brittle fillers showed high radial pressure during compaction (MDP), ($p < 0.05$). Visually, plastic/brittle fillers showed greater tendencies for adhesion to punches than viscoelastic fillers, while the later showed

⁶ "Reprinted from Pharm Dev Tech, Vol./No., S. Abdel-Hamid and G.Betz, A novel tool for the prediction of tablet sticking during high speed compaction, Pages 1-8, Copyright (2011), with permission from Informa Healthcare"

higher tendencies for adhesion to the die-wall. This was confirmed by higher values of axial stress transmission for plastic/brittle than viscoelastic fillers (higher punch surface/powder interaction), and higher residual die-wall and ejection forces for viscoelastic than plastic/brittle fillers, ($p < 0.05$). Take-off force was not a useful tool to estimate sticking due to cohesive failure of the compacts. **Conclusion:** Radial die-wall pressure monitoring is suggested as a robust tool to predict sticking.

Key words: sticking, adhesion, radial die-wall pressure, mefenamic acid, compaction simulation

Introduction

Sticking is a serious problem in tableting that could affect the manufacturability of the process [1, 2]. Sticking refers to the adhesion of materials to punch surface and to die-wall. Filming is a slow form of sticking related to powder moisture. Picking is another type of sticking in which particles stick to embossing or debossing on the punch faces. Sticking tendency increases by increasing compression force, reducing lubricant concentration, increasing tablet diameter, and reducing tablet thickness [3]. Tablet sticking was estimated by measuring different forces like slipping force between the tablet surface and upper punch [4], stripping force [5], and sweep-off force [3] from the lower punch, or detachment force from an instrumented upper punch [6]. Other indicators of sticking were increasing ejection and take-off forces [7-9]. Adhesion of effervescent tablets to punch tips was determined using electron microscopy, surface roughness measurements, quantification of punch weight variations, and atomic force microscopy guided by molecular simulation [10, 11]. Factors affecting adhesion are particle size, shape, and surface roughness, moisture content, temperature, surface finish of stainless steel, and tooling geometry [9, 12-19]. Mechanism of antiadherents to prevent sticking of powder to punch face is the reduction of surface energies for these powders [20]. Amorphous materials have higher surface energy than crystalline [21], hence they have higher tendency for

adhesion. Forces responsible for adhesion include: van der Waals forces, electrostatic forces, electrical double layer formation, capillary forces, and other interfacial phenomena such as salt bridge formation and contact melting [22-24]. Adhesion takes place commonly by forming a mechanical interfacial layer on a rough porous surface where surface mobility and mechanical stabilization takes place [25]. Thus, adhesion depends on shear strength and plasticity of the materials. Surface treatment such as polishing or coating could tremendously affect adhesion [25]. The physicochemical properties of powder and metal surface on molecular basis determine the onset of adhesion and other mechanical factors such as compression force determine the degree of adhesion. Sticking is a complex problem which has material related causes like particle surface condition, particle size, melting point, and moisture content; and machinery related causes like punch surface condition, compression pressure, and speed. Sticking usually appears after increasing the duration of the tablet press running time at the end stages of drug product development, so using compaction simulation provides a fundamental understanding and early discovery of this phenomenon. The aim of this chapter was to investigate powder related factors such as particle size, surface condition, drug loading, and machinery related factors such as compression pressure and speed on sticking. This was done by radial die-wall pressure monitoring aided by a fully instrumented compaction simulator to

understand the fundamental aspects of sticking through quantitative parameters such as radial die-wall pressure, axial stress transmission, as well as ejection, and take-off forces. The use of an instrumented die is suggested in literature to explain the interaction of particles and punch surface under pressure and speed [26, 27], hence was applied in the present work.

Materials and Methods

Materials

Microcrystalline cellulose MCC (Avicel[®] PH102, FMC Corporation, DE, US), directly compressible mannitol (Pardeck[®] M200, Merck KGaA, Darmstadt, Germany), calcium hydrogen phosphate dihydrate CHPD (Emcompress[®], JRS Pharma, Rosenberg, Germany), pregelatinized starch (Sta-Rx[®] 1500, Colorcon, Idstein, Germany), spray dried lactose monohydrate (Flowlac[®] 100, Meggle, Wasserburg, Germany), mefenamic acid (Sigma-Aldrich, Steinheim, Germany), magnesium stearate (Mg stearate, supplied by Sandoz AG, Basel, Switzerland).

Methods

Preparation of powder mixtures

Mixtures of different fillers and mefenamic acid at three different loadings; 25, 50 and 75 % (w/w) were prepared by mixing for 2 min at 100 rpm in a Turbula[®] mixer (Type T2A, Wilhelm A. Bachofen AG, Switzerland). All formulations had 1% (w/w) Mg stearate as a lubricant.

Powder Characterization

True density

True density of powders was measured by AccuPyc 1330 helium pycnometer (Micrometrics, Norcross, GA, US). A known weight of the samples was placed into the sample cell. Values were expressed as the mean of five parallel measurements.

Particle-size distribution

The average particle size was determined by laser diffraction with a Malvern Mastersizer X (Malvern Instruments, Worcestershire, UK). The measurements were carried out three times for each sample. Obscuration value between 10 to 30% was got in all measurements. The function “polydisperse” was activated. Mean, median particle size, and span were recorded.

Morphological studies

Particle morphology for MA was assessed by scanning electron microscopy (SEM) (Nova NanoSem 230, Eindhoven, Netherlands). Samples were mounted on aluminum stubs using double side adhesive carbon tape and sputter coated with gold 20 nm (BalTec MED 020 Coating System, Lichtenstein).

Powder compaction

Powder compaction was carried out using a compaction simulator (PressterTM, Metropolitan Computing Corp., NJ, US) simulating the tablet press Korsch PH336 (36 stations). The compaction rolls used were 300 mm in diameter. Accordingly, a flat-faced B-tooling with a diameter of 10 mm was used to make tablets of 250 mg in weight. Powder feed was manually done. The machine was set to perform compaction pressures of 50, 150, and 300 MPa at the compaction speeds of 0.5, 1, and 2 m/s corresponding to the following dwell times 19, 6.4, and 4.8 ms, respectively. Six tablets were compressed at the same experimental conditions and the mean was calculated. Working conditions were 29-30°C and 40-45 %RH. Residual die-wall pressure (RDP), maximum die-wall pressure (MDP), work of compaction (WC), ejection force (EF), and take-off force (TO) were measured. The die-wall pressure reaches a maximum value, MDP, just after the upper and lower punches show maximum compression values, and shows a constant residual value, RDP, after upper and lower punch forces become zero. Axial to radial stress ratio (SR) (MDP to the average of upper and lower compression pressures) was also calculated.

Compact characterization

Radial tensile strength (RTS)

Crushing strength of a compact was determined by pressing it diametrically on a Pharmatron tablet tester (model 8D, Dr Schleuniger Pharmatron Inc., Solothurn, Switzerland). Radial tensile strength σ (MPa) was calculated according to:

$$\sigma = 2F/\pi dh \quad (1)$$

Where F is the force required to cause failure in tension (N), d is the compact diameter (mm), h is the compact thickness (mm), and π is a constant equals 3.1416. Compact dimensions were measured using a micrometer with a precision of 0.01mm (Mitutoyo, Japan).

Porosity

Compact porosity was calculated from compact apparent density and in-die dimensions according to the following equation:

$$\varepsilon = 1 - \left[(m / \pi . r^2 . h) / \rho_T \right] \quad (2)$$

Where ε is the in-die porosity, m is the compact mass (mg), r is the compact radius (5 mm), h is the in-die compact height (mm), ρ_T is the true density (mg/mm³) of powders.

Elastic recovery (% ER₀)

The % ER₀ for a compact was calculated from “zero pressure thickness” that could be seen from the force vs. thickness plot, and “minimum punch gap” (thickness at maximum compression), features of Presster[®] software.

$$ER_0(\%) = T_i - T_m / T_m \cdot 100 \quad (3)$$

Where T_i is the compact thickness at zero pressure just before ejection, T_m is the minimum compact thickness at maximum compression force.

Data interpretation

To study the effect of different compaction variables, runs were generated according to an experimental design using STAVEX[®] 5.0 (Aicos, Switzerland), applying a Box-Behnken design, optimization mode, **Table 22**. Compaction pressure, speed, and drug loading (3 levels) were the factors. RDP, MDP, SR, EF, TO, ER₀, RTS, WC, and porosity were the responses. Least squares analysis was applied for the fitted model of optimization. The model was evaluated in terms of statistical significance using analysis of variance (ANOVA) at a level of significance (p< 0.05).

Table 22 Experimental design generated by STAVEX[®] 5.0 to study the effect of mefenamic acid (MA) loading on radial die-wall pressure

Run	Compression Pressure (MPa)	Compression Speed (m/s)	Drug Loading (%)
1	50	0.5	50
2	50	2	50
3	50	1	25
4	50	1	75
5	300	0.5	50
6	300	2	50
7	300	1	25
8	300	1	75
9	150	0.5	25
10	150	2	25
11	150	0.5	75
12	150	2	75
13	150	1	50

Results and Discussion

Effect of particle size and surface, and MA loading on sticking

Table 23 shows the median and mean diameters, and span (particle size distribution), as well as the true density of the investigated powders. Mean particle size of MCC, lactose, and mannitol were nearly equal, CHPD showed the largest mean particle size and narrowest particle size distribution while MA showed the smallest particle size and the widest particle size distribution. CHPD showed the highest density while densities of the other powders were almost the same except for MA was the lowest. Mean particle size of MA was fine (around 60 μm); however this value was larger than the values reported in literature where it was reported to have a size of 8-18 μm . This could be due to particle aggregation and was confirmed with the wide particle size distribution. This fine size of MA led to poor compressibility of the formulations especially at high drug loading which led to capping and sticking to the punch surface, **Figure 53**. MA is a good model to study tableting problems such as capping and sticking [28]. Fine particles were reported to have a high tendency for adhesion [13-15, 19]. SEM picture shows MA as microcrystalline aggregated plate-like particles, **Figure 54**. MA was reported to have two different crystal habits depending on crystallization method applied during bulk manufacturing [29, 30].

Table 23 Median, and mean diameters, span, and true density of the investigated powders

Powder	Median [μm] \pm SD	Mean [μm] \pm SD	Span \pm SD	True density [g/cm^3] \pm SD
MCC	124.63 \pm 0.93	136.57 \pm 0.94	1.68 \pm $1 \cdot 10^{-3}$	1.5859 \pm $1.9 \cdot 10^{-3}$
Mannitol	131.15 \pm 1.99	149.22 \pm 2.55	1.73 \pm $2.22 \cdot 10^{-2}$	1.5154 \pm $0.7 \cdot 10^{-3}$
Lactose	124.87 \pm 1.10	131.44 \pm 1.01	1.43 \pm $6.66 \cdot 10^{-3}$	1.5419 \pm $1.2 \cdot 10^{-3}$
Pregelatinized Starch	86.51 \pm 0.16	94.90 \pm 0.03	1.87 \pm $8.72 \cdot 10^{-3}$	1.4964 \pm $0.6 \cdot 10^{-3}$
CHPD	181.71 \pm 3.02	188.02 \pm 2.90	0.86 \pm $1.38 \cdot 10^{-2}$	2.4818 \pm $1.6 \cdot 10^{-3}$
MA	38.93 \pm 2.12	59.28 \pm 3.37	3.62 \pm 0.07	1.2617 \pm $0.9 \cdot 10^{-3}$

Different crystal forms have different specific surface areas and surface free energies. Adhesion is a surface phenomenon and crystal habits of MA affect its mechanical properties due to controlling contact points, frictional, and adhesive forces in relation to crystal faces as well as packing geometry [31]. Particle shape and surface roughness were reported to have a big effect on adhesion. Paracetamol was reported to have high adhesion due to particle irregularity and surface roughness [13], and the lamellar shape of PEG 4000 allowed more asperity contact points with stainless steel surface [14].

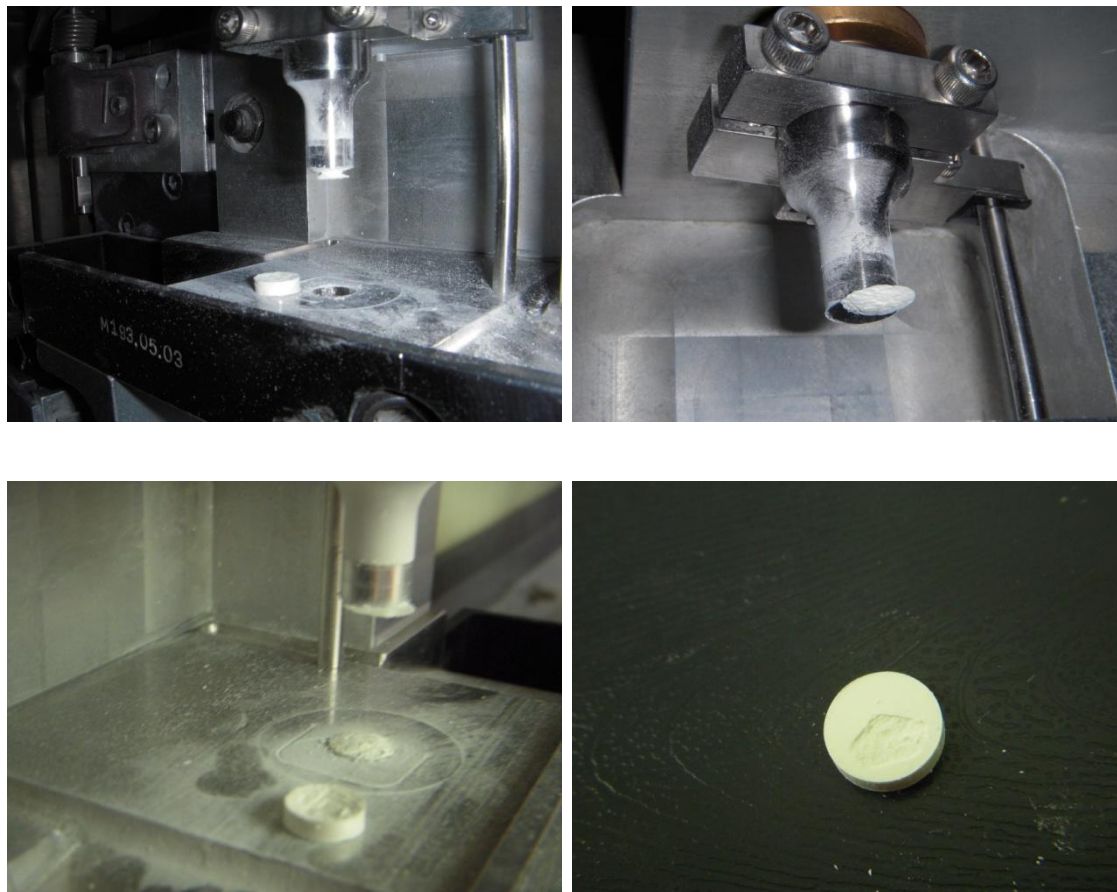


Figure 53 Sticking and capping of different MA formulations

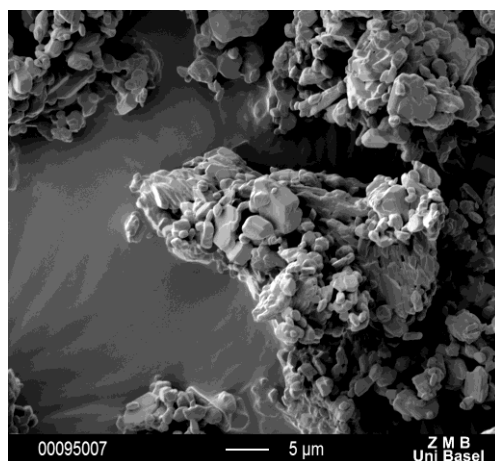


Figure 54 SEM picture for MA particles

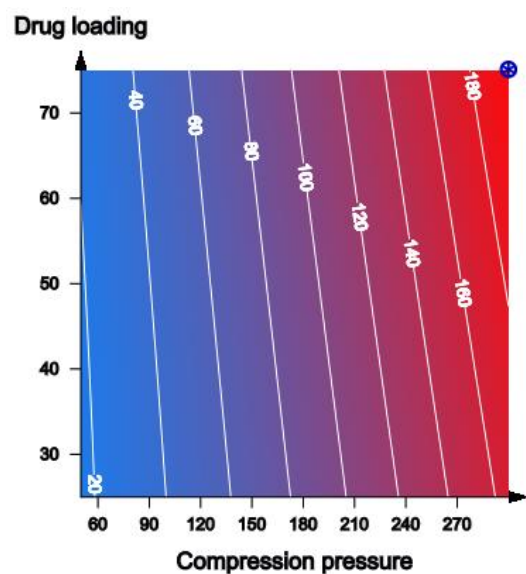
Effect of compression pressure and speed on sticking

Regardless of drug loading, sticking was visually inspected on both upper and lower punches at high compression pressure and speed. High compression pressure increased the area of contact between powder bed and punch surface due to excessive deformation. This led to higher probability for bonding and adhesion. Plastic deforming materials tend to be more liable for adhesion due to time dependency which would lead to the formation of more adhesive bonds [3, 6, 32]. Moreover, deformable particles tend to have higher tendency for adhesion than rigid particles due to larger area of contact [33]. In this study, sticking was inspected at high compaction speeds although it was reported that shortening the penetration time of the lower punch resulted in less time and area of contact, and hence reduced bonding of powder bed to punch face [3]. It could be then concluded that particle physicochemical properties and compression pressure are rather the most critical factors for sticking while speed is more relevant to capping problem.

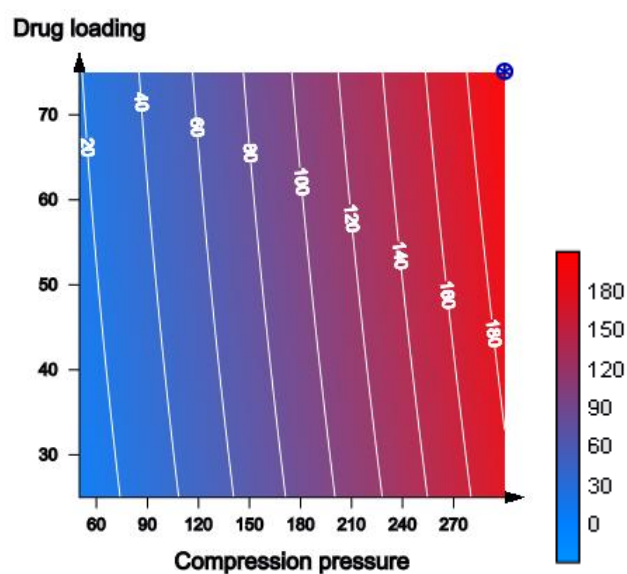
Radial die-wall pressure for sticking prediction

By increasing drug loading, viscoelastic fillers MCC and pregelatinized starch showed no effect on maximum die-wall pressure (MDP). Plastic/brittle fillers (mannitol, lactose, CHPD) showed an increase in MDP, ($p < 0.01$). **Figure 55** shows the increase of MDP for lactose and CHPD by increasing both compression pressure

and drug loading (transfer from blue to red zones). There was a higher axial to radial stress transmission through powder bed for these fillers in comparison to viscoelastic fillers. This resulted in greater tendencies for plastic/brittle fillers' formulations to interact with punch surface, and hence sticking. Visually these formulations showed sticking at most of the compaction cycles especially for lactose. This was further confirmed by higher stress ratio (SR) for such formulations in comparison to viscoelastic fillers' formulations, ($p < 0.02$), **Figure 56**. On the other hand viscoelastic fillers' compacts showed higher residual die-wall pressure (RDP) and ejection force in comparison to plastic/brittle fillers' compacts, ($p < 0.002$). **Figure 57** shows the increase of RDP and ejection force for MCC by increasing drug loading. This was due to higher radial frictional interactions for viscoelastic fillers' compacts after compaction. This showed that by increasing drug loading, viscoelastic fillers showed adhesion to die-wall or radial sticking while plastic/brittle fillers showed adhesion to punch faces or axial sticking. These results are in accordance with what is reported by Mitrevej and Augsburger [34], that ejection force is reduced with time during compaction due to improvement of force transmission. Moreover, Kikuta and Kitamori [35] found a direct correlation between ejection and radial forces for different lubricants, and estimated lubricants' adhesion to be almost zero. It is also reported that MA tablets show high ejection forces due to high sticking tendency to surfaces [36].

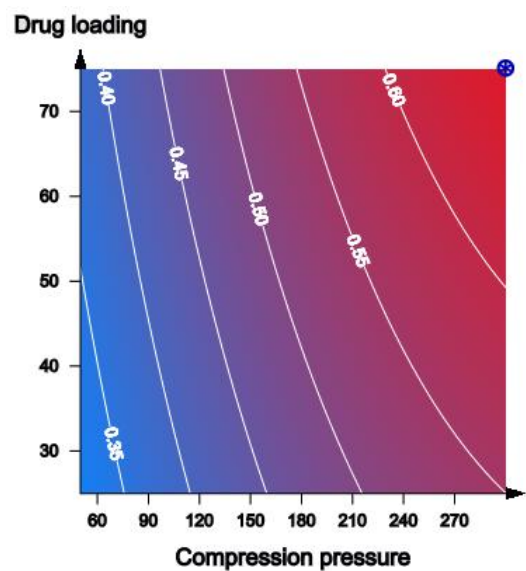


(a)

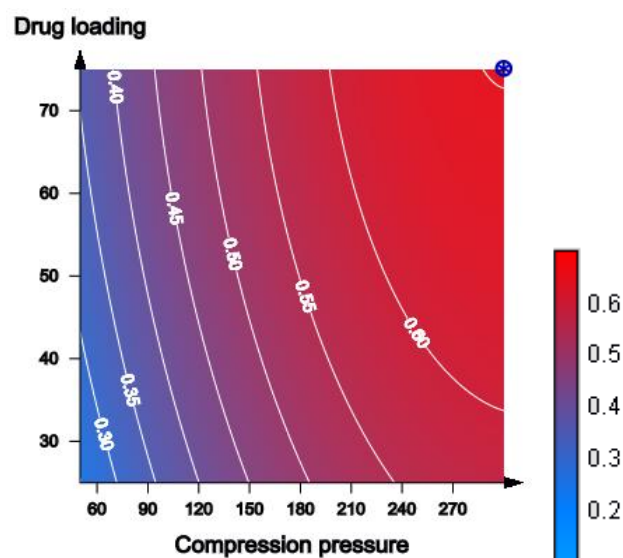


(b)

Figure 55 Contour plots of MDP for (a) Lactose (b) CHPD



(a)



(b)

Figure 56 Contour plots of SR for (a) Lactose (b) CHPD

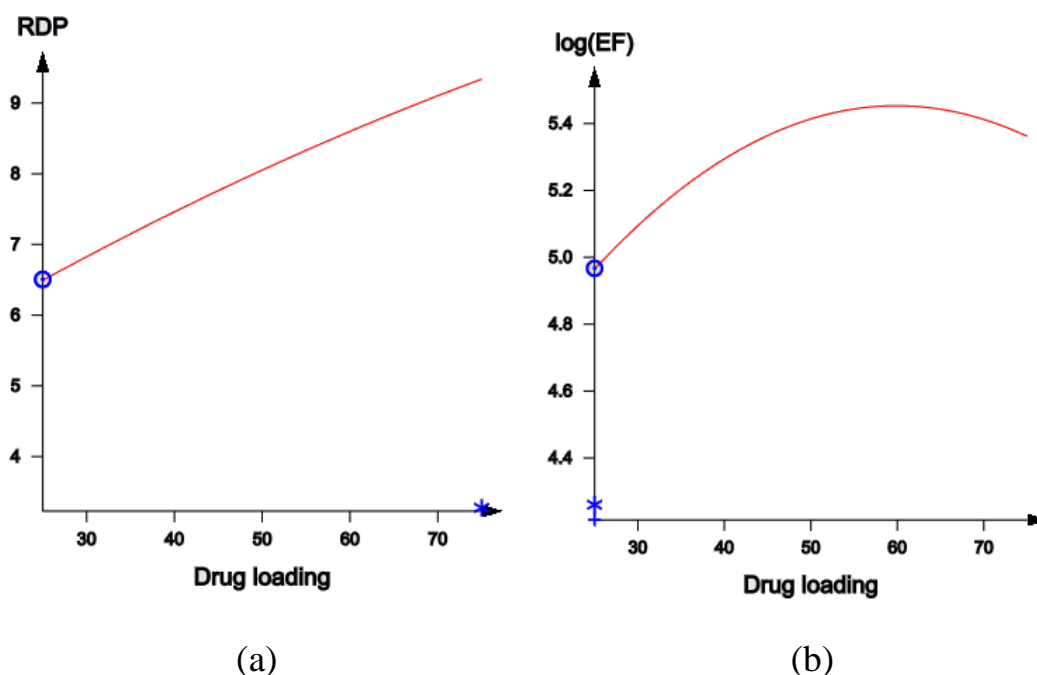


Figure 57 Linear plots for MCC showing (a) RDP (b) EF

Take-off force for sticking prediction

By increasing MA loading, take-off force showed no change for all formulations although sticking was inspected visually. Wang and coworkers [9] mentioned that addition of diluents to sticking profens reduced take-off force and resulted only in picking or filming rather than significant sticking for the pure drugs. Moreover in this study, cohesive failure of compacts led to insignificant change in take-off force because adhesion was stronger than cohesion, **Figure 53**. Capping mainly occurred and in fewer cases, failure to make a compact, but this happened only at runs 8 and 12 in the design (see **Table 22**) for all fillers due to high drug loading/compression pressure/ speed. Other fillers like pregelatinized starch and lactose showed also this

phenomena at runs 2, 4 and 6 for pregelatinized starch and runs 4 and 6 for lactose where the first showed failure to make a compact and the second showed mainly capping. Weak cohesion was confirmed by the low tensile strength for compacts of the remaining runs. In previous studies, cohesive failure led to improper adhesion measurement [6, 37, 38]. Also, it was reported that chipping of tablets changed surface characteristics and hindered adhesion measurement [3, 34].

Effect of MA loading on Radial Tensile Strength (RTS), Elastic Recovery (ER_0), Work of Compaction (WC), and Porosity

RTS was calculated for intact compacts that did not show cohesive failure.

RTS was reduced for all compacts' formulations by increasing MA loading, ($p < 0.01$), **Figure 58**. This was due to poor compressibility of MA because of weak particle bonding related to its fine particle size. Fine particles showed high interparticulate friction and resulted in lower densification of powder and hence poor contact. Similar results were previously reported [39, 40]. Another reason was the brittle nature of MA [30], where continuous fragmentation resulted in failure of interparticulate bond formation. It was reported that increasing the amount of brittle materials would lead to a reduction in crushing strength [41]. The brittle nature of MA resulted also in reduction of porosity for plastic/brittle fillers due to filling of voids on fragmentation, ($p < 0.004$). Regarding elastic recovery, only plastic/brittle

fillers showed high ER_0 by increasing MA loading, ($p < 0.04$), **Figure 59**. This result confirmed the behavior of interacting axially and adhering to punch surfaces for such formulations. MA acted as Paracetamol which was reported to be highly elastic with brittle fracture [42-44]. This led to the highest incidence of capping for such formulations due to further weakening of bonding [45, 46]. By increasing MA loading, work of compaction was increased for lactose and CHPD, ($p < 0.05$), **Figure 60**. These materials showed the highest sticking propensity, so a high work of compaction was required to overcome adhesion and friction forces with the metal surfaces. It was reported that reducing friction resulted in reduction of the work required to compact a powder [2].

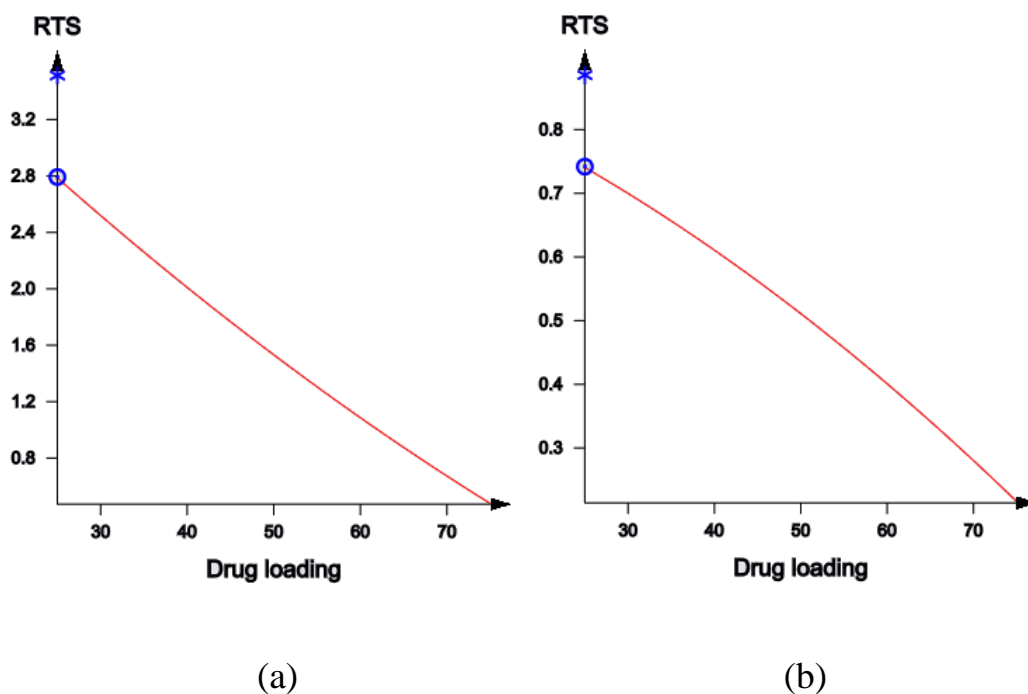


Figure 58 Linear plots of RTS for (a) MCC (b) Lactose

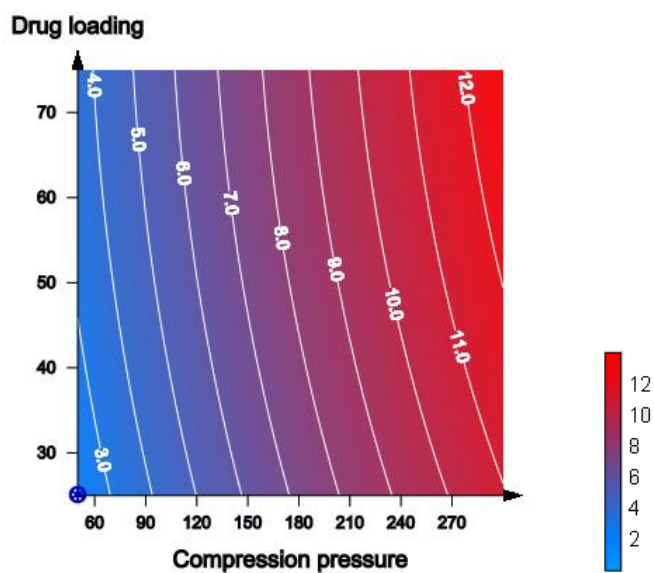


Figure 59 Contour plot of ER_0 for lactose

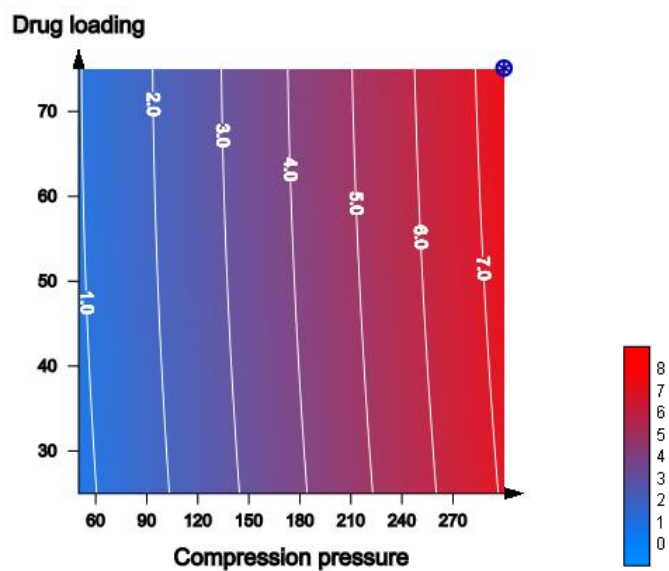


Figure 60 Contour plot of WC for lactose

Conclusion

Tablet sticking could highly affect the smoothness of the compaction process as well as the production time. Radial die-wall pressure monitoring was a successful tool to assess sticking. Depending on powder deformation behavior, plastic/brittle formulations showed high axial interaction which led to adhesion to punch surfaces confirmed by high MDP and SR values while viscoelastic formulations showed higher radial interaction led to adhesion to die-wall and confirmed by high RDP and ejection forces. Although it is a well known tool to detect sticking, take-off force in this study was insensitive to estimate sticking due to cohesive failure of the compacts. Tooling polishing or coating could be an expensive solution for this problematic surface phenomenon, however sticking sometimes is inherent for materials like MA and also related to compaction process parameters like increasing compression pressure. So it is advised to investigate this problem in early development by using robust tools such as radial die-wall to optimize the formulation and compromise the machine parameters from the beginning.

References

- [1] Moody G, Rubinstein MH, Fitz Simmons RA. Tablet lubricants 1. Theory and modes of action. *Int J Pharm* 1981; 9: 75-80.
- [2] Stainforth JN, Cryer S, Ahmed HA, Davies SP. Aspects of pharmaceutical tribology. *Drug Dev Ind Pharm* 1989; 15: 2265-2294.
- [3] Mitrevej A, Augsburger LL. Adhesion of tablets in a rotary tablet press I. Instrumentation and preliminary study of variables affecting adhesion. *Drug Dev Ind Pharm* 1980; 6: 331-377.
- [4] Naito SI, Nakamichi K. Studies on techniques of manufacturing pharmacy I. Prediction of tableting troubles such as capping and sticking. *Chem Pharm Bull* 1969; 17: 2507-2514.
- [5] Ritter M, Dürrenberger M, Sucker H. Messmethode zur Quantifizierung des Klebens von Tabletten. *Pharm Ind* 1978, 40 : 1181-1183.
- [6] Waimer F, Krumme M, Danz P, Tenter U, Schmidt PC. A novel method for the detection of sticking of tablets. *Pharm Dev Technol* 1999; 4: 359-367.
- [7] Schmid PC, Tenter U. Preßkraft- und Weg-Zeit- Charakteristik von Rundlauftablettenpressen; 5. Mitt.: Messung und Auswertung von Ausstoßkräften. *Pharm Ind* 1989; 51: 183-187.

- [8] Jahn T, Steffens KJ. Press chamber coating as external lubrication for high speed rotary presses: lubricant spray rate optimization. *Drug Dev Ind Pharm* 2005; 31: 951-957.
- [9] Wang JJ, Guillot MA, Bateman SD, Morris KR. Modeling of adhesion in tablet compression II. Compaction studies using a compaction simulator and an instrumented tablet press. *J Pharm Sci* 2004, 93: 407-417.
- [10] Sendall FE, Staniforth JN. A study of powder adhesion to metal surfaces during compression of effervescent pharmaceutical tablets. *J Pharm Pharmacol* 1986; 38: 489-493.
- [11] Wang JJ, Li T, Bateman SD, Erck R, Morris KR. Modeling of adhesion in tablet compression I. Atomic force microscopy and molecular simulation. *J Pharm Sci* 2003, 92: 798-814.
- [12] Otsuka A. Adhesive properties and related phenomena for powdered pharmaceuticals. *Yakugaku Zasshi* 1998; 118: 127-142.
- [13] Shimada Y, Yonezawa Y, Sunada H. Measurement and evaluation of the adhesive force between particles by the direct separation method. *J Pharm Sci* 2003; 92: 560-568.
- [14] Lam KK, Newton JM. Investigation of applied compression on the adhesion of powders to a substrate surface. *Powder Technol* 1991; 65: 167-175.

- [15] Lam KK, Newton JM. Influence of particle size on the adhesion behavior of powders, after application of an initial press-on force. *Powder Technol* 1992; 73: 117-125.
- [16] Lam KK, Newton JM. Effect of temperature on particle solid adhesion to a substrate surface. *Powder Technol* 1992; 73: 267-274.
- [17] Shimada Y, Sunada M, Mizuno M, Yonezawa Y, Sunada H, Takebayasi K, Yokosuka M, Kimura H. Measurement of the adhesive force of fine particles on tablet surfaces and method of their removal. *Drug Dev Ind Pharm* 2000; 26: 149-158.
- [18] Podczek F. Investigations into the reduction of powder adhesion to stainless steel surfaces by surface modification to aid capsule filling. *Int J Pharm* 1999; 178: 93-100.
- [19] Danjo K, Kamiya K, Otsuka A. Effect of temperature on the sticking of low melting point materials. *Chem Pharm Bull* 1993; 41: 1423-1427.
- [20] Swaminathan V, Cobb J, Saracovan I. Measurement of the surface energy of lubricated pharmaceutical powders by inverse gas chromatography. *Int J Pharm* 2006; 312: 158-165.
- [21] Buckton G, Darcy P. Water mobility in amorphous lactose below and close to the glass transition temperature. *Int J Pharm* 1996; 136: 141-146.

- [22] Coelho MC, Harnby N. Moisture bonding in powders. *Powder Technol* 1978; 20: 201-205.
- [23] Visser J. Van der Waals and other cohesive forces affecting powder fluidization. *Powder Technol* 1989; 58: 1-10.
- [24] Boonyai P, Bhandari B, Howes T. Stickiness measurement techniques for food powders: a review. *Powder Technol* 2004; 145: 34-46.
- [25] Pulker HK, Perry AJ, Berger R. Adhesion. *Surf Technol* 1981; 14: 25-39.
- [26] Abdel-Hamid S, Betz G. Study of radial die-wall pressure changes during pharmaceutical powder compaction. *Drug Dev Ind Pharm* 2011; 37: 387-395.
- [27] Doelker E, Massuelle D. Benefits of die-wall instrumentation for research and development in tableting. *Eur J Pharm Biopharm* 2004; 58: 427-444.
- [28] Adam A, Schrimpl L, Schmidt PC. Factors influencing capping and cracking of mefenamic acid tablets. *Drug Dev Ind Pharm* 2000; 26: 489-497.
- [29] Panchagnula R, Sundaramurthy P, Pillai O, Agrawal S, Raj YA. Solid-state characterization of Mefenamic acid. *J Pharm Sci* 2004; 93: 1019-1029.
- [30] Adam A, Schrimpl L, Schmidt PC. Some physicochemical properties of Mefenamic acid. *Drug Dev Ind Pharm* 2000; 26: 477-487.

- [31] Garekani HA, Sadeghi F, Badiie A, Mostafa SA, Rajabi-Siahboomi AR. Crystal habit modifications of ibuprofen and their physicochemical characteristics. *Drug Dev Ind Pharm* 2001; 27: 803-809.
- [32] Lam KK, Newton JM. The influence of the time of application of contact pressure on particle adhesion to a substrate surface. *Powder Technol* 1993; 76: 149-154.
- [33] Feng JQ. Adhesive contact of elastically deformable spheres: A computational study of pull-off force and contact radius. *J Colloid Interface Sci* 2001; 238: 318-323.
- [34] Mitrevej KT, Augsburger LL. Adhesion of tablets in a rotary tablet press II. Effects of blending time, running time, and lubricant concentration. *Drug Dev Ind Pharm* 1982; 8: 237-282.
- [35] Kikuta J, Kitamori N. Frictional properties of tablet lubricants. *Drug Dev Ind Pharm* 1985; 11: 845-854.
- [36] Kimura G, Betz G, Leuenberger H. Influence of loading volume of mefenamic Acid on granules and tablet characteristics using a compaction simulator. *Pharm Dev Technol* 2008; 13: 57-64.
- [37] Felton LA, McGinity JW. Adhesion of polymeric films to pharmaceutical solids. *Eur J Pharm Biopharm* 1999; 47: 3-14.

- [38] Roberts M, Ford JL, MacLeod GS, Fell JT, Smith GW, Rowe PH, Dyas AM. Effect of lubricant type and concentration on the punch tip adherence of model ibuprofen formulations. *J Pharm Pharmacol* 2004; 56: 299-305.
- [39] Roberts RJ, Rowe C. The effect of the relationship between punch velocity and particle size on the compaction behavior of materials with varying deformation mechanisms. *J Pharm Pharmacol* 1986; 38: 567-571.
- [40] York P. Particle slippage and rearrangement during compression of pharmaceutical powders. *J Pharm Pharmacol* 1978; 30: 6-10.
- [41] Cespi M, Bonacucina G, Misici-Falzi M, Golzi R, Boltri L, Palmieri GF. Stress relaxation test for the characterization of the viscoelasticity of pellets. *Eur J Pharm Biopharm* 2007; 67: 476-484.
- [42] Roberts RJ, Rowe RC. The effect of punch velocity on the compaction of a variety of materials. *J Pharm Pharmacol* 1985; 37: 377-384.
- [43] Doelker E, Shotton E. The effect of some binding agents on the mechanical properties of granules and their compression characteristics. *J Pharm Pharmacol* 1977; 29: 193-198.
- [44] Ruegger CE, Çelik M. The effect of compression and decompression speed on the mechanical strength of compacts. *Pharm Dev Technol* 2000; 5: 485-494.

- [45] Esezobo S, Pilpel N. Effects of applied load and particle size on the plastoelasticity and tablet strength of some directly compressible powders. *J Pharm Pharmacol* 1987; 39: 303-304.
- [46] Travers DN, Çelik M, Buttery TC. A computer aided investigation on strain movement in compacts under constant stress within the die. *Drug Dev Ind. Pharm* 1983; 9, 139-157.

Discussion and Outlook

A challenging task in this thesis was to resolve the conflicts and contradictory claims reported in literature about radial die-wall pressure measurement during high speed compaction of pharmaceutical materials. The results showed that a continuous increase of the residual value of radial die-wall pressure would indicate increasing tendency for friction, and hence probability for capping. On the other hand, a high constant value of the maximum radial die-wall pressure during compaction would provide an evidence for plastic behavior and high stress transmission through powder bed. Thus, radial die-wall pressure changes were good predictors to mechanical parameters such as tensile strength and elastic recovery, as well as to powder compressibility, and density non homogeneity under variable physico-chemical/mechanical conditions. Moreover, regarding the aforementioned results, radial die-wall pressure showed also robustness as a tool for sticking prediction.

Future prospective would include studying compaction with a temperature controlled die, so changes of material physico-chemical characteristics could be investigated, such as polymorphism. This could be guided by on-line X-Ray Microtomography which allows 3D characterization of the compact microstructure and Atomic Force Microscopy for surface scanning and characterization.

Sameh Abdel-Hamid

PERSONAL INFORMATION

Nationality	Egyptian
Place of Birth	Cairo, Egypt
Gender	Male

EDUCATION

December 2007 – June 2011	PhD Natural sciences (Summa cum laude) “Instrumentation of tableting machines: High speed compaction investigation through simulation and radial die-wall pressure monitoring” Industrial Pharmacy Lab, University of Basel, Basel, Switzerland
October 2001- December 2005	MSc Pharmaceutical Sciences (Drug Technology) “Formulation and Evaluation of Mebeverine HCl as a Local Anesthetic for Oral and Dental Use” Faculty of Pharmacy, Ain Shams University, Cairo, Egypt
September 1995- May 2000	BSc Pharmaceutical Sciences (Excellent with Honors) Faculty of Pharmacy, Ain Shams University, Cairo, Egypt

PUBLICATIONS

Sameh Abdel-Hamid, S.E. Abdel-Hady, A.A. El-Shamy, H.F. El-Dessouky. Formulation of an antispasmodic drug as a topical local anesthetic. **Int J Pharm** 2006, 326: 107-118.

Sameh Abdel-Hamid, S.E. Abdel-Hady, A.A. El-Shamy, H.F. El-Dessouky. A novel formulation for mebeverine hydrochloride. **Drug Dev Ind Pharm** 2007, 11: 1-12.

Sameh Abdel-Hamid, G.Betz. Study of radial die-wall pressure changes during pharmaceutical powder compaction. **Drug Dev Ind Pharm** 2011, 37(4): 387–395.

Sameh Abdel-Hamid, M. Koziolk, G.Betz. Effect of lubricant, binder, and drug loading on radial die-wall pressure. **Drug Dev Ind Pharm**. In press

Sameh Abdel-Hamid, F. Alshihabi, G.Betz. Investigating the effect of particle size and shape on high speed tableting through radial die-wall pressure monitoring. **Int J Pharm** 2011, 413: 29-35.

Sameh Abdel-Hamid, G.Betz. Radial die-wall pressure as a reliable tool for studying the effect of powder water activity on high speed tableting. **Int J Pharm** 2011, 411: 152-161.

Sameh Abdel-Hamid, G.Betz. Investigating the effect of punch geometry on high speed tableting through radial die-wall pressure monitoring. **Pharm Dev Technol**. In press

Sameh Abdel-Hamid, G.Betz. A novel tool for the prediction of tablet sticking during high speed compaction. **Pharm DevTechnol**. In press